

CENTER FOR

ADVANCED NUCLEAR ENERGY SYSTEMS

Massachusetts Institute of Technology
77 Massachusetts Avenue, 24-215
Cambridge, MA 02139-4307

(617) 452-2660
canes@mit.edu
canes.mit.edu



Nuclear Fuel Cycle Program

Levelized Cost of Fuel (LCOF) studies for microreactors using TRISO fuel in hydride and berylli- um-based composite modera- tors in open and closed fuel cycles

Sai Prasad Balla and Jacopo Buongiorno

Department of Nuclear Science and Engineering
Massachusetts Institute of Technology

MIT-NFC-TR-135
March 2025

CANES PUBLICATIONS

Topical and progress reports are published under six series:

Advanced Nuclear Power Technology Program (MIT-ANP-)
Nuclear Energy and Sustainability Program (MIT-NES-)
Nuclear Fuel Cycle Technology and Policy Program (MIT-NFC-)
Nuclear Space Applications (MIT-NSA-)
Nuclear Systems Enhanced Performance Program (MIT-NSP-)
MIT Reactor Redesign Program (MIT-MRR-)

Please visit our website (canes.mit.edu) to view more publication lists.

MIT-NFC-TR-135	S. Prasad Balla and J. Buongiorno Levelized Cost of Fuel (LCOF) studies for microreactors using TRISO fuel in hydride and beryllium-based composite moderators in open and closed fuel cycles (2025).
MIT-NFC-TR-134	S. Shaner; K. Shirvan; E. Pilat, and R. Ballinger, Opportunity for Innovation in the Existing LWR Fuel Cycle (2016).
MIT-NFC-TR-133	S. Passerini; E. Shwageraus; M.S. Kazimi, Sensitivity Analysis and Optimization of the Nuclear Fuel Cycle: A Systematic Approach (2012).
MIT-NFC-TR-132	J.W. Fricano; J. Buongiorno, Integrated Fuel Performance And Thermal-Hydraulic Sub-Channel Models For Analysis Of Sodium Fast Reactors (2012).
MIT-NFC-TR-131	T.P. Gerrity; B. Forget; T. Newton, MCODE-3: Time-Dependent Depletion Isotopics with MCNP-5 and SCALE-6.1 (2012).
MIT-NFC-TR-130	N. Andrews; A. Karahan; M.S. Kazimi, Development Of Fission Gas Swelling And Release Models For Metallic Nuclear Fuels (2012).
MIT-NFC-TR-129	A.J. Mieloszyk; M.S. Kazimi, An Improved Structural Mechanics Model For The Frapcon Nuclear Fuel Performance Code (2012).
MIT-NFC-TR-128	T. Kwak; M.W. Golay, Nuclear Non-Proliferation Regime Effectiveness: An Integrated Methodology for Analyzing Highly Enriched Uranium Production Scenarios at Gas Centrifuge Enrichment Plants (May 2012).
MIT-NFC-TR-127	F.E. Dozier; M.J. Driscoll; J. Buongiorno, Feasibility of Very Deep Borehole Disposal of US Nuclear Defense Wastes (June 2011).
MIT-NFC-TR-126	B.R. Herman; E. Shwageraus; B. Forget; M.S. Kazimi, Cross Section Generation Strategy for High Conversion Light Water Reactors (June 2011).
MIT-NFC-TR-125	E.A. Bates; J. Buongiorno; M.J. Driscoll, A Drop-In Concept for Deep Borehole Canister Emplacement (June 2011).
MIT-NFC-TR-125	G. Haratyk; J. Buongiorno; M.J. Driscoll, Nuclear-Renewables Energy System for Hydrogen and Electricity Production (June 2011).
MIT-NFC-TR-124	B. Feng; M.S. Kazimi; B. Forget, Feasibility of Breeding in Hard Spectrum Boiling Water Reactors with Oxide and Nitride Fuels (June 2011).
MIT-NFC-TR-123	A.C. Kadak; K. Yost, Key Issues Associated with Interim Storage of Used Nuclear Fuel (December 2010).
MIT-NFC-TR-122	M. Massie; B. Forget, A Generalized Optimization Methodology for Isotope Management (September 2010).
MIT-NFC-PR-121	K.G. Jensen; M.J. Driscoll, Plugging of Deep Boreholes for HLW Disposal (July 2010).

Executive Summary

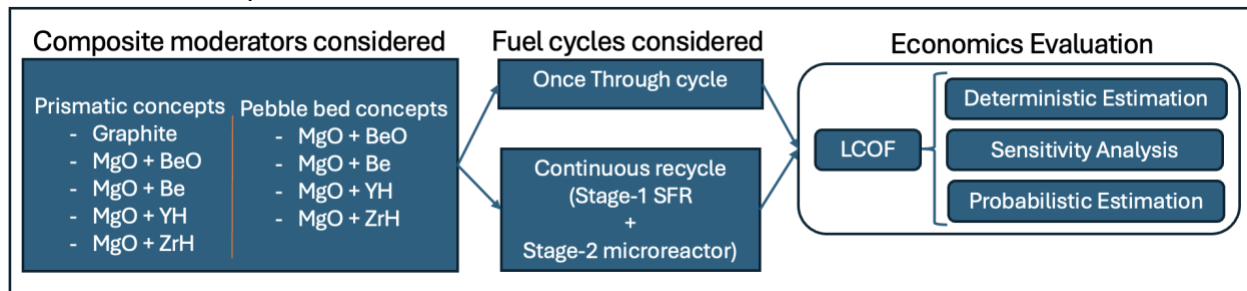
Nuclear batteries (NBs) are small, advanced microreactors with a thermal output of under 20 MW_{th} [1]. These compact reactors promise plug-and-play capability, ensuring reliable operation with high capacity factors and reducing expensive transmission infrastructure requirements in remote areas. The bulk of these microreactors are based on graphite-moderated high-temperature gas-cooled reactor (HTGR) design. Graphite exhibits unfavorable properties under irradiation and tends to undergo non-uniform shrinkage followed by volumetric expansion and increased residual stress during irradiation, limiting its operational lifespan. Composite moderators, which combine a radiation- and chemically-stable magnesium oxide (MgO) host matrix with an entrained beryllium or hydride moderating phase, have shown potential as suitable alternatives for the graphite used in HTGRs [2].

Dr. Brown's research group at the University of Tennessee Knoxville under DOE's ARPA-E ONWARDS program [3] has developed microreactor point designs for the state-of-the-art graphite moderator and pebble-bed and prismatic microreactor point designs using the composite moderator IMF concepts. Both open and continuous recycle fuel cycles are developed with substantially reduced overall nuclear waste. However, these concepts must demonstrate financial competitiveness to be commercially successful and for large-scale adoption. This study conducted a comparative economic evaluation of these novel fuel concepts using industry-standard, albeit imperfect, Levelized Cost of Fuel (LCOF) metric.

A deterministic LCOF analysis was first performed using fixed material and process cost estimates for various fuel cycle configurations. For the Once-Through cycle, all fuel cycle costs—from mining and milling to spent fuel management—are discounted to the initial fuel load timeline, annualized via capital recovery factors, and then normalized by the reactor's annual electricity production.

The continuous recycle fuel cycle features a two-stage process: Stage 1 employs a sodium-cooled fast reactor (SFR) to breed surplus plutonium, which is then reprocessed and used to fuel multiple Stage-2 microreactors, optimizing fuel utilization and minimizing waste. The continuous recycle analysis was conducted using two complementary methods. First, a standalone Stage-2 methodology was applied where all cost components specific to Stage-2—such as remote-handled TRISO fuel fabrication, deconsolidation, pyroprocessing, and waste management—are mapped along the Stage-2 timeline, discounted to the Stage-2 fuel load timeline, annualized via capital recovery factor, and normalized by the microreactors' annual electricity production. Second, a combined or fleet-mode approach was used where the entire fuel cycle Stage-1 and Stage-2 perspective. In this approach, the full spectrum of Stage-1 costs—including mining, milling, blanket, and driver fuel fabrication, reprocessing (pyroprocessing), U-Pu-MA storage, and waste disposal—is mapped and discounted to the Stage-1 fuel load event. Stage-2 costs are similarly adjusted to reflect the cumulative effect of fueling multiple microreactors from one SFR. The aggregated, discounted costs are then annualized by capital recovery factor and normalized by the total annual electricity production of the integrated system, yielding the overall LCOF measured at the Stage-1 fuel load.

Sensitivity analyses were carried out to assess the critical cost drivers. Individual cost parameters were systematically varied by $\pm 20\%$ from baseline values to identify their impact on the LCOF. Monte Carlo analysis accounting for multiple simultaneous uncertainties, including potential reduction in fuel fabrication costs for NOAK system, potential increase in enrichment costs due to Category-II facility requirements (Category-II Enrichment Facility (10-20% U-235) employ increased security, physical protection, material accounting requirements than existing Category-III Enrichment Facility (U-235 <10% LEU)), and historical variations in raw material costs, was carried out for 200,000 iterations, which provided a comprehensive distribution of possible LCOF outcomes. [Figure E-1](#) provides a complete overview of the reactor concepts and the economic analysis carried out.



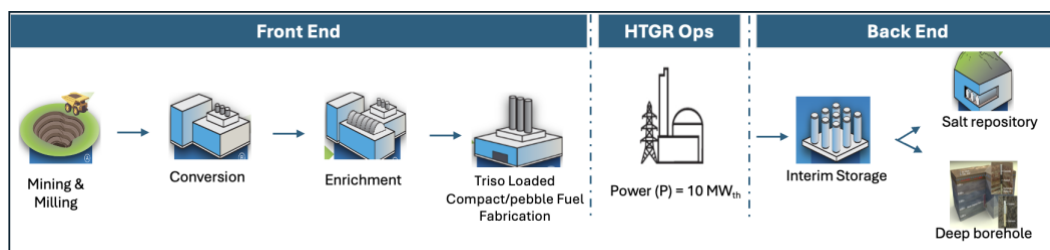
E- 1 Full scope of analysis

While performing the literature review for the costs associated with different fuel cycle steps, the spot prices were readily available for mining & milling, conversion, and enrichment. However, there was a considerable gap in fuel fabrication cost estimation for the composite moderator concepts. Also, there was little guidance on the back-end disposal of advanced microreactor concepts.

As part of this study, detailed microreactor fuel fabrication steps were examined, and an effort was made to analogously estimate the manufacturing cost from the known graphite baseline case. After this, the total fabrication cost was estimated for the different concepts using the cost of composite moderators based on commercial providers and expert consultation and adding to the manufacturing cost. For the final disposal, using the existing disposal options as a baseline, a step-by-step comparison was carried out to identify the requirement/ constraint that sets the design limit- referred to as the 'limiting factor'. The limiting factor was considered to arrive at the cost of the disposal option.

Once-through cycle, LCOF estimation results:

[Figure E- 2](#) was used as the reference fuel cycle for the once-through fuel cycle in which the microreactor fuel undergoes a single pass through the reactor and is directly disposed of without recycling. The results are discussed next.



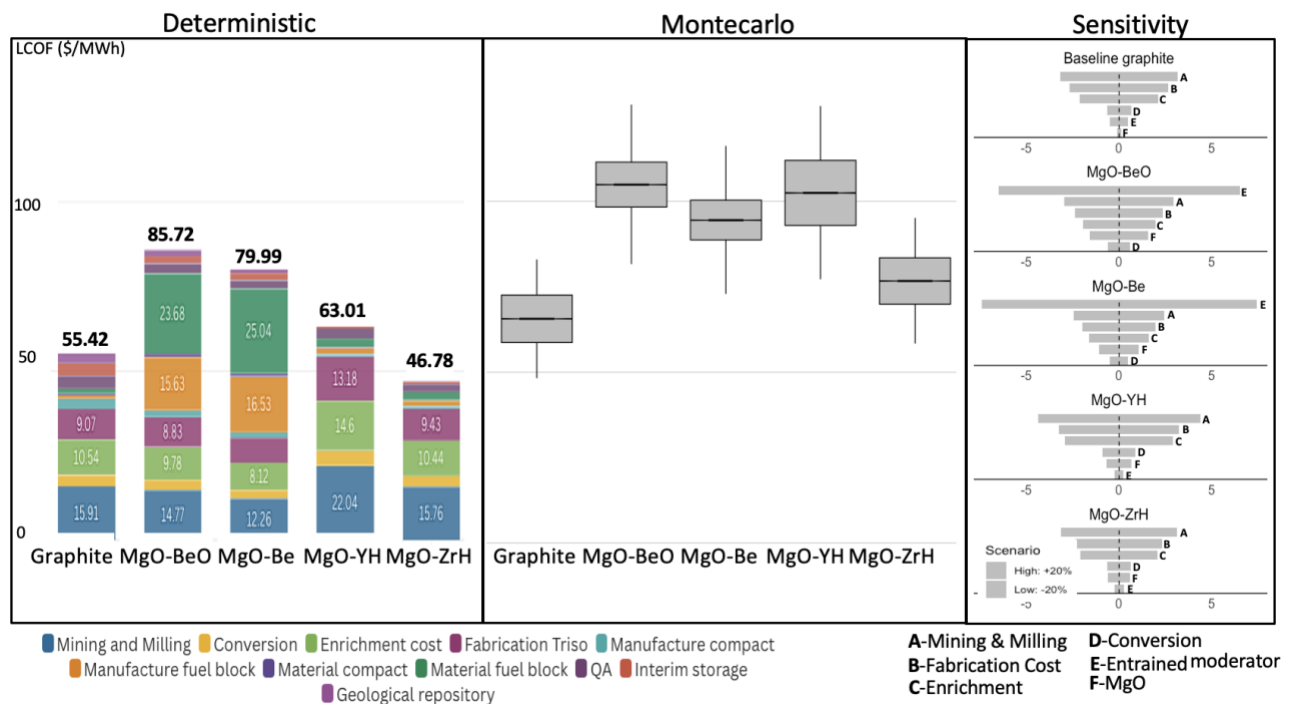
E- 2 Reference Open fuel cycle major steps. Icons taken from [4]

Prismatic concepts:

Figure

E- 3 presents the results of LCOF analysis for the Once-through prismatic concepts. The baseline prismatic graphite design incurs an LCOF of \$55.42/MWh. In contrast, advanced moderator concepts exhibit a wide cost range: MgO–ZrH, at \$46.79 (16% below baseline), presents the lowest deterministic LCOF, while MgO–BeO and MgO–Be reach \$85.72 (53% above) and \$79.99 (43% above), respectively, and MgO–YH stands at \$63.01 (13% above).

It was observed that fuel block manufacturing and material costs are the significant cost drivers for the prismatic concepts. The new LCOF was calculated assuming fuel blocks would be recycled after every reload. The results indicated that introducing fuel block recycling will yield substantial savings for beryllium-based cores—MgO–Be’s LCOF declines 52% (to \$38.54), and MgO–BeO’s drops 46% (to \$46.49)—whereas graphite, MgO–YH, and MgO–ZrH see modest 5–8% improvements. These economic gains would also lead to operational and safety advantages, including reduced handling and waste volumes. However, detailed additional analysis for fuel block performance under higher irradiation, irradiated block inspection, and regulatory compliance would be needed. A separate cost-threshold modeling indicated that beryllium-based prismatic reactors may achieve baseline parity if raw beryllium dips below \$798/kg or BeO remains under \$54/kg. In contrast, it was seen that the MgO–YH cannot match baseline graphite economics even under favorable moderator pricing.



E- 3 Deterministic, Monte Carlo, and sensitivity LCOF results for once-through prismatic concepts

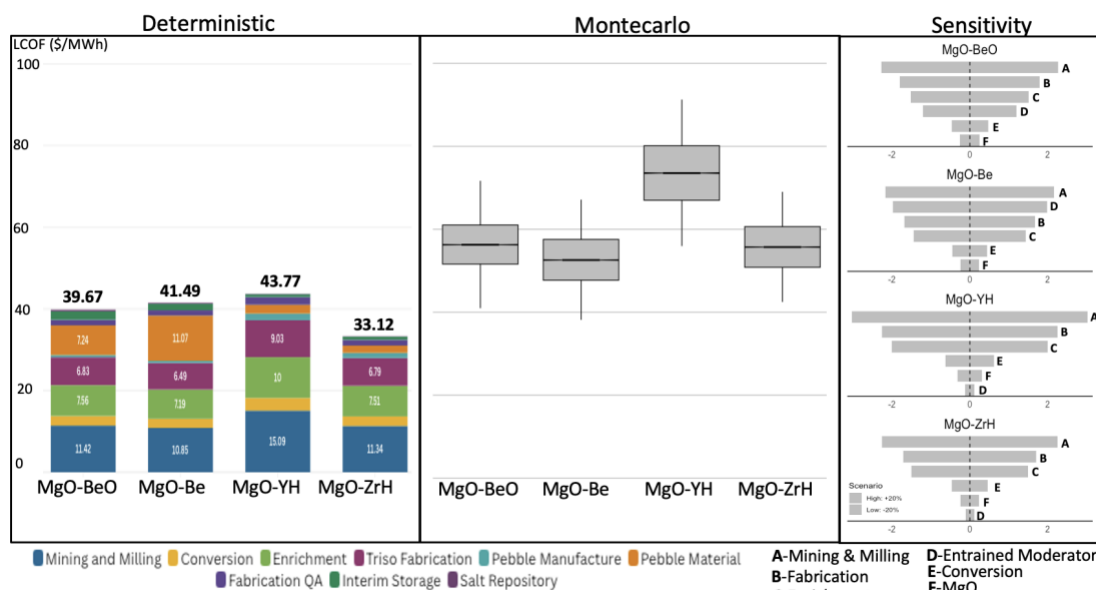
Sensitivity analyses reveal that the advanced moderators face elevated price risks, particularly for beryllium-based concepts ($\pm \$6.5$ – $\$7.4$ /MWh swings), while MgO–YH depends heavily on raw uranium availability ($\pm \$4.4$ /MWh for mining and milling). Monte Carlo simulations confirm these vulnerabilities and potential cost escalations: although the baseline graphite sees an 18% rise (to \$65.73) over its deterministic estimate, MgO–ZrH’s cost can spike by 64% (to \$76.80), while MgO–BeO and MgO–Be increase by roughly 23% and 18%, respectively, reflecting supply-chain uncertainties; MgO–YH, at a 63% jump (to \$102.61), emerges as the most volatile. At the

lower end of the spectrum, these findings also suggest that novel moderators—especially ZrH and beryllium-based options—can rival graphite under certain optimistic conditions, that is, stable supply chains and advanced manufacturing processes like additive manufacture that minimize material loss.

Pebble bed concepts:

The results of the LCOF analysis for the Once-through pebble bed concepts are shown in [Figure E- 4](#). MgO–ZrH, at \$33.12/MWh, demonstrates the most substantial cost advantage, largely due to lower mining and enrichment expenditures; MgO–BeO follows at \$39.67/MWh, avoiding the high moderator cost penalties seen in prismatic systems. MgO–Be totals \$41.49/MWh, reflecting a moderate beryllium premium that remains significantly lower than prismatic levels, and MgO–YH stands at \$43.77/MWh, primarily driven by its higher mining and enrichment requirements.

Sensitivity analyses reveal that front-end variables—notably mining and fabrication—dominate cost uncertainty, whereas moderator expenses, though nontrivial, are notably less volatile than in prismatic designs. Monte Carlo simulations underscore this stability: MgO–BeO, MgO–Be, and MgO–ZrH each display tighter standard deviations ($\sigma \approx 6$) than prismatic equivalents, while MgO–YH’s higher mean (\$73.60/MWh, $\sigma = 7.88$) still exhibits reduced variability compared to its prismatic counterpart. Collectively, these findings demonstrate that pebble-bed architecture substantially lowers moderator-driven costs and narrows overall LCOF spreads (roughly 10.65 units from lowest to highest), indicating a more predictable economic profile dominated by mining, milling, and fuel fabrication factors, thereby enhancing the commercial viability of pebble-bed reactor deployment.



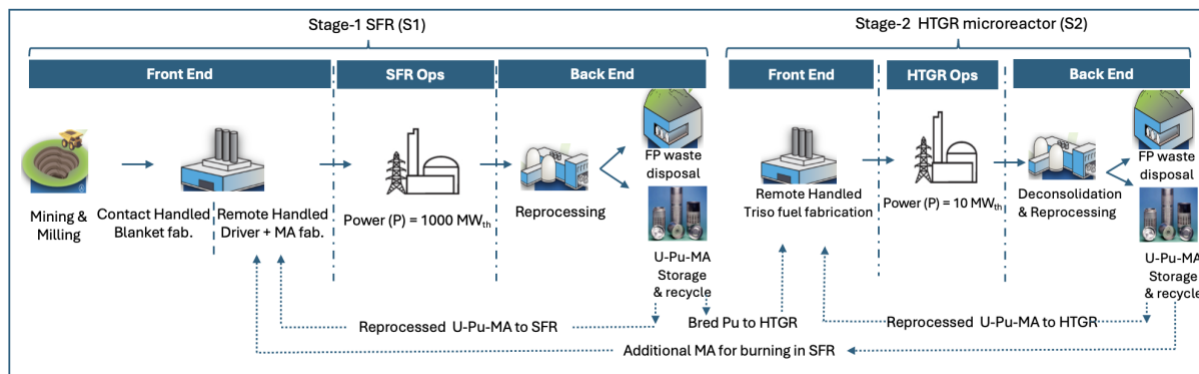
E- 4 Deterministic, Monte Carlo, and sensitivity LCOF results for once-through pebble bed concepts

It was also noted that the absolute contribution to the LCOF from the back-end operations is not as significant. However, the volume of spent fuel emerged as the limiting factor both in deep borehole and geological repository options. Deconsolidation of the fuel matrix is one of the proposed solutions to reduce the SNF volume. In the analysis, with deconsolidation, spent

fuel volume reductions up to 90-98% were observed, which would result in a steep decline in required repository potentially capacity, leading to siting and public acceptance benefits.

Continuous recycle fuel cycle, LCOF estimation results:

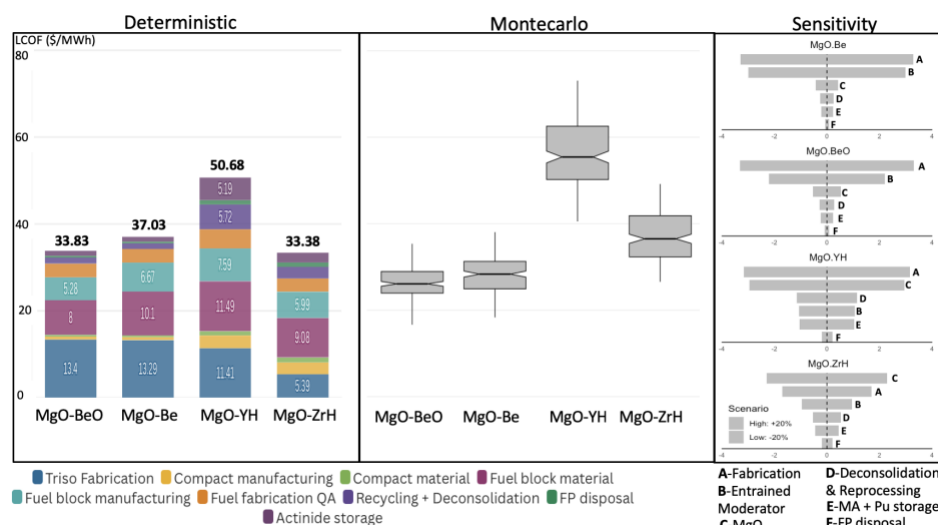
Figure E- 5 provides an overview of this transuranic recycling approach, in which a single fast reactor (Stage 1) supports one or more microreactors (Stage 2).



E- 5 Continuous recycle fuel cycle major steps. Icons are taken from [4]

Prismatic concepts (Stand-alone microreactor):

The results of the LCOF analysis for the continuous recycle prismatic concepts under the standalone stage—2 methodology are shown in Figure E- 6. Under continuous-recycle (CR) conditions, prismatic microreactors demonstrate substantial cost reductions relative to a once-through graphite baseline of approximately \$55.96/MWh. MgO–ZrH exhibits the lowest deterministic LCOF at \$33.38/MWh, followed closely by MgO–BeO (\$33.83/MWh) and MgO–Be (\$37.03/MWh), amounting to 34–40% decreases vis-à-vis once-through graphite. By contrast, with an LCOF of \$50.68/MWh, MgO–YH achieves only a 9% reduction.



E- 6 Deterministic, Monte Carlo, and sensitivity LCOF analyses for continuous recycle prismatic concepts on standalone microreactor consideration.

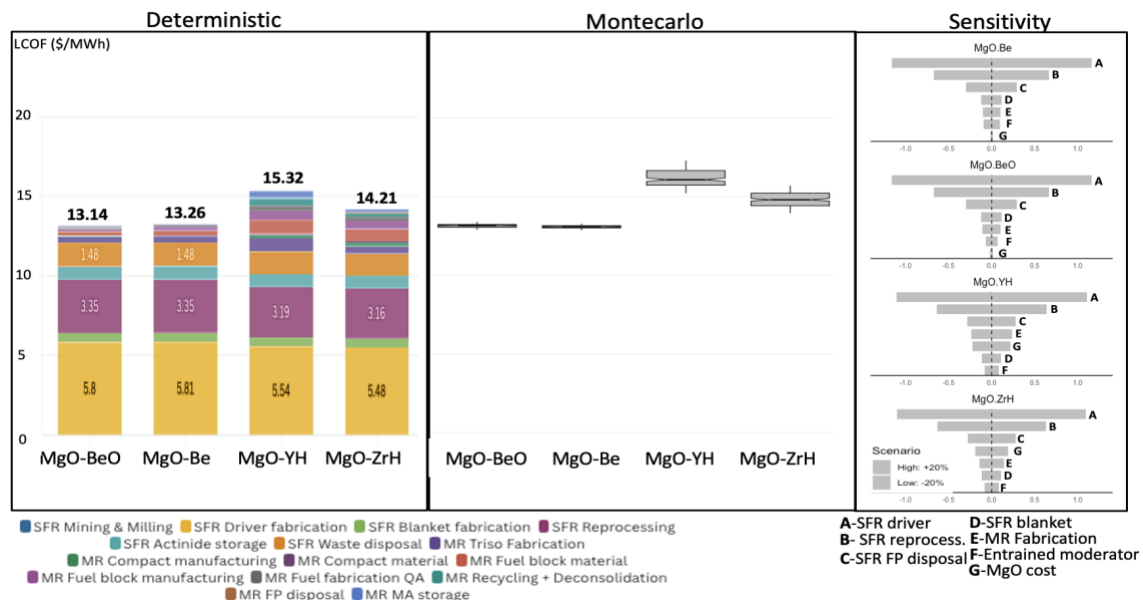
Sensitivity analyses indicate that fabrication and moderator-material swings remain the principal cost levers, whereas reprocessing exerts relatively minor effects. Monte Carlo simulations underscore the upside potential of MgO–Be and MgO–BeO, whose mean LCOFs (\$28.17/MWh and \$26.22/MWh, respectively) often fall well below deterministic values when

favorable input assumptions coincide. MgO–ZrH’s mean cost (\$37.08/MWh) remains competitive despite periodic unfavorable draws related to zirconium hydride pricing. MgO–YH, conversely, remains the least cost-effective, as its higher heavy metal loading needs and, consequently, higher reprocessing expenses push its mean LCOF (\$56.27/MWh) near or above once-through graphite levels in many simulation outcomes. As category-II enrichment costs are not required, the potential for cost escalation is reduced, thereby improving LCOF outcomes under conditions of uncertainty.

Prismatic concepts - combined SFR and microreactor

Figure E- 7 presents the LCOF results for this scenario. Introducing fuel cycle expenses for the sodium-cooled fast reactor (SFR), which provides plutonium to Stage 2, shows that SFR-related expenses dominate—accounting for 87–92% of total costs. As a result, differences among the microreactors, while present, become comparatively minor. Specifically, MgO–BeO and MgO–Be costs cluster between \$13.14 and \$13.26 per MWh, MgO–ZrH increases to \$14.21 per MWh, and MgO–YH reaches \$15.32 per MWh.

Sensitivity results confirm that $\pm 20\%$ shifts in SFR driver fabrication and reprocessing overshadow moderator-cost fluctuations, reinforcing that any improvements in SFR fabrication or reprocessing efficiency throughput directly reduce the overall LCOF. Monte Carlo results mirror these trends: both beryllium-based concepts (MgO–Be and MgO–BeO) converge tightly around \$13/MWh, while MgO–ZrH and MgO–YH exhibit higher mean costs (\$14.80/MWh and \$16.16/MWh, respectively) and broader uncertainty ranges. Consequently, although moderator selection retains some minor influence, targeted advancements in SFR driver fabrication and reprocessing performance remain the most impactful strategies for lowering system-wide fuel costs in an integrated CR configuration.

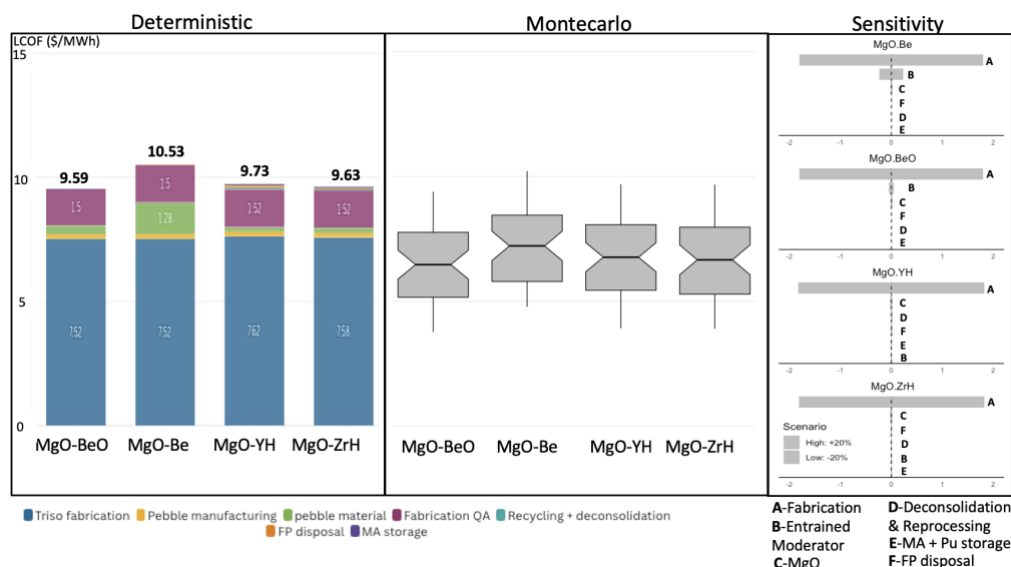


E- 7 Deterministic, Monte Carlo, and sensitivity LCOF results for the continuous recycle prismatic concepts based on combined SFR and microreactor consideration.

Pebble bed concepts - Stand-alone microreactor:

The LCOF results for the pebble bed concepts are presented in Figure E- 8. The four continuous-recycle pebble-bed microreactor designs exhibit leveled costs of fuel (LCOF) in the range of

\$9.59–\$10.53 per MWh. This relatively narrow cost band is primarily attributable to three interlinked factors: (1) a pronounced reduction in moderator mass, estimated at approximately 87–93% reduction relative to prismatic counterparts; (2) exceptionally high burnup levels reaching up to 415.3 GWd/MT, and (3) extended core residence times of up to a century in certain beryllium-based configurations. The dominant cost driver, evident from the data, is recycled TRU-based TRISO fuel fabrication costs, which contribute between \$7.52 and \$7.62 per MWh across all four concepts.



E- 8 Deterministic, Monte Carlo, and sensitivity LCOF results for the continuous recycle pebble bed concepts based on standalone microreactor consideration.

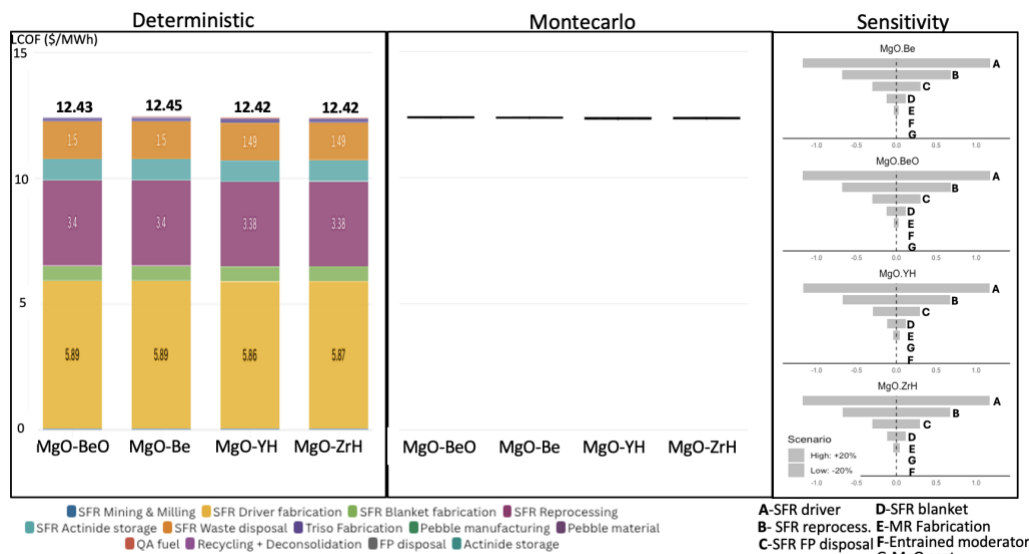
Sensitivity analyses further indicate that $\pm 20\%$ fluctuations in fabrication expenses account for the most significant LCOF variations, significantly overshadowing all other factors. The long incore residence time forces the backend costs to be a minor contributor to LCOF. Moreover, Monte Carlo simulations demonstrate mean LCOF values that can be 24–38% lower than the deterministic baselines, highlighting the probabilistic advantage due to lowering fabrication cost, limited entrained moderator costs, and absence of enrichment requirements. Although promising, the proposed burnup levels and long residence times exceed current qualifications for TRISO fuel. This suggests that additional research is required to validate long-term operational stability and reliability.

Pebble bed concepts - combined SFR and microreactor:

When a sodium-cooled fast reactor (SFR) is introduced to supply plutonium and manage reprocessing for these microreactors, the economic analysis reveals a shift in the cost distributions. Figure E- 9 depicts that the SFR contribution to the overall LCOF reaches approximately 98–99%, resulting in total fuel costs converging to \$12.40–\$12.45 per MWh regardless of the microreactor’s moderator configuration. Consequently, the microreactors’ share is confined to \$0.12–\$0.18 per MWh, rendering differences among beryllium- or hydride-based moderators almost negligible at the fleet scale.

Sensitivity analyses validated that $\pm 20\%$ variations in SFR driver fabrication and reprocessing can shift LCOF by \$1.18 or more, eclipsing the marginal effects of uncertainties in moderator material pricing or pebble fabrication. Furthermore, the Monte Carlo simulations produce tight

clusters of cost outcomes near \$13 per MWh, further reinforcing the conclusion that SFR-related expenditures dominate the overall economics. In line with earlier prismatic studies, these findings indicate that targeted advancements in fast-reactor driver fabrication and reprocessing activities may yield substantially larger economic benefits.



E- 9 Deterministic, Monte Carlo, and sensitivity LCOF results for the continuous recycle prismatic concepts based on combined SFR and microreactor consideration.

The major takeaway is that advanced moderators can significantly reduce microreactor costs, but this economic promise relies heavily on stable supply chains, mature fabrication methods, and proven high-burnup fuel performance. Once-Through Pebble-bed designs, in particular, appear more robust against swings in raw material prices because they use less moderator per MWh and can operate with extended residence times, thereby reducing front-end fuel demand. Continuous recycle scenarios further lower LCOFs by offsetting higher reprocessing costs with savings in uncertain enrichment costs in Category-II facilities for HALEU fuels—an advantage magnified when paired with a large fast reactor (SFR) whose expenses dominate the overall fuel cycle. However, achieving and sustaining ultra-high burnups remains a major technical challenge requiring extensive R&D into long-duration TRISO fuel integrity, in-situ inspection, and safe handling.

Acknowledgments

The DOE ARPA-E funded this work under contract DE-AR0001620 as part of the “MATRICY: Matrix Engineered TRISO Compacts Enabling Advanced Reactor Fuel Cycles” Program.

Professor Nick Brown’s team from the University of Tennessee Knoxville and Professor Jason from Stony Brook University provided help with the necessary support or the reactor design specifications. Discussions with Dr. Lance Snead provided vital insights into composite moderator fabrication. Dr. Dave Petti helped to understand the nuances of the TRISO fabrication process.

Cambridge, MA

March 2, 2025

Table of Contents

Executive Summary	1
Acknowledgments	9
List of abbreviations	13
List of Tables	15
List of Figures	16
1 Scope and Objective	18
2 Reactor designs, moderator concepts and TRISO types considered for analysis	21
2.1 High-temperature gas-cooled reactor point designs	21
2.1.1 The prismatic microreactor point design	21
2.1.2 The pebble bed microreactor point design	23
2.2 Composite moderators considered for analysis	25
2.3 TRISO kernels used for study	26
3 Generalized methodology for LCOF analysis	27
3.1 Deterministic estimation: LCOF cost drivers	27
3.2 Sensitivity analysis	29
3.3 Monte Carlo analysis	30
4 Fuel cycle major activities and cost considerations	31
4.1 Once-Through cycle	31
Once-Through Front-end processes	31
4.1.1 Mining and Milling	31
4.1.2 Conversion	31
4.1.3 Enrichment	31
4.1.4 Fuel fabrication process	32
Once-through back-end processes	36
4.1.5 Ultimate disposal	38
4.2 Continuous recycle fuel cycle: Major steps and cost considerations	39
Stage-1 SFR Front-end process	41
4.2.1 Mining and milling	41
4.2.2 Contact handled blanket fabrication	41
4.2.3 Remote-handled driver fabrication	41
Stage-1 SFR Back-end process	41
4.2.4 Reprocessing	42
4.2.5 U-Pu-MA storage & recycle	42
4.2.6 FP waste disposal	42
Stage-2 HTGR Front-end process	42
4.2.7 Remote-handled TRISO fuel fabrication	43
Stage-2 HTGR Back-end process	43
4.2.8 Deconsolidation & Pyroprocessing	43
4.2.9 U-Pu-MA storage & recycle	44
4.2.10 FP waste disposal	44

4.3	Material costs	44
5	<i>Fabrication cost estimation methodology and calculation for Once-Through and continuous recycle reactor concepts</i>	46
5.1	Fabrication cost estimation methodology for prismatic reactor concepts:	46
5.1.1	TRISO fabrication consideration	46
5.1.2	Prismatic fuel assembly fabrication (including compacts)	47
5.1.3	QA costs during each of the above processes:	48
5.2	Fuel fabrication costs estimation methodology for pebble-bed concepts	49
5.2.1	TRISO fabrication costs	49
5.2.2	Pebble fabrication costs	49
5.2.3	Pebble QA cost	50
6	<i>Methodology and cost estimation for Spent Nuclear Fuel Disposal activity from Microreactors</i>	51
6.1	Interim storage – microreactor equivalency assessment:	51
6.2	Deep borehole - microreactor concepts equivalency assessment.....	52
6.3	Geological repository microreactor equivalency assessment	53
6.4	Back-End disposal constraints and costs	54
	Threshold-Cost Analysis.....	55
7	<i>LCOF Estimation</i>	56
7.1	Levelized Cost of Fuel (LCOF) estimation for once-through cycle.....	56
7.2	Levelized Cost of Fuel (LCOF) estimation for continuous recycle fuel cycle	58
7.3	Sensitivity analysis	61
7.4	Montecarlo analysis	61
8	<i>Results & Discussion LCOF using deterministic approach, Sensitivity Analysis & Montecarlo Analysis</i>	64
8.1	Once-Through cycle Prismatic microreactor	65
8.1.1	LCOF cost drivers.....	65
8.1.2	Sensitivity Analysis	67
8.1.3	Monte Carlo analysis.....	68
8.1.4	Key implications and recommendations.....	69
8.2	Once-Through cycle Pebble-bed microreactor	71
8.2.1	LCOF cost drivers.....	71
8.2.2	Sensitivity analysis.....	72
8.2.3	Monte Carlo analysis.....	73
8.2.4	Key implications and recommendations.....	74
8.3	Deconsolidation merits and limiting cost for the deconsolidation process	75
8.4	Continuous recycle (Only stage-2) Prismatic microreactor	78
8.4.1	LCOF cost drivers.....	78
8.4.2	Sensitivity analysis.....	79
8.4.3	Monte Carlo analysis.....	80
8.4.4	Key Implications and Recommendations	81
8.5	Continuous recycle (Stage-1 & Stage-2 combined) Prismatic micro Reactor.....	82
8.5.1	LCOF cost drivers.....	82
8.5.2	Sensitivity analysis.....	83

8.5.3	Monte Carlo analysis.....	84
8.5.4	Key implications and recommendations.....	85
8.6	Continuous recycle (Only Stage-2) Pebble-bed micro reactor	86
8.6.1	LCOF cost drivers.....	86
	Combined Impact of High Burnup and Long Residence Time	86
8.6.2	Sensitivity analysis.....	87
8.6.3	Monte Carlo analysis.....	88
8.6.4	Key implications and recommendations.....	88
8.7	Continuous recycle (stage-1 & stage-2 combined) Pebble bed microreactor	90
8.7.1	LCOF cost drivers.....	90
8.7.2	Sensitivity analysis.....	91
8.7.3	Monte Carlo analysis.....	91
8.7.4	Key implications and recommendations.....	92
9	Conclusion and future work	93
	References.....	96
	Appendix 1 Sodium-cooled fast reactor design specification	99
	Appendix 2 Calculations for the front end of the cycle	101

List of abbreviations

Acronym	Description
ARPA-E	Advanced Research Projects Agency–Energy
BU	Burnup
Cat-II	Category-II Facility
CDF	Cumulative Distribution Function
CF	Capacity Factor
CFR	Code of Federal Regulations
CR	Continuous Recycle
CRF	Capital Recovery Factor
DPC	Dual-Purpose Canister
DOE	Department of Energy (United States)
EFPD	Effective Full Power Days
EPY	Effective Full Power Years
FOAK	First-of-a-Kind
FP	Fission Product
FSAR	Final Safety Analysis Report
GWd/MT	Gigawatt-days per Metric Ton
HALEU	High-Assay Low-Enriched Uranium
HLW	High-Level Waste
HM	Heavy Metal
HTGR	High-Temperature Gas-Cooled Reactor
IMF	Inert Matrix Fuel
ISFSI	Independent Spent Fuel Storage Installation
LCOF	Levelized Cost of Fuel
LLW	Low-Level Waste
MA	Minor Actinides
MC	Monte Carlo
MATRICY	Matrix Engineered TRISO Compacts Enabling Advanced Reactor Fuel Cycles
MEITNER	Modeling-Enhanced Innovations Trailblazing Nuclear Energy Reinvigoration
MgO	Magnesium Oxide
MPC	Multipurpose Canister
MW _{th}	Megawatts Thermal
NB / NBs	Nuclear Battery / Nuclear Batteries
NOAK	N _{th} -of-a-Kind
NPV	Net Present Value
NRC	Nuclear Regulatory Commission (United States)
ONWARDS	Optimizing Nuclear Waste and Advanced Reactor Disposal Systems
O[I]PyC	Outer [Inner] Pyrocarbon Layer
SFR	Sodium-Cooled Fast Reactor
SiC	Silicon Carbide
SNF	Spent Nuclear Fuel
SWU	Separative Work Unit

TRISO	Tristructural Isotropic
TRU	Transuranic
UCO	Uranium OxyCarbide
UF ₆	Uranium Hexafluoride
UN	Uranium Nitride
UNH	Uranyl Nitrate Hexahydrate
UTK	University of Tennessee, Knoxville

List of Tables

Table 2-1 Once-Through prismatic reactor design specification.....	22
Table 2-2 Continuous recycle prismatic reactor design specification	23
Table 2-3 Once-Through pebble bed reactor design specification	24
Table 2-4 Continuous recycle pebble bed reactor design specification.....	25
Table 2-5 Volume fraction of moderating materials for prismatic and pebble bed concepts [10].	26
Table 2-6 Features of the TRISO particles for the state-of-the-art and IMF concepts	26
Table 4-1 MPC design specifications based on Holtec international final safety analysis report	37
Table 4-2 Summary of canister design specifications [22].....	38
Table 4-3 Design specification for MPC	39
Table 6-1 Equivalency estimation methodology for baseline graphite case.....	51
Table 6-2 Limiting parameter identification and storage costs for interim storage (full core basis). The values in rows 1-5 indicate the fraction of interim storage casks required for disposal of full core as dictated by criteria in column 1.	52
Table 6-3 Limiting parameter identification and storage costs (full core basis) for deep borehole disposal. The values in rows 1-3 indicate the number of borehole casks required for disposal of full core as dictated by criteria in column 1.	53
Table 6-4 Limiting parameter identification and storage costs(full core basis) for salt repository disposal. The values in rows 1-3 indicate the number of MPC's required for disposal of full core as dictated by criteria in column 1.	53
Table 6-5 Permanent disposal cost comparison. (full core basis).....	54
Table 7-1 Mass of ore, SWU, and fuel mass for different concepts	56
Table 7-2 Cost basis table for Once-Through prismatic IMF concepts.....	57
Table 7-3 Cost basis table for Once-Through pebble-bed IMF concept	57
Table 7-4 Cost basis for stage-1 SFR	59
Table 7-5 Cost basis for continuous recycle prismatic concepts	59
Table 7-6 Cost basis for continuous recycle pebble bed concepts.....	60
Table 7-7 Variables considered for sensitivity analysis:	61
Table 7-8 Summary of the Monte Carlo range for process and material costs.....	63
Table 8-1 Equivalent deep borehole canisters required per microreactor (after deconsolidation). The values in rows 1-3 indicate the number of borehole canisters dictated by criteria in column 1	75
Table 8-2 Equivalent MPCs required per microreactor for the geological repository (after deconsolidation). The values in rows 1-3 indicate the percentage of MPC filled dictated by criteria in column 1	75
Table 8-3 Threshold deconsolidation costs for economic benefit	77

List of Figures

Figure 2-1 Radial (left) cross cut of the Once-through prismatic microreactor. Prismatic microreactor compact assembly (center). Radial (left) cross cut of the continuous recycle prismatic microreactor. Taken from [7]. Figures are not to scale.....	21
Figure 2-2 Axial and radial cross-section of the pebble bed micro reactor point designs for Once-through (left) and continuous recycle fuel cycle (right). Taken from[8].....	24
Figure 2-3 Composite moderator concept and notional properties of the structural matrix and entrained moderating phase. Taken from [8].....	25
Figure 3-1 A generalised four-step framework to calculate the LCOF for a standalone reactor..	27
Figure 3-2 Fuel cycle considered by Ganda et al [11]	28
Figure 3-3 A generalized four-step framework to calculate the LCOF for a combined (stage-1 + stage-2) continuous recycle configuration.	29
Figure 4-1 Once-through fuel cycle diagram showing major steps.	31
Figure 4-2 Block flow diagram of UO kernel fabrication process. Taken from [14]	33
Figure 4-3 Block flow diagram of the UO ₂ kernel to UN kernel fabrication process. Taken from [14].....	33
Figure 4-4 Major steps of UO ₂ kernel fabrication. Taken from [15]	33
Figure 4-5 Major steps during coating process. Taken from [16]	34
Figure 4-6 Schematic of the GA coater (Noren 1991) used for NPR fuel. Taken from [17]	34
Figure 4-7 Summary of fabrication process for fuel compacts. Taken from [16]	35
Figure 4-8 Complete cylindrical compact. Taken from [18]	35
Figure 4-9 Pebble fuel manufacture. Taken from [16]	36
Figure 4-10 Completed spherical compact and furnace mold. Taken from [19].....	36
Figure 4-11 Hi-Storm 100s Overpack with MPC partially inserted. Taken from [21].....	37
Figure 4-12 MPC-32 Basket. Taken from [21].....	37
Figure 4-13 Generalized concept for deep borehole disposal of high-level radioactive waste. Figure taken from [22]	38
Figure 4-14 Conceptual drawing for the salt repository concept with in-drift emplacement in long parallel drifts and emplacement of crushed salt backfill. Taken from [23]	39
Figure 4-15 Continous recycling of transuranic fuel cycle with SFR and microreactor stage	40
Figure 4-16 Generic flowsheet for application of pyroprocessing to pebble-type fuels. Taken from [26]	44
Figure 5-1 Baseline graphite case cost split.....	46
Figure 5-2 Similarity between compact/ pebble fabrication.....	49
Figure 7-1 Major activities in a Once-Through prismatic fuel cycle with timeline	57
Figure 7-2 Major activities in a continuous recycle fuel cycle with timeline.....	59
Figure 7-3 Historical data of Beryllium, Yttrium and Zirconium	63
Figure 8-1 LCOF distribution across different Once-Through prismatic reactor concepts [fuel block single use]	65
Figure 8-2 LCOF distribution across different Once-Through prismatic reactor concepts w/wo fuel block recycling.....	66
Figure 8-3 Sensitivity analysis of LCOF components for different OT prismatic reactor concepts	67
Figure 8-4 Histogram and cumulative distribution function (CDF) of LCOF for different OT prismatic reactor concepts. The blue histograms show the frequency distribution of LCOF outcomes, while the red curves represent cumulative probabilities, providing insights into the likelihood of achieving specific cost targets.	69
Figure 8-5 LCOF distribution across different Once-through pebble-bed reactor concepts	71

Figure 8-6 Sensitivity analysis of LCOF components for different Once-Through Pebble bed reactor concepts	72
Figure 8-7 Histogram and cumulative distribution function (CDF) of LCOF for different OT Pebble-bed reactor concepts	73
Figure 8-8 Disposal contribution to LCOF with and without deconsolidation for deep borehole	76
Figure 8-9 Disposal contribution to LCOF with and without deconsolidation for disposal in geological repository	76
Figure 8-10 LCOF distribution for standalone stage-2 reactor concepts	78
Figure 8-11 Sensitivity analysis for continuous recycle prismatic concepts	79
Figure 8-12 LCOF Probability distributions for continuous recycle prismatic reactor Concepts (Stage-2 microreactor only).	80
Figure 8-13 LCOF Distribution Across Combined Stage-1 and Stage-2 Reactor Concepts	82
Figure 8-14 Sensitivity Analysis of LCOF for Combined SFR + Microreactor Prismatic Reactor Concepts	83
Figure 8-15 LCOF probability distributions for continuous recycle prismatic reactor concepts.	84
Figure 8-16 LCOF distribution across continuous recycle pebble reactor concepts (microreactor Only)	86
Figure 8-17 Sensitivity analysis of LCOF for continuous recycle pebble concepts (microreactor Only)	87
Figure 8-18 LCOF probability distributions for pebble bed continuous recycle concepts. The blue histograms depict the frequency of LCOF outcomes, while the red curves represent the cumulative probability, highlighting the likelihood of achieving specific cost targets.	88
Figure 8-19 LCOF distribution across combined SFR + Microreactor pebble-bed reactor concepts	90
Figure 8-20 Sensitivity analysis of LCOF for combined SFR + microreactor pebble reactor concepts	91
Figure 8-21: LCOF probability distributions for continuous recycle prismatic reactor concepts.	92

1 Scope and Objective

Nuclear batteries are a special category of microreactors that support plug-and-play capability. These are envisaged to be factory assembled, factory fuelled, and transported by road by fitting into ISO standard shipping containers [1]. The development of nuclear batteries is gaining traction, driven by the need to address energy challenges in areas with limited power infrastructure. As an example, Project Pele, launched by the U.S. Department of Defense, aims to develop a mobile microreactor to reduce logistical challenges and reliance on diesel in remote or forward-operating bases [5]. There are also use cases for remote applications like Alaska, where existing electricity prices are expensive [6].

The HTGR-based microreactors represent a promising design for the next generation of commercial microreactors in this power range and size limitations. However, they face considerable challenges related to the use of graphite as a moderator, which results in low core power density and unfavorable properties under irradiation. These challenges have motivated studies to explore two-phase composite moderators using beryllium and hydride-containing moderating phases entrained within a stable ceramic matrix. It is demonstrated that such composite structures can produce advanced moderators with enhanced neutronic performance and greater stability compared to graphite [2].

Under the Department of Energy's ONWARDS program [3], Dr. Nick Brown's research group at the University of Tennessee, Knoxville, has developed point designs for microreactors employing composite moderators in prismatic and pebble-bed configurations. These designs incorporate high-assay low-enriched uranium (HALEU) TRISO fuel with uranium nitride (UN) kernels and utilize composite moderators composed of a magnesium oxide (MgO) matrix entraining either a hydride or beryllium based moderator. Preliminary results indicate that these composite moderator systems can reduce waste volume by a factor of ten compared to conventional graphite designs.

However, adopting these new moderator systems has significant implications for both the front and back ends of the nuclear fuel cycle. On the front end, the reliance on HALEU increases enrichment costs, while modifications to TRISO fuel fabrication processes and the introduction of novel moderator materials create new complexities. On the back end, the altered spent fuel characteristics may necessitate different interim storage and disposal strategies and could affect reprocessing steps where applicable. Consequently, the overall fuel-cycle costs for reactors using composite moderators may differ substantially from those of graphite-moderated systems. Demonstrating economic viability—by accounting the cost of different enrichment and potential manufacturing challenges against improved reactor performance and waste reduction—is therefore essential if these advanced moderator concepts are to gain widespread market acceptance.

Against this backdrop, this thesis performs a techno-economic analysis of these microreactor fuels using composite moderators concepts. Both prismatic and pebble-bed HTGR microreactor designs are examined under once-through and continuous-recycle fuel cycles. The principal aim is to see how the introduction of composite moderators might affect the economics of microreactors.

Primary Research Questions

1. How do the front-end and back-end fuel cycle costs of composite moderator-based microreactors compare to traditional graphite moderated microreactors across both once-through and continuous-recycle strategies?
2. Which advanced moderator materials—beryllium-based (Be, BeO) or hydride-based (ZrH, YH)—offer the most promising economic performance under different reactor configurations (prismatic vs. pebble-bed)?
3. To what extent can continuous recycle and deconsolidation strategies mitigate back-end disposal costs and enhance the overall economic viability of these microreactors?
4. What are the key cost drivers and sensitivities for microreactors adopting composite moderators, and how do they compare to those of the baseline graphite design?

The study uses the Levelized Cost of Fuel (LCOF) as the principal metric to quantify these questions. By summing all front-end (e.g., enrichment, fabrication) and back-end (e.g., spent fuel storage, geological disposal, reprocessing) costs, then annualizing and normalizing over total electricity production, the LCOF enables direct comparisons among different reactor designs. Although it cannot capture every nuance of the electricity market or regulatory conditions, levelized cost remains the industry's preferred yardstick for comparing alternative nuclear fuel-cycle strategies.

This report is organized as follows: Chapter 2 introduces prismatic and pebble-bed configurations, details the properties of composite moderator concepts, and specifies TRISO fuel characteristics for each design variant. These technical parameters form the basis for subsequent economic evaluation.

An analytical framework is developed in Chapter 3, outlining a general methodology for LCOF calculation. This includes approaches for deterministic cost estimation, sensitivity analysis, Monte Carlo simulation methods, and mathematical models for both standalone and combined cycle analysis.

Chapter 4 examines the front-end as well as back-end activities for both the Once-through cycle and continuous recycle fuel cycles. This chapter also establishes cost data sources for materials and fuel cycle activities.

A detailed examination of fabrication costs follows in Chapter 5. This chapter develops models for TRISO particle production, fuel compact and pebble manufacturing, and quality assurance requirements. It also establishes cost-scaling relationships.

Chapter 6 addresses the spent nuclear fuel disposal from the microreactors. It establishes methodologies for assessing interim storage requirements, evaluating deep borehole disposal options, and analyzing geological repository considerations. The chapter develops cost equivalency assessments to enable comparison across different disposal strategies and concludes with a discussion on deconsolidation along with a methodology to quantify its benefits.

These analyses are integrated in Chapter 7, which establishes LCOF calculation methodology across multiple scenarios. This includes the evaluation of once-through cycle configurations and continuous recycle scenarios (Both stand-alone and combined fast reactor with microreactor analysis). The chapter also presents the calculations for cost sensitivities and Montecarlo analysis to provide a complete economic picture.

Comprehensive results are presented in Chapter 8, providing detailed cost breakdowns by reactor type, sensitivity analysis findings, and Monte Carlo simulation outcomes. This chapter offers economic comparisons across designs and identifies key insights and recommendations for technology development.

The thesis concludes in Chapter 9 with a summary of major findings regarding economic viability, including this analysis' limitations. It also highlights critical areas for future research and technology development.

2 Reactor designs, moderator concepts and TRISO types considered for analysis

Detailed microreactor designs developed by Dr. Brown's team at the University of Tennessee–Knoxville (UTK) under the U.S. Department of Energy's ONWARDS program were leveraged for the present analysis. The overarching goal of the ONWARDS program was to reduce overall nuclear waste for once-through and continuous recycle scenarios [3]. Prismatic and pebble-bed microreactor point designs were generated using a baseline graphite moderator and advanced composite moderators. Parametric sweeps were performed for both once-through and continuous-recycle options to find the optimum combination of TRISO packing fraction, fuel pin pitch, and reflector thickness that maximizes discharge burnup while satisfying key microreactor size constraints. This section summarizes the microreactor point designs, followed by an introduction of the four composite moderator concepts used for this study.

2.1 High-temperature gas-cooled reactor point designs

Two HTGR microreactor concepts—prismatic cores and pebble-bed cores—were developed by the UTK team. Both of these concepts incorporated TRISO fuels embedded in composite moderators. In each case, design variations were created for:

1. Once-through cycles, where spent fuel is disposed of directly and
2. Continuous-recycle fuel cycles, where fissile materials are recovered and reused.

2.1.1 The prismatic microreactor point design

For all prismatic microreactor calculations, the total power was set to 10MW_{th} . The microreactor design considers both a conventional HTGR fuel form, UCO TRISO encapsulated in a graphite matrix, and Fully Ceramic Microencapsulated (FCM) fuel, which is UN TRISO particles encapsulated in MgO.

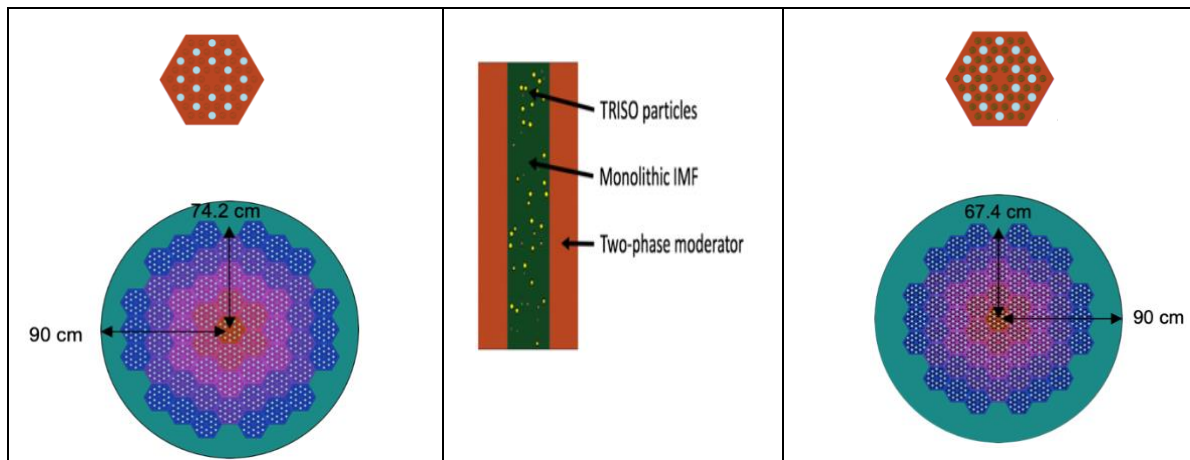


Figure 2-1 Radial (left) cross cut of the Once-through prismatic microreactor. Prismatic microreactor compact assembly (center). Radial (left) cross cut of the continuous recycle prismatic microreactor. Taken from [7]. Figures are not to scale.

Figure 2-1 shows a radial cross-section (left), an axial cross-section (middle), and the fuel assembly (right) of the prismatic microreactor. The radius from the center of the core to the outer edge of the reflector is 90 cm, and the total height of the microreactor is 395.5 cm, which includes a 79.1 cm upper reflector and lower reflector made of composite moderator material.

A concise summary of core features for the once-through prismatic variants (including discharge burnup, cycle length, and moderator mass) is given in Table 2-1, while the continuous-recycle prismatic configurations are detailed in Table 2-2. These tables also document the relevant fuel-cycle mass balances, in-core residence times, and masses of MgO and entrained moderator phases for each scenario.

Table 2-1 Once-Through prismatic reactor design specification

Reactor concept	Graphite	MgO-BeO	MgO-Be	MgO-YH _{x=1.9}	MgO-ZrH _{x=1.9}
Discharge burnup (GW-d/MT)	51.72	59.3	74.2	75.9	94.2
Cycle length (years)	3.48	5.7	7.1	32.9	27.2
Number of compacts	110880	110880	110880	110880	110880
Number of fuel blocks	2640	2640	2640	2640	2640
Number TRISO particles	82051200	82051200	82051200	369230400	246153600
Mass of TRISO particles (kg)	358	453	453	2039	1360
Volume of TRISO particles (m ³)	0.07	0.07	0.07	0.30	0.20
Total MgO mass (kg) in core (Compact + Fuel block)	NA	10132.5	8461.4	12612.6	10607.7
Total MgO mass in compacts (kg)	1026.1 (Graphite)	2160.7	2159.9	1320.4	1680.5
Total MgO mass in fuel blocks (kg)	6308.7 (Graphite)	7971.8	6301.5	11292.2	8927.2
Total entrained moderator mass (kg) BeO/Be/YH/ZrH in core	NA	4483.2	2170.9	2371.2	2481.9
Spent Fuel Values					
Fuel mass for final disposal (kg)	8832	15067	11027	17021	14457
Fuel volume for final disposal (m ³)	4.38	4.38	3.60	4.38	3.60
Photons [photon/s]					
	Graphite	MgOBeO	MgOBe	MgOYH _{x=1.9}	MgOZrH _{x=1.9}
5 Years after core unload	1.70E+15	2.82E+15	3.56E+15	1.11E+16	9.89E+15
20 Years after core unload	8.84E+14	1.43E+15	1.78E+15	6.36E+15	5.53E+15
Spontaneous Fissions [sf/s]					
	Graphite	MgOBeO	MgOBe	MgOYH _{x=1.9}	MgOZrH _{x=1.9}
5 Years after core unload	1.03E+06	4.77E+06	1.02E+07	8.05E+07	7.50E+07
20 Years after core unload	6.72E+05	2.85E+06	5.96E+06	4.65E+07	4.32E+07
Decay Heat [Watts]					
	Graphite	MgOBeO	MgOBe	MgOYH _{x=1.9}	MgOZrH _{x=1.9}
5 Years after core unload	525	836	1040	3636	3148
20 Years after core unload	299	499	627	2511	2122

Table 2-2 Continuous recycle prismatic reactor design specification

Reactor concept	MgO-BeO	MgO-Be	MgO-YH _{x=1.9}	MgO-ZrH _{x=1.9}
Cycle Length (years)	31.1	31.8	3.7	4.0
Discharge burnup (GWD/MT)	86.5	88.5	52.1	111.3
Number of compacts	110880	110880	110880	110880
Number of fuel blocks	2640	2640	2640	2640
Total MgO mass (kg) in core (Compact + Fuel block)	5977.5	5976.3	14710.8	11207.0
Total MgO mass in compacts (kg)	1200.3	1200.4	2159.7	2280.3
Total MgO mass in fuel blocks (kg)	4777.2	4775.9	12551.1	8926.7
Total entrained moderator mass (kg) BeO/Be/YH/ZrH in core	2686.6	1601.4	2635.3	2490.6
Fresh fuel composition front end				
Plutonium (kg)	1064.5	1063.5	212.5	106.4
Minor Actinides (kg)	119.5	119.4	23.9	11.9
Spent fuel composition back end				
Recycled Uranium (kg)	7.7	8.0	0.2	0.1
Plutonium (kg)	908.2	904.7	197.7	92.7
Minor Actinides (kg)	150.7	150.4	23.4	10.7
Fission Products (kg)	107.8	107.7	12.7	13.5
Number of micro reactors per SFR				
Plutonium produced by SFR for stage-2	196.1 kg-Pu			
Plutonium required for stage-2	1064.5- 908.2 =156.3	1063.5- 904.7 =158.8	212.5-197.7 = 14.8	106.4-92.7 = 13.7
Number of micro reactors per SFR	196.1/156.3 =1.26	196.1/158.8 =1.24	196.1/14.8 =13.3	196.1/13.7 =14.3

2.1.2 The pebble bed microreactor point design

The pebble bed microreactor point design is illustrated in Figure 2-2. The size constraints of the pebble bed microreactor limit the moderating material available and make the IMF concepts a particularly favorable option for the compact nature of a microreactor. As with the prismatic concepts, the thermal power was set to 10MW_{th}. The upper and lower reflector height was also taken from the prismatic design and used in developing the initial pebble bed core.

Depletion calculations employed a linear reactivity discharge model with an eight-batch fuel management scheme to estimate discharge burnup. The optimized parameters, including discharge burnup, fueling rates, and moderator volumes, are summarized for the once-through pebble-bed variants in Table 2-3, while the continuous-recycle pebble-bed cases are shown in Table 2-4. As in the prismatic analysis, these appendices include details on fuel-cycle mass balances, MgO usage, and entrained moderator quantities for both once-through and continuous-recycle scenarios.

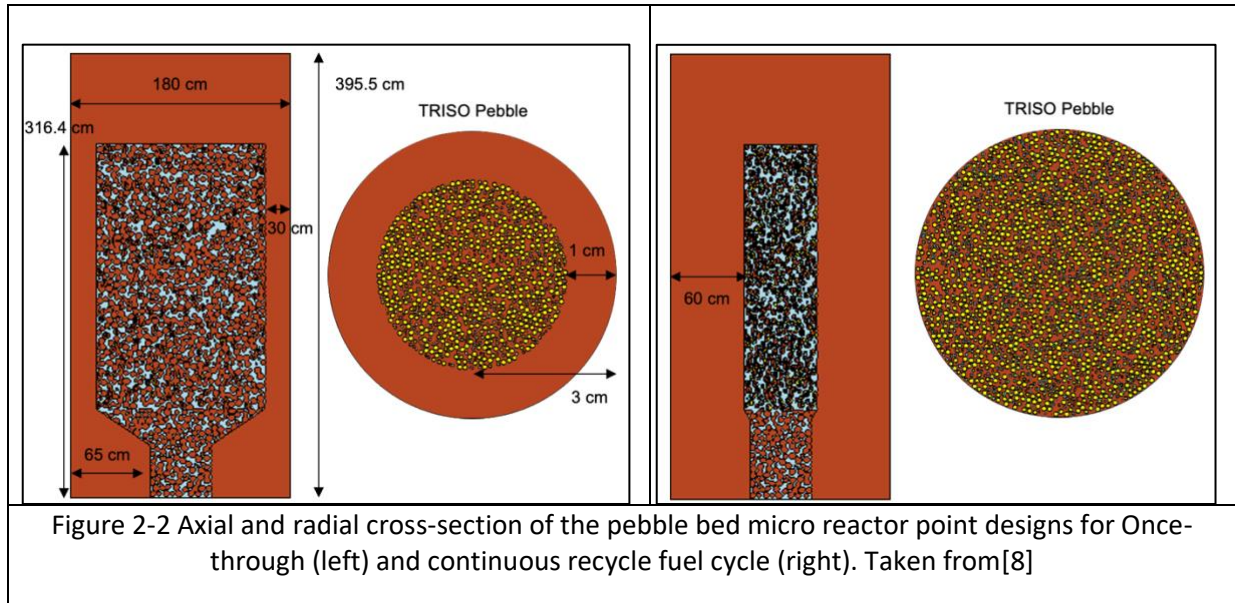


Table 2-3 Once-Through pebble bed reactor design specification

Reactor concept	MgO-BeO	MgO-Be	MgO-YH _{x=1.9}	MgO-ZrH _{x=1.9}
Cycle length (years)	9.6	16.0	31.0	30.5
Discharge burnup (GWD/MT)	85.1	105.6	106.7	140.4
Number Pebbles	4342	5911	25733	19702
Number of TRISO particles	213918786	213918786	304752448	304752448
Total MgO mass (kg) in core	3685.3	4966.3	8931.3	6898.8
Total entrained moderator mass (kg) BeO/Be/YH/ZrH in core	2072.5	1710.9	1875.4	1917.9
Mass of TRISO particles (kg)	530	719	1329	1024
Volume of TRISO particles (m ³)	0.08	0.11	0.20	0.15
Spent Fuel Values				
Fuel mass for final disposal	5642	7330	12127	9843
Fuel volume for final disposal (m ³)	1.79	2.42	3.13	2.42
Photons [photon/s]				
	MgOBeO	MgOBe	MgOYH _{x=1.9}	MgOZrH _{x=1.9}
5 Years after core unload	5.00E+15	7.74E+15	1.14E+16	1.19E+16
20 Years after core unload	2.36E+15	3.73E+15	6.13E+15	6.10E+15
Spontaneous Fssions [sf/s]				
	MgOBeO	MgOBe	MgOYH _{x=1.9}	MgOZrH _{x=1.9}
5 Years after core unload	2.31E+07	8.59E+07	1.17E+08	2.21E+08
20 Years after core unload	1.33E+07	4.90E+07	6.72E+07	1.27E+08
Decay Heat [Watts]				
	MgOBeO	MgOBe	MgOYH _{x=1.9}	MgOZrH _{x=1.9}
5 Years after core unload	1429	2307	3648	3782
20 Years after core unload	863	1457	2450	2472

Table 2-4 Continuous recycle pebble bed reactor design specification

Reactor concept	MgO-BeO	MgO-Be	MgO-YH _{x=1.9}	MgO-ZrH _{x=1.9}
Cycle length (years)	99.9	99.0	69.1	75.5
Discharge burnup (GWD/MT)	415.3	411.6	287.5	314.1
Number of pebbles	3619	3619	3619	3619
Total MgO mass (kg)	601.5	601.6	852.0	852.1
Total entrained moderator mass (kg) BeO/Be/YH/ZrH in core	338.3	201.7	178.9	237.8
Fresh fuel composition				
Plutonium (kg)	711.0	710.7	710.9	710.5
Minor Actinides (kg)	79.8	79.8	79.8	79.8
Spent fuel composition				
Recycled Uranium (kg)	24.0	24.01	15.0	17.03
Plutonium (kg)	366.8	364.1	458.4	438.32
Minor Actinides (kg)	55.5	54.9	73.9	70.1
Fission Products (kg)	335.5	338.3	234.3	255.8
Number of micro reactors per SFR				
Plutonium produced by SFR for stage-2	196.1			
Plutonium required for stage-2	=711-366.8 =344.2	=710.7-364.1 =346.6	=710.9-458.4 =252.5	=710.5-438.32 =272.18
Number of micro reactors per SFR	=196.1/344.2 = 0.57	=196.1/346.6 = 0.57	=196.1/252.5 = 0.77	=196.1/272.18 = 0.72

2.2 Composite moderators considered for analysis

In the case of composite moderators, a highly moderating phase is entrained within a continuous and environmentally stable matrix [8]. The conceptual architecture for such a composite and the desired attributes for a composite moderator are shown in Figure 2-3. Potential enabling attributes of these advanced composite moderators as compared to nuclear graphite are decreased core size, decreased uranium loading (for the same power level and enrichment), and less drastic property changes under irradiation.

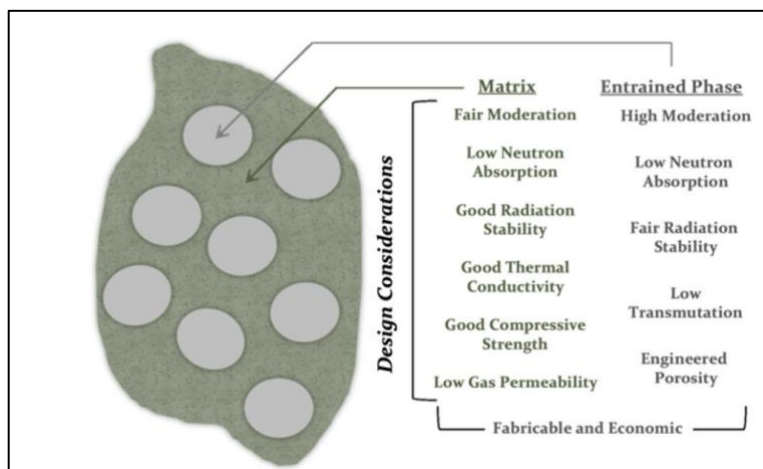


Figure 2-3 Composite moderator concept and notional properties of the structural matrix and entrained moderating phase. Taken from [8]

Table 2-5 lists the moderating materials, host matrix, and entrained phase volume fractions considered in this analysis for the different reactor concepts.

Composite moderators composed of a radiation and chemically stable magnesia (MgO) host matrix with an entrained beryllium [3] or hydride moderating phase [9] are considered.

Table 2-5 Volume fraction of moderating materials for prismatic and pebble bed concepts [10].

Reactor concepts	Host material	Moderating material
MgO-BeO	MgO-60% by volume	BeO-40% by volume
MgO-Be	MgO-60% by volume	Be-40% by volume
MgO-YH	MgO-85% by volume	YH _{x=1.9} -15% by volume
MgO-ZrH	MgO-85% by volume	ZrH _{x=1.9} -15% by volume

2.3 TRISO kernels used for study

Two types of TRISO were considered for this study: Uranium oxy-carbide (UCO) fuel kernel and uranium nitride (UN) fuel kernel. UCO TRISO was used as the baseline fuel, whereas UN TRISO was used in other variants because of the higher kernel density of UN fuel. Table 2-6 summarizes the properties of both types of TRISO particles.

Table 2-6 Features of the TRISO particles for the state-of-the-art and IMF concepts

Parameter		Graphite baseline	IMF concept	Units
Kernel				
	Material	UCO (UC _{0.5} O _{1.5})	UN	-
	Density	10.9	14.3	g/cm ³
	Outer radius	0.0425	0.0425	cm
Buffer layer				
	Material	Porous graphite		-
	Density	1.0		g/cm ³
	Outer radius	0.0475		cm
Inner PyC layer				
	Material	Carbon		-
	Density	1.9		g/cm ³
	Outer radius	0.0510		cm
SiC layer				
	Material	Silicon carbide		-
	Density	3.2		g/cm ³
	Outer radius	0.0545		cm
Outer PyC layer				
	Material	Carbon		-
	Density	1.9		g/cm ³
	Outer radius	0.0580		cm

3 Generalized methodology for LCOF analysis

This chapter establishes a generalized methodology to evaluate the Levelized Cost of Fuel (LCOF) for various microreactor configurations operating under once-through and continuous-recycle fuel cycles. This section first introduces a standalone approach in which a single reactor is modeled. The discussion then moves to a multi-stage analysis, wherein a Stage-1 reactor's spent fuel is reused in multiple Stage-2 units, thus capturing the plutonium and Minor Actinides (MA) interdependencies. Finally, a generalized methodology for sensitivity analysis and Monte Carlo simulation is also described. The methodology presented here serves as the framework for economic analysis carried out in the subsequent chapters.

3.1 Deterministic estimation: LCOF cost drivers

Methodology 1: For Once-Through and standalone stage-2 analysis for continuous recycle fuel cycle. In the first approach, all major fuel cycle activities are mapped to a chronological timeline before the initial fuel load (T_l) and after the final unload event (T_u). Activities taking place before T_l are often referred to as front-end costs, while those after T_u are referred to as back-end costs. Once each activity is identified, its cost is assessed and aligned with the appropriate time interval.

These costs are then discounted to a single reference point (commonly T_l) using a present value (PV) calculation. After deriving the PV of all activities, these values are annualized across the operational period of the reactor. A capital recovery factor translates each PV into an annualized cost. Finally, dividing by the reactor's annual electricity production yields each activity's contribution to the Levelized fuel cost (LCOF). Summing those contributions provides the total LCOF for the standalone scenario, thus offering a straightforward measure of how all front-end and back-end expenses combine over the reactor's life. The framework, as discussed, is shown schematically in Figure 3-1.

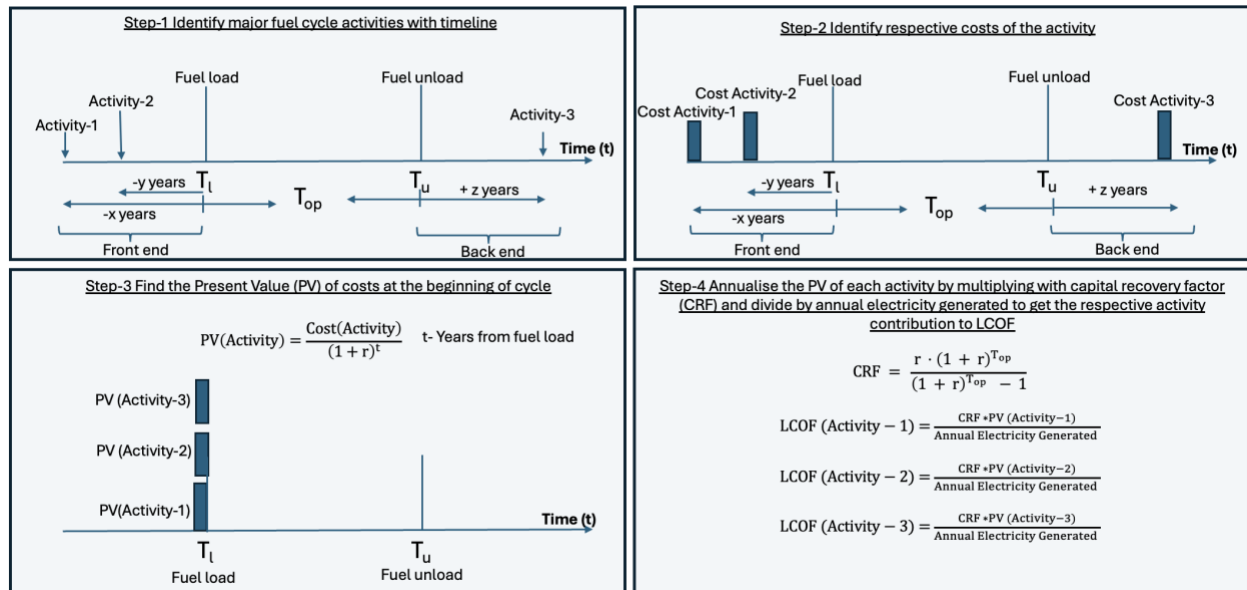


Figure 3-1 A generalised four-step framework to calculate the LCOF for a standalone reactor

Methodology 2: Combined stage-1 and stage-2 analysis for continuous recycle fuel cycle

In the combined cycle approach, a stage-1 reactor's spent fuel is directed to multiple stage-2 reactors. Activities for stage 1 (e.g., fuel fabrication, reactor operation, and discharge) are tracked much like the standalone case but are now linked to subsequent stage 2 processes. The timeline for stage-2 activities typically begins once the stage 1 reactor's spent fuel is reprocessed for reuse. Costs for these stage-2 tasks are again discounted to a common reference time. To calculate LCOF for the complex cycles, a modified version of the levelized cost of fuel expression is adapted from continuous recycle models developed by Ganda et al[11].

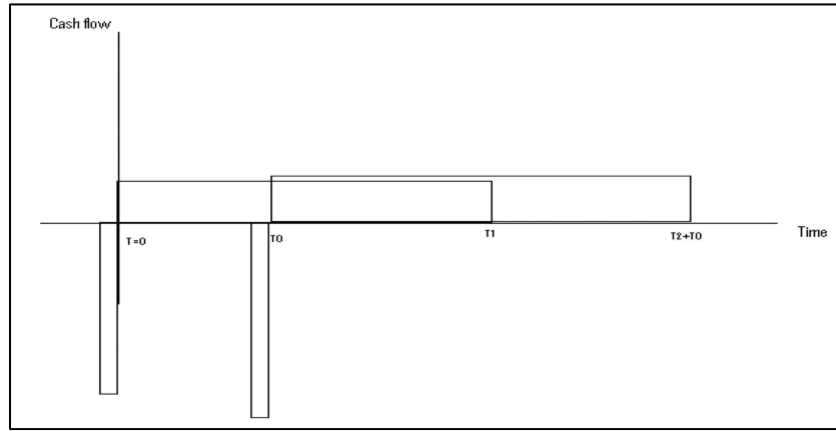


Figure 3-2 Fuel cycle considered by Ganda et al [11]

$$\begin{aligned}
 &NPV_1 + NPV_2 e^{-r T_0} \\
 &= C_{\text{combined}} \\
 &\times E_1 \left[\int_0^{T_0} e^{-r t} dt + (1 + \alpha) \int_{T_0}^{T_{\text{plant1}}} e^{-r t} dt + \alpha \int_{T_{\text{plant1}}}^{T_0 + T_{\text{plant2}}} e^{-r t} dt \right]
 \end{aligned}$$

Where:

r : discount rate,

T_{plant1} : reactor operating time for stage-1

T_{plant2} : reactor operating time for stage-2

T_0 : Time gap between stage-2 and stage-1

E_1 : Annual electricity generated by stage-1 reactor

E_2 : Annual electricity generated by stage-2 reactors

α = Ratio of electricity units generated in stage-2 to electricity units generated in stage-1 (E_2/E_1)

The two-stage equation, as derived by Ganda et al, differs from the present formulation in two principal ways. First, this study has no operational overlap between the Stage-1 and Stage-2 reactors. Thus, the overlap region—where both cycles generate electricity simultaneously—is removed from the LCOF calculations (middle term in RHS). Second, because a single Stage-1 reactor may feed multiple Stage-2 microreactors, the net present value (NPV) for Stage-2 (i.e., NPV_2) as well as the Stage-2 power generation term are each multiplied by the number of microreactors. This adjustment ensures that both costs and

electricity outputs are scaled appropriately. The revised expression for the combined Levelized Cost of Fuel (LCOF), reflecting these modifications, is shown below.

$$C_{\text{combined}} (\text{LCOF}) = r \cdot \frac{PV_1 + N \cdot PV_2 \cdot e^{-rT_2}}{E_1 \cdot (1 - e^{-rT_1}) + N \cdot E_2 \cdot (e^{-rT_2} - e^{-rT_3})}$$

The discussed methodology is shown schematically in Figure 3-3.

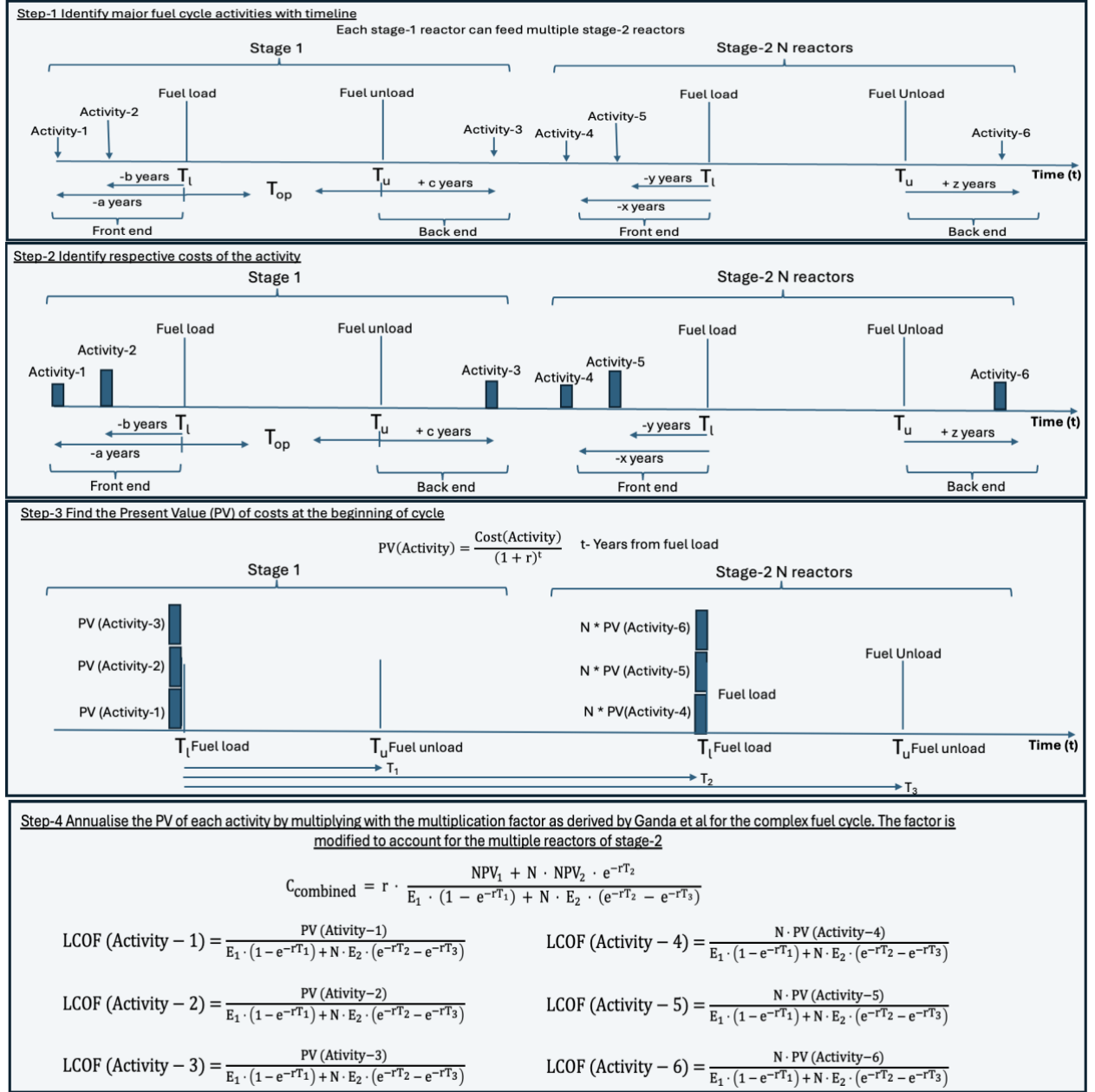


Figure 3-3 A generalized four-step framework to calculate the LCOF for a combined (stage-1 + stage-2) continuous recycle configuration.

3.2 Sensitivity analysis

Once a baseline LCOF has been calculated for either the standalone or the combined-reactor framework, a sensitivity analysis is performed to identify parameters exerting the greatest influence on the final cost. Typically, each parameter is varied by a fixed percentage (e.g.,

$\pm 20\%$) while all other parameters remain at nominal values. By recalculating the LCOF under these variations, the relative significance of each parameter is established, thereby highlighting critical cost drivers that merit further investigation or potential optimization.

3.3 Monte Carlo analysis

A Monte Carlo approach employs probability distributions for variables to capture deeper uncertainties that may not be fully explored through simple parameter adjustments. Rather than specifying a single value or a ± 20 percent range, each parameter is given a continuous distribution based on historical data or expert judgment. In each iteration, the model samples a random draw from every parameter's distribution, calculates the LCOF under that specific set of conditions, and records the result. Repeating this process a large number of times generates a probability distribution of LCOF outcomes. Examining the mean, standard deviation, range, and full histogram of these results offers insights into the probability that the LCOF will fall below (or exceed) certain thresholds. In so doing, Monte Carlo analysis provides a thorough assessment of future economic risks and opportunities.

The generalized methodology outlined here—comprising both a standalone viewpoint and a multi-stage or continuous recycle viewpoint explained in terms of activity 1, activity 2, etc—forms the backbone of the economic evaluations in later chapters. The next section begins the application of this framework to once-through and continuous recycle fuel cycles by detailing the major front-end and back-end processes along with the respective cost estimates.

4 Fuel cycle major activities and cost considerations

This chapter identifies the key processes and associated costs in the nuclear fuel cycle, focusing first on the once-through scenario and subsequently introducing a continuous recycle scenario. Each subsection provides a concise overview of the technical steps and cost estimates based on current literature.

4.1 Once-Through cycle

Figure 4-1 provides the primary reference for this fuel cycle in which the microreactor fuel undergoes a single pass through the reactor and is directly disposed of without any form of recycling. The subsequent sub-sections present a concise description of each activity.

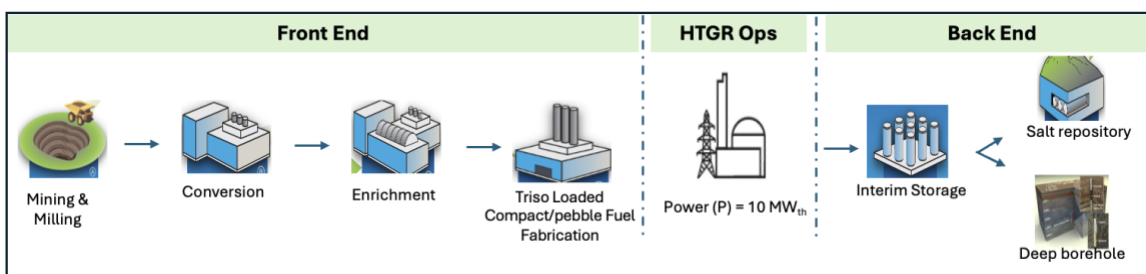


Figure 4-1 Once-through fuel cycle diagram showing major steps.

Once-Through Front-end processes

The once-through front-end processes encompass all the steps required to prepare nuclear fuel for loading into the reactor. This includes uranium ore mining and milling, conversion, enrichment, and fuel fabrication.

4.1.1 Mining and Milling

Uranium ore is the starting material for all once-through fuel cycles. The cost of uranium is influenced by a combination of factors affecting supply and demand. Online websites like Ux Consulting continually update market data for uranium spot pricing. This analysis uses a mining and milling cost of \$160 per kg [12].

4.1.2 Conversion

The mined natural uranium oxide concentrate (U_3O_8) undergoes purification and conversion into uranium hexafluoride (UF_6), ready for use as feedstock at uranium enrichment facilities. This process includes receiving feed material, conducting chemical conversion, and shipping the final UF_6 in cylinders. Similar to mining and milling, spot prices are maintained by various online sources. The current work uses a conversion cost of \$40/kg [12].

4.1.3 Enrichment

The uranium hexafluoride (UF_6) produced from the conversion facility is enriched to increase the uranium-235 content from its natural level of 0.71% to 19.9%. This process involves

receiving UF_6 in cylinders, evaporating it, enriching the gas-phase uranium, and subsequently condensing the enriched and depleted UF_6 solids. The enriched product is then shipped in cylinders to fuel fabrication facilities. Enrichment cost is typically measured in terms of Separative Work Unit (SWU), which is typically used to quantify the effort required in the uranium enrichment process. An enrichment cost of \$138 per SWU [12] is adopted for this work.

4.1.4 Fuel fabrication process

TRISO fuel particles are produced through a carefully controlled multi-step manufacturing process. The fuel kernels are synthesized using a gel-precipitation technique, which can be conducted via internal, external, or total gelation methods. Following kernel preparation, multiple protective layers, including pyrolytic carbon and silicon carbide, are applied using Chemical Vapor Deposition (CVD) in a high-temperature coater [13]. These layers encapsulate the kernel, providing mechanical integrity and containment of fission products. Finally, the coated fuel particles are mixed with matrix materials, such as graphite filler and binder, and then pressed and heat-treated to form the final fuel element, ready for use in a nuclear reactor.

Reference cost. The TRISO particle fuel production process, together with the ‘embedding in graphite’ step, is very complex compared to LWR-UOX fuel fabrication. There are a lot of gaps in the economic information for this type of fuel. There is no single process for all particle fuels and many processes are proprietary [13]. The FCRD cost basis document [13] refers to multiple sources for the TRISO fuel fabrication costs ranging in value from \$2000 – 30000/ kgHM. A nominal price of \$10000/ kgHM [13] was considered for the analysis for baseline estimates, with the variation in cost to be factored in the sensitivity and Monte Carlo analysis.

Since the different microreactor concepts considered under the scope of this study use different types of TRISO and different materials for fuel fabrication, each of the sub-processes involved with fuel fabrication is discussed in detail. This discussion will help to formulate the cost basis based on similarities with the established process.

4.1.4.1 Kernel fabrication

Figure 4-2 shows a generic TRISO fuel fabrication process. A sol-gel or similar fluidization process renders liquid spheres into hard solid spheres to get uniform spheres. A liquid solution such as uranyl nitrate hexahydrate (UNH) is produced from UF_6 . Uniform UNH solution drops of the desired size are formed and contacted with ammonia to form gel spheres (gel-precipitation process). These gel spheres are washed with water, dried to a low-density form, calcined to a medium-density form, and then sintered to a high-density microsphere ‘kernel’ [14].

The production of UN TRISO particles from UO TRISO particles can be subdivided into two distinct steps, as shown in Figure 4-3. Feedstock UO_3+C spheres produced using a sol-gel method are converted to $\text{UC}_x\text{N}_{1-x}$ by carbothermic reduction, occurring in two calcining steps followed by a nitriding step to form the final nitride product [14]. Figure 4-4 depicts the kernel evolution through the kernel fabrication steps.

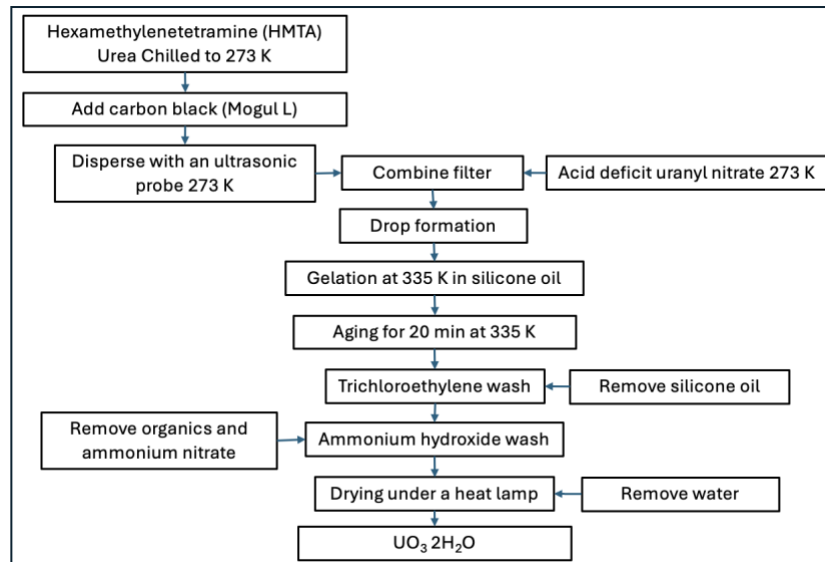


Figure 4-2 Block flow diagram of UO kernel fabrication process. Taken from [14]

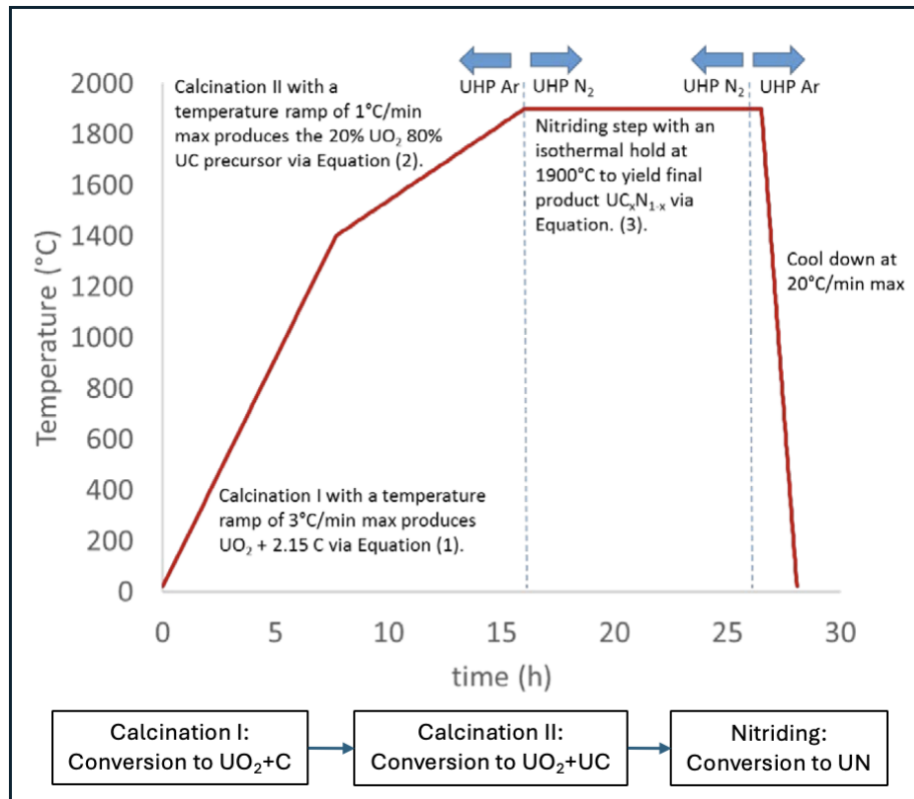


Figure 4-3 Block flow diagram of the UO₂ kernel to UN kernel fabrication process. Taken from [14]

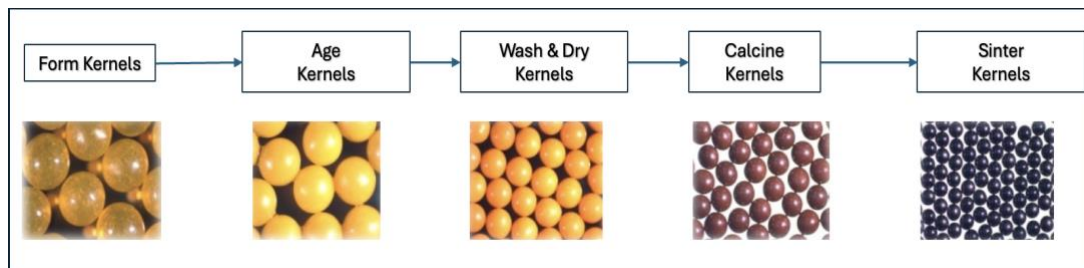


Figure 4-4 Major steps of UO₂ kernel fabrication. Taken from [15]

4.1.4.2 Coating Deposition

A typical flow diagram of the process used for coating deposition is shown in Figure 4-5. The four coating layers are deposited on kernels in a heated furnace (Figure 4-6) by chemical vapor deposition (CVD). Flowing gases in the furnace suspend the kernels to form a fluidized bed. Coating gases are chosen to decompose and deposit certain constituents of theirs on the kernels' surfaces at temperatures up to 1600°C.

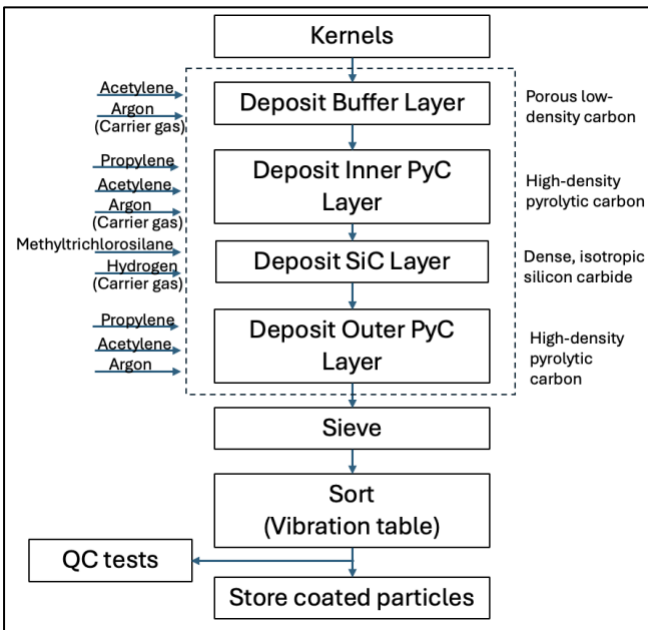


Figure 4-5 Major steps during coating process. Taken from [16]

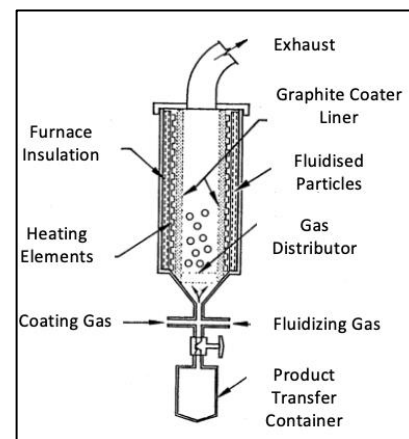


Figure 4-6 Schematic of the GA coater (Noren 1991) used for NPR fuel. Taken from [17]

There are two primary fuel forms used for the different reactor concepts: The prismatic concept, in which a fuel assembly or 'block' is in the shape of a hexagonal cylinder with holes drilled for the flow of the gas coolant. These hexagonal blocks are stacked and arrayed inside a machined graphite core. Each prismatic block has smaller graphite-suitable circular cylinders or 'compacts', laden with TRISO particles and embedded in other vertical holes in the block. The other fuel assembly form is that of a billiard-ball-sized graphite sphere or "pebble" with the TRISO particles embedded within it.

4.1.4.3 Fabrication of the Fuel compacts

Coated TRISO fuel particles are fabricated into fuel compacts by dispersing them in a graphite matrix and sintering them. The process begins by overcoating the TRISO particles with a graphitic matrix material (Figure 4-7). The overcoated particles are then warm-pressed into a compact shape using metallic dies. These compacts are heated to around 800°C in an inert nitrogen atmosphere to carbonize the phenolic resin binder [16]. Subsequently, they undergo heat treatment at 1800°C in a vacuum annealing furnace to remove impurities and degas the compacts, ensuring they are suitable for use in the reactor. The formation of cylindrical compacts is homogenous, with no fuel-free regions. A finished cylindrical compact is shown in Figure 4-8. The designs considered for analysis assume that compacts containing the fuel

particles use only MgO as the base material, whereas fuel blocks are composed of composite moderators (MgO + Entrained moderator).

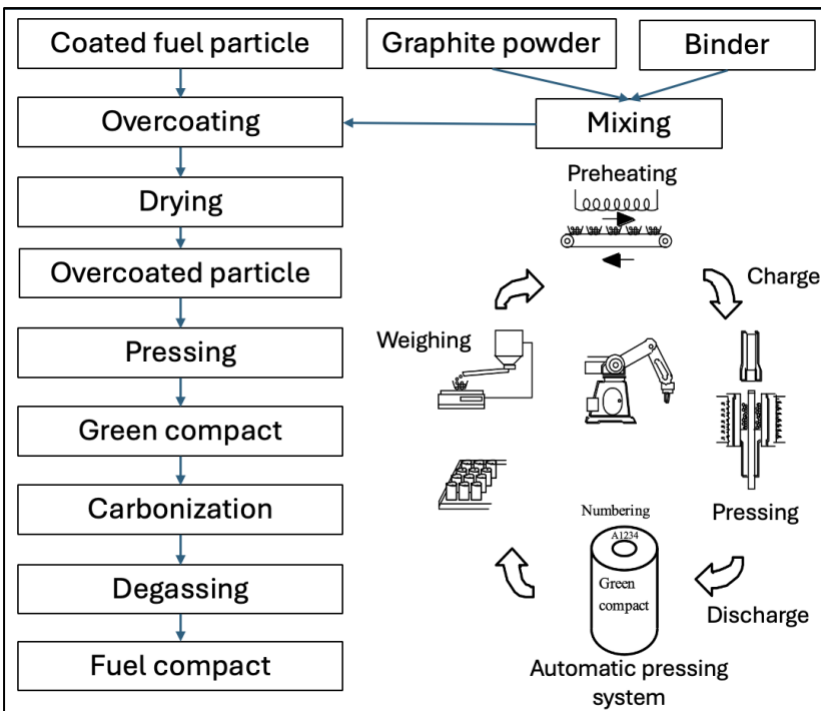


Figure 4-7 Summary of fabrication process for fuel compacts. Taken from [16]



Figure 4-8 Complete cylindrical compact. Taken from [18]

4.1.4.4 Fabrication of the Fuel pebbles

The first step involves coating the TRISO particles with the resinated graphite powder to a coating thickness needed to acquire the desired packing fraction once compacted (Figure 4-9). The powder and particles are mixed at a certain ratio in a rotating drum, spinning sufficiently fast to fix the mixture to the drum walls [16]. An agitator's arm is then inserted to separate the mixture from the wall so it falls through a methanol mist provided by a jet nozzle. The methanol ensures proper adherence of the graphite powder to the particles and sufficient lubricant during compacting to allow the movement of particles into open spaces.

The next step incorporates the prepressed fuel sphere with a fuel-free zone. Spherical compacts have a central fuel region pre-formed and then incorporated with a layer of non-TRISO-containing graphite surrounding it. The lower half of the layer is first put into the compression chamber, the fuel region placed on top, and the rest of the graphite powder is fed into the top of the chamber to fill the rest of the mold. The filled mold is pressed at 300 MPa with little concern that TRISO particles will be damaged since the fuel region is pre-formed. The spherical shape requires quasi-isostatic compression. A finished pebble is shown in Figure 4-10. For the microreactors considered in the analysis, the starting material is the composite mixture of MgO and entrained moderator. The rest of the manufacturing steps are envisaged to be similar to baseline graphite case.

Based on this background information, the fabrication costs for the advanced moderator concepts will be estimated in Chapter 5.

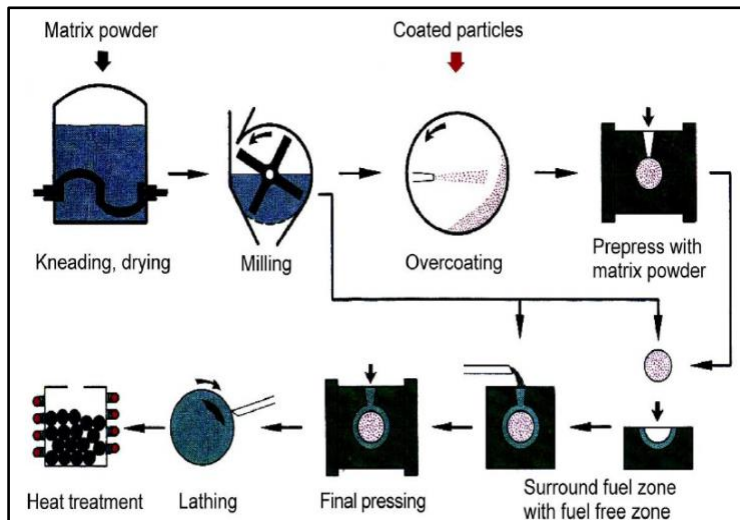


Figure 4-9 Pebble fuel manufacture. Taken from [16]



Figure 4-10 Completed spherical compact and furnace mold. Taken from [19]

Once-through back-end processes

The fuel spent is typically stored in a cooling pond for five years. Upon leaving the cooling pond, the spent fuel is stored above-ground in dry casks (interim storage), awaiting ultimate disposal (either in a geologic repository or deep borehole). In the next sections, these back-end processes are discussed with respect to the current state of the art and the associated costs.

4.1.4.5 Spent fuel pool

Spent nuclear fuel storage in a spent fuel pool is usually required in all open and closed fuel cycles. There are large safety and economic incentives to allow the radioactivity of SNF to decrease before transport, processing, or disposal. Upon reactor shutdown, SNF is intensely radioactive and generates large quantities of decay heat equal to about 6% of the reactor's power output. However, the radioactive decay heat decreases rapidly, reaching 0.5% in one week. Some advanced reactor designs (HTR-10, Xe-100) incorporate dry storage to store the SNF [20]. Nonetheless, all reactors store the fuel in the nuclear power plant (wet or dry storage) before moving the fuel to interim storage. The cost for this storage is generally included in the reactor capital and operating cost figures, so this charge will not be separately accounted for in this study.

4.1.4.6 Interim dry storage

Interim dry storage has become essential to nuclear waste management, addressing capacity issues, enhancing safety, reducing costs, and providing flexibility as the industry works towards long-term disposal solutions. The Multipurpose cask (MPC) (Figure 4-11) is a multi-purpose SNF storage device for fuel assemblies. The MPC is engineered as a cylindrical prismatic structure with square cross-section storage cavities (Figure 4-12). The number of storage locations depends on the type of fuel. Regardless of the storage cell count, the construction of the MPC is fundamentally the same; it is built as a honeycomb of cellular elements positioned within a circumscribing cylindrical canister shell [13].

The storage overpack is designed to provide the necessary neutron and gamma shielding to comply with the provisions of 10CFR72 for dry storage of SNF at an ISFSI. The overpack is constructed from steel and concrete, with long, proven histories of usage in nuclear applications. The overpack combines many desirable features of previously approved concrete and metal module designs. Since the interim storage casks are not designed to store the spent fuel from microreactors, it was assumed that any intact fuel assembly that falls within the geometric, thermal, and radiation shielding limits established for the design basis intact fuel assembly can be safely stored. Holtec International a leading provider of spent fuel storage and transportation solutions, published the Final Safety Analysis Report (FSAR) for the HI-STORM 100 Cask System [21], which was referred to identify the design basis specifications—including geometric, thermal, and radiological shielding criteria.

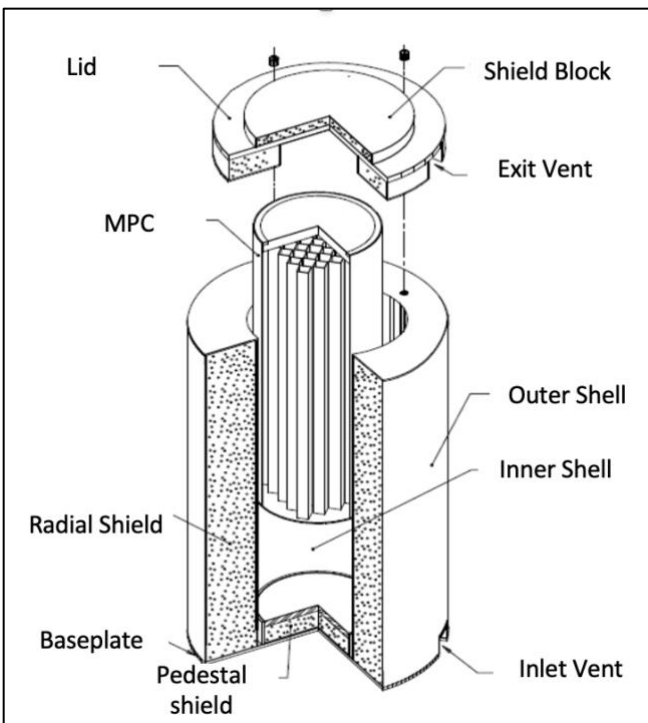


Figure 4-11 Hi-Storm 100s Overpack with MPC partially inserted. Taken from [21]

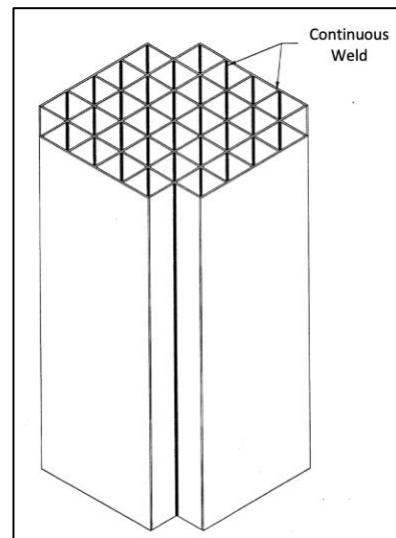


Figure 4-12 MPC-32 Basket. Taken from [21]

Table 4-1 shows the design parameters and values for the Holtec HI-STORM MPC [21].

Table 4-1 MPC design specifications based on Holtec international final safety analysis report

Structural limits		Thermal limits		Radiation limits	
Volume (m ³)	6.95	Thermal power (kwatts)	34	Neutron/ sec	2.68E+8
Mass (kg)	24595			Photon/ sec	3.85E+15

Reference cost - According to the Advanced Fuel Cycle Cost Basis Report [13], the service contract labor costs for implementing the procedures start at \$200,000 per cask. The capital costs for the storage container and dry storage overpack also begin at \$1 million. Thus, a ballpark cost of \$1.2 million/ MPC is considered for this study.

4.1.5 Ultimate disposal

4.1.5.1 Option-1 Deep borehole

Deep borehole disposal is one concept postulated for permanent SNF storage. As part of the background study, the 2010 MIT master's thesis by Jonathan Sutton Gibbs was leveraged, in which a detailed study of the feasibility of lateral emplacement in very deep borehole disposal of high-level nuclear waste was conducted [22].

The generalized deep borehole disposal concept is illustrated in Figure 4-13. The concept consists of drilling a borehole (or array of boreholes) into crystalline basement rock to a depth of about 5,000 m, emplacing waste canisters containing used nuclear fuel or vitrified radioactive waste from reprocessing in the lower 2,000 m of the borehole, and sealing the upper 3,000 m of the borehole. Waste in the deep borehole disposal system is an order of magnitude deeper than typical mined repositories, resulting in greater natural isolation from the surface and near-surface environment. The disposal zone in a single borehole could contain about 400 waste canisters of approximately 5 m in length.

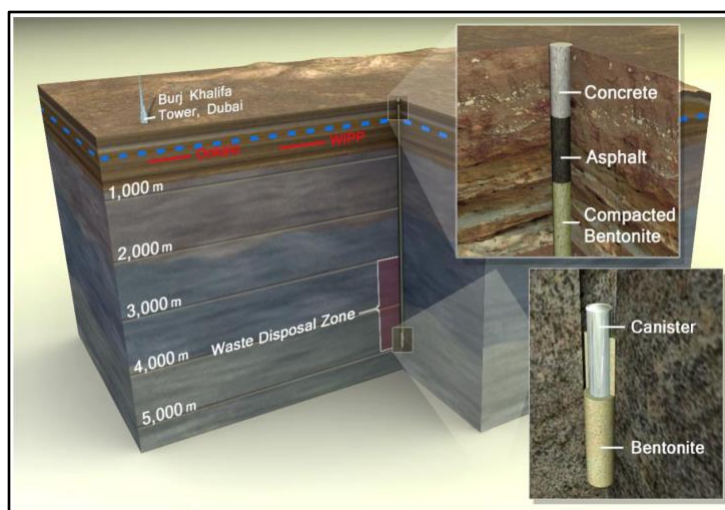


Figure 4-13 Generalized concept for deep borehole disposal of high-level radioactive waste. Figure taken from [22]

The deep borehole canister design specifications are given in Table 4-2.

Table 4-2 Summary of canister design specifications [22]

Structural basis		Thermal basis	
Volume	38,639 cm ³	Heat	340 watts
Mass	729 kg		

Reference cost - The deep borehole disposal cost for a single borehole was estimated to be around \$40.1 million, not including transportation or any associated storage charges.

4.1.5.2 Option-2 Deep Geological Repository

The deep geological repository presents another secure, long-term solution for nuclear waste management. Sandia National Lab report on the DPC disposal concept of operations [23]

reports that the deep geological repository would be situated at depths between 500 to 1,000 meters to provide isolation and take advantage of overburden stress that encourages the natural sealing of storage spaces. The report envisions a modular design, incorporating extensive emplacement tunnels radiating from a central core to accommodate an inventory of roughly 140,000 MTU across nearly 10,000 DPC-based waste packages. The repository's planning includes specific provisions for drift spacing, limiting areal thermal load to manage temperature increase and ensure structural integrity over time. The repository effectively controls the peak salt temperature by adhering to a thermal power limit of 10 kW per package and maintaining strategic distances between them (Figure 4-14 [23]).

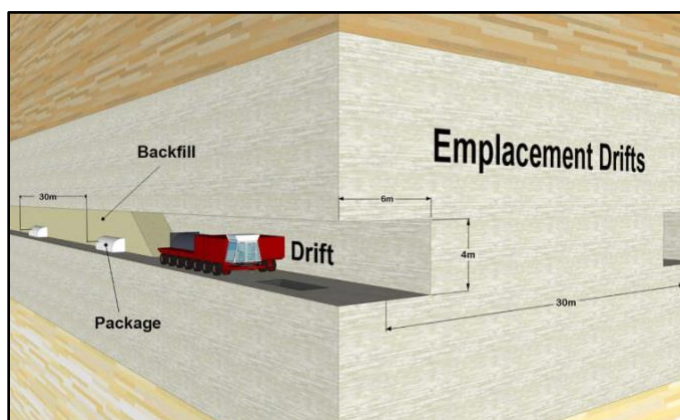


Figure 4-14 Conceptual drawing for the salt repository concept with in-drift emplacement in long parallel drifts and emplacement of crushed salt backfill. Taken from [23]

The design specification for the MPC [23] to be disposed of in a salt-based deep geological repository is as per Table 4-3.

Table 4-3 Design specification for MPC

Structural basis		Thermal basis	
Volume	6.95 m ³	Heat	10 kwatt
Mass	15867 kg-HM		

Reference cost – Hardin et al [24] estimates the total cost, including the repository's design, construction, start-up, operation, closure, and monitoring, to accommodate 140,000 metric tons of spent nuclear fuel (SNF), ranging from USD 24.33 billion to USD 32.48 billion. Given that the repository is designed to store a total of 10,000 dual-purpose casks, the upper limit on the cost of storing a single cask is determined to be approximately USD 3.2 million.

Back-end cost estimation key takeaway: The number of casks required for disposing of the used nuclear fuel depends on characteristics such as decay heat, mass, volume, neutron, and gamma irradiation levels. Chapter 6 proposes an equivalency assessment method, which evaluates the number of casks required for each microreactor concept. The number of casks thus identified, along with the per unit cask cost, will result in back-end cost estimation.

4.2 Continuous recycle fuel cycle: Major steps and cost considerations

The continuous recycling of plutonium and uranium in a closed fuel cycle involves a two-stage process that integrates both fast and thermal reactors, thereby enhancing resource utilization and minimizing nuclear waste. In the first stage, a sodium-cooled fast reactor (SFR) is employed,

which utilizes natural uranium and recycled plutonium as its primary fuel. This reactor not only generates energy but also breeds more plutonium (breeds) than it consumes; the surplus plutonium is then directed to the second stage. In this subsequent stage, the surplus plutonium, along with recycled plutonium, is incorporated into TRISO fuel embedded in a magnesium oxide (MgO)-based Inert Matrix Fuel (IMF) and loaded into the reactor to produce electricity. The Minor Actinides (MA) separated in Stage 2 are sent to Stage 1 for fissioning under the SFR hard neutron spectrum. Figure 4-15 provides an overview of this transuranic recycling approach, in which a single fast reactor (Stage 1) supports one or more microreactors (Stage 2).

Facilities supporting continuous recycling are unavailable commercially, so the ‘spot prices’ that exist for once-through processes (like uranium mining, conversion, or enrichment) are unavailable for continuous recycle fuel cycle steps. Consequently, the analysis for evaluating the costs of continuous recycled fuel cycle activities relies heavily on the DOE’s Fuel Cycle Research & Development (FCRD) cost basis report [13], which provides a comprehensive set of cost data to support the cost analysis for advanced fuel cycle.

The following subsections outline each step, from front-end processes to back-end operations, and reference relevant cost estimates.

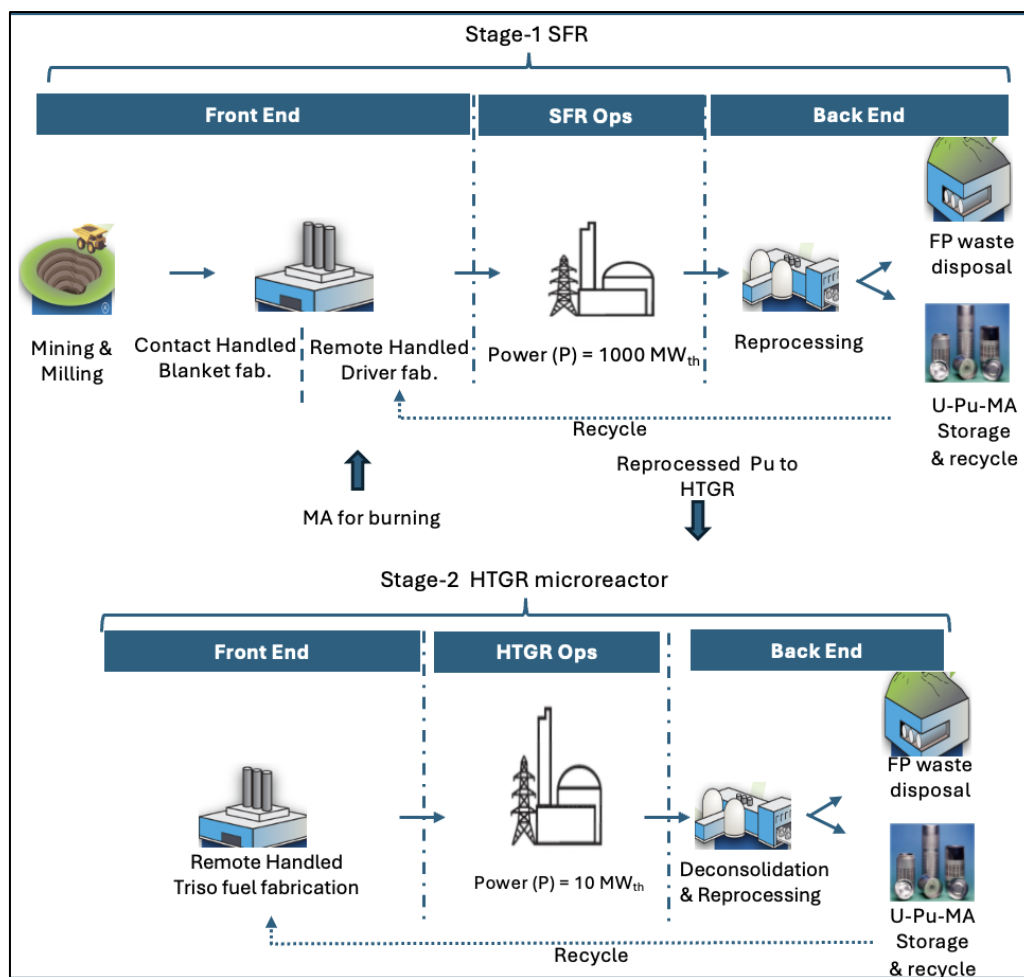


Figure 4-15 Continuous recycling of transuranic fuel cycle with SFR and microreactor stage

Stage-1 SFR Front-end process

The front-end processes include all the fuel cycle activities leading to fuel load in a sodium-cooled fast reactor.

4.2.1 Mining and milling

The initial mining and milling step is the same as the Once-Through fuel cycle. Refer to section 4.1.1 for a discussion on the process and associated costs.

4.2.2 Contact handled blanket fabrication

Fresh blankets made from fertile/recycled uranium for producing plutonium-239 typically exhibit very low radiation levels, allowing them to be handled directly. Uranium dioxide (UO_2) blanket fuel can be produced in a standard industrial facility with minimal security and radiation protection requirements. Given the lack of significant concerns related to criticality or radiotoxicity, the cost of fabricating blanket fuel is expected to be comparable to that of fabricating low-enriched uranium (LEU) fuel [13].

Reference cost- The contact-handled blanket fabrication per unit cost is based on an advanced fuel cycle cost basis document [13], which estimates the mean cost of fabricating FR pelletized ceramic NATUO_2 or DUO_2 blanket fuel to be \$487 per kgHM.

4.2.3 Remote-handled driver fabrication

In contrast to the blanket fuel, remote handling will be required for the spent fuels arising from continuous recycling and re-fabrication of higher-actinide-bearing fuel types, especially those involving electrochemical pyrochemical recycling or multiple-pass recycling.

Reference cost - The advanced fuel cycle cost basis document [13] estimates remote driver fabrication costs about \$5,060 per kg HM. This figure is based on subtracting the cost of UREX+1a reprocessing from integrated reprocessing-plus-fabrication values reported in related literature [25].

Stage-1 SFR Back-end process

The spent fuel will be given a cooling time of 5 years to allow radioactivity levels to reduce. As with the Once-through concepts, the associated costs are accounted for under O&M costs and thus are not considered for further analysis.

The spent fuel after 5 years is reprocessed, and the separated U-Pu-MA are stored for further loading into the SFR core (under equilibrium conditions) and stage-2 microreactor. The fission product waste is disposed of as LLW after 300 years of monitored storage.

4.2.4 Reprocessing

Reprocessing is usually carried out by the standard pyroprocessing process, which uses electrochemical reactions to extract fissile material from used fuels and generate source material suitable for recycling. Pyroprocessing typically begins with a head-end treatment tailored to the fuel type by either chopping clad metallic fuel or electro-reducing oxide fuel to metal. The main separation step in a pyroprocessing flowsheet is electrorefining, wherein constituents in the used nuclear fuel are oxidized and dissolved into molten salt, and then actinides are selectively reduced and deposited as alloys that can be used as source materials for new fuel. Most of the fuel is recovered as separate alloys of by-product uranium and mixed actinides. Waste from the process consists of process salt and metallic waste streams with fission products and fuel cladding. The volume of HLW and its activity are decreased by pyroprocessing compared to direct disposal [26].

Reference cost- Based on the FCRD cost basis document [13] and the references therein [27], [28] the mean reference costs for integrated pyroprocessing and remote refabrication are estimated at \$2600 per kgHM.

4.2.5 U-Pu-MA storage & recycle

Recovered uranium, plutonium, and minor actinides must be stored under stringent security measures and criticality controls. Handling high-fissile-content materials typically involves heavily shielded containment, remote robotics, and sophisticated radiation protection systems.

Reference Cost - The FCRD document [13] cites a mean storage cost of \$5,206 per kg of Pu-MA per year, assuming a 50 MT facility capacity and compliance with current U.S. security requirements.

4.2.6 FP waste disposal

The fission product (FP) waste generated during the pyroprocessing of spent nuclear fuel requires careful long-term management due to its radioactivity and heat generation. One of the proposed solutions in advanced fuel cycles is 300-year decay storage for immobilized FP waste. This storage period is intended to significantly reduce the radioactivity and thermal output of the waste, making subsequent disposal as low-level waste (LLW) feasible.

Reference cost - The estimated cost for managing the FP waste is \$17190 per kg-FP [13].

Stage-2 HTGR Front-end process

During Stage-2, the surplus plutonium recovered from Stage-1 and recycled plutonium during the equilibrium state are fabricated into TRISO particles, which are subsequently loaded into the microreactor in the form of compacts/ pebbles. This process differs from fresh-U TRISO fabrication due to higher radiation fields and associated remote-handling requirements.

4.2.7 Remote-handled TRISO fuel fabrication

The fabrication of TRISO fuel has traditionally been centered on fresh uranium. However, incorporating recycled transuranic elements into TRISO fuel production will introduce several significant challenges requiring a detailed examination. The next few paragraphs explore the considerations of using recycled TRU for TRISO fabrication and the economic implications of adapting the production process.

Recycled TRU TRISO Fuel Fabrication Process: The basic clean TRISO fuel fabrication process is discussed in section 4.1.4. One key issue envisaged for recycled TRU-based TRISO manufacture is the handling and processing of radioactive recycled TRU. Due to the elevated radiation levels compared to clean uranium, the TRISO fuel fabrication process must be adapted to incorporate shielding and remote handling technologies. Specialized facilities would be required to accommodate these safety measures, and these facilities must be equipped with hot cells, gloveboxes, and other protective systems to manage the radiation safely.

Reference cost estimates:

The current literature lacks specific estimates for the fabrication of TRU-based TRISO fuel under remote handling conditions, highlighting the uncertainty surrounding the economic implications of this process. Mixed oxide (MOX) fuel fabrication appears to be the closest analog, which involves blending plutonium recovered from spent nuclear fuel with uranium oxide. In standard light-water reactor (LWR) operations, the cost of conventional uranium dioxide fuel fabrication is approximately \$230 per kilogram [13], whereas MOX fuel can exceed \$1600 per kilogram [13]. This substantially higher cost primarily stems from the need for specialized facilities to handle plutonium, stringent safety protocols, and the economic implications of small-batch processing.

The current estimate for TRISO fuel fabrication using a fresh uranium approach is \$10,000 per kilogram [13]. This higher cost reflects the inherently small-batch nature of TRISO production and the specialized precision equipment required, indicating that penalties associated with limited throughput and specialized handling are already embedded in the current TRISO fabrication expenditure. Consequently, rather than applying a multiplicative factor to account for remote handling of TRU-based TRISO fuel, an additive escalation strategy is deemed more appropriate, given that the baseline TRISO cost (\$10,000 per kilogram) has already internalized many of the cost drivers—particularly those arising from small-batch production. Applying a 50% uncertainty premium to this cost results in the TRU-based TRISO fabrication cost of approximately \$12,000 per kilogram (\$10,000 + \$2,000). This cost will be considered as a baseline fuel fabrication cost for recycled TRU-based TRISO manufacturing to derive costs for other advanced continuous recycling concepts.

Stage-2 HTGR Back-end process

4.2.8 Deconsolidation & Pyroprocessing

The coating that microencapsulates each kernel must be breached so that, during pyroprocessing, the molten salt electrolyte can penetrate the coating and make contact with

the fuel kernel [26]. Therefore, before beginning pyro processing, a head-end process is required to separate the kernels from the matrix material and then breach the coatings.

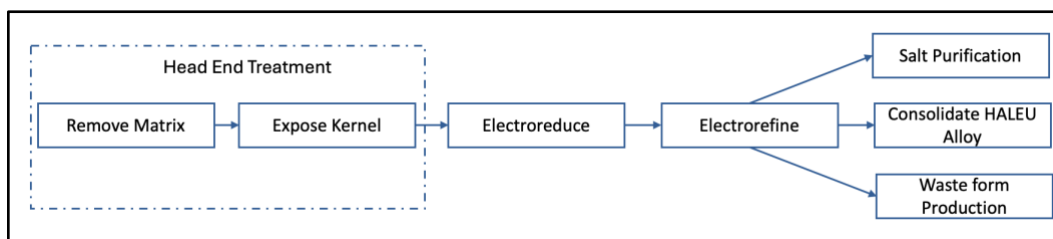


Figure 4-16 Generic flowsheet for application of pyroprocessing to pebble-type fuels. Taken from [26]

Figure 4-16 illustrates a high-level concept for applying pyroprocessing to pebble-type fuels [26]. It is postulated that preparing TRISO-type fuels for pyroprocessing by breaching the pyrolytic carbon layers using a molten salt electrochemical technique may be compatible with the current pyroprocessing flowsheet [26]. This technique involves the electrochemical formation of lithium metal from a molten salt onto the carbon surface, which then intercalates and destroys the graphite [29].

Reference cost - No cost-related estimates currently exist for the head-end process associated with breaching the TRISO layers. Nevertheless, due to the suggested proximity of this technique to the pyroprocessing process, the head-end process cost is assumed to be similar to that of the existing pyroprocessing process. Thus, as a simplifying assumption for this analysis, it is assumed that two pyroprocessing processes are run in series: the first process performs the head-end treatment, and the second process performs the actual pyroprocessing. Thus, the cost of deconsolidation and reprocessing is assumed to be $2 \times 2600 = \$5200$ per kgHM.

4.2.9 U-Pu-MA storage & recycle

Refer to section 4.2.5 for technology discussion and cost estimates.

4.2.10 FP waste disposal

Refer to section 4.2.6 for technology discussion and cost estimates

4.3 Material costs

Due to stringent purity requirements, proprietary manufacturing processes, and restricted markets, nuclear-grade material costs are challenging to ascertain. The specialized nature of nuclear-grade materials means that only a few qualified suppliers exist, often leading to confidentiality clauses and variable pricing.

To circumvent these challenges, multiple strategies were employed, including direct consultation with commercial suppliers, historical price analysis, and expert input. Information on cost was obtained from suppliers like Materion, American Beryllia, and MSE Supplies. For the cases when costs from reliable sources could not be sourced, a historical price analysis was resorted to. Insights from subject-matter experts helped validate assumptions and refine cost

estimates, particularly for yttrium hydride. The various cost estimates for entrained moderator material, along with the sources, are discussed next.

Beryllium Oxide (BeO)

Estimates from American Beryllia (USA), Materion (USA), and Nantong TaiYang Advanced Material (China) were collected as part of the ARPA-E MEITNER project [30]. American Beryllia (USA) offers BeO at \$1,102/kg with 99.5% purity, representing the premium end of the market. Materion (USA) provides a more competitive option at \$727.5/kg without specified purity levels. Nantong TaiYang Advanced Material (China) offers the most economical option at \$620/kg with 99.5% purity.

These price variations reflect differences in manufacturing capabilities, supply chain reliability, quality assurance processes, and geographic production locations. A mean price of \$816/kg was used for LCOF estimation.

Beryllium (Be)

Nuclear-grade beryllium price is quoted at \$2,313/kg by Materion (USA) [30]. This relatively high price point reflects the complexity of beryllium extraction and processing. While purity specifications were not specified, Materion's established position in the nuclear supply chain suggests costs reflecting nuclear specifications.

Zirconium Hydride (ZrH)

The cost for nuclear-grade ZrH was derived based on values used in earlier research. Buongiorno [31] considered a base zirconium metal price range of \$90-110/kg in 2006, along with the hydriding process adding approximately 30% to base material costs (from Allegheny Technologies). USGS data shows relative stability in raw zirconium sponge costs, from \$31/kg in 2004 to \$28/kg in 2024 [32]. Thus, assuming a stable base zirconium metal price and applying the 51.6% inflation adjustment (2004-2024) [33] to processing costs yields a 2024 estimate of \$160/kg for nuclear-grade ZrH.

Yttrium Hydride (YH)

Consultation with Dr. Lance Snead suggests that the base metal cost for yttrium exceeds zirconium by approximately \$10/kg. Assuming identical hydriding and purification costs, the estimated cost for nuclear-grade YH of \$175/kg is considered.

5 Fabrication cost estimation methodology and calculation for Once-Through and continuous recycle reactor concepts

In this chapter, a structured methodology is discussed, which is used to estimate the fuel fabrication costs of composite moderators under both Once-Through and continuous recycle concepts. Recognizing the inherent complexity of TRISO-loaded fuel assembly fabrication, a bottom-up approach has not been adopted. Instead, an analogous evaluation approach is used that systematically extends established graphite-based costs to advanced reactor concepts.

5.1 Fabrication cost estimation methodology for prismatic reactor concepts:

For ease of analysis, the fabrication process for TRISO-loaded prismatic fuel assemblies is subdivided into the following sub-processes:

- TRISO fabrication
- Prismatic fuel assembly fabrication (including compacts)
- QA during each of the above processes

Personal communication with Dr. Dave Petti [34] leads to understanding the cost split between these three sub-processes in the 48%, 32%, and 20% ratio, respectively.

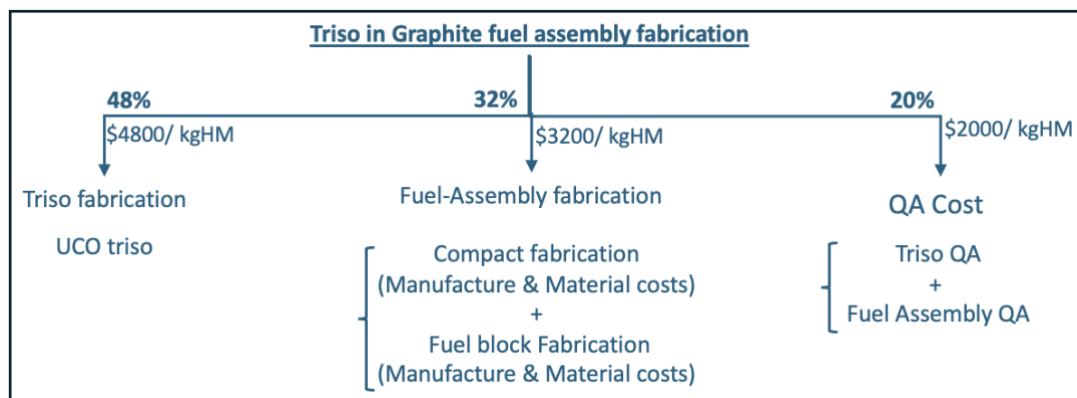


Figure 5-1 Baseline graphite case cost split.

In the next subsections, a deep dive is made into each subprocess to establish the cost estimation strategy for advanced moderator concepts under consideration.

5.1.1 TRISO fabrication consideration

a) Consideration for the Once-Through concepts

As discussed in section 2.3, UN TRISO is considered for the different reactor concepts as it results in higher uranium loading. Also, as discussed in section 4.1.4.1, the principal distinction between UCO and UN kernel production is an additional nitriding step required for UN kernels. Both kernel types undergo sol-gel production, calcination, and a fluidized-bed chemical vapor deposition (CVD) process for coating. However, the UN route involves converting $\text{UO}_2 + \text{UC}$ into UN before the final coating stage. As per personal communication with Dr. Dave Petti [34], adding this extra step would introduce a minor cost addition. Consequently, as an upper limit, UN TRISO production is estimated to be about 5% more expensive than UCO TRISO. As a second

rough approximation, this increment is derived by adding a single stage to the existing 20-step process, as shown in Figure 4-2, yielding an approximate 5% premium. Thus, the UN TRISO fuel fabrication cost is estimated at \$5,040/kgHM.

b) Consideration for the continuous recycle concepts

Under continuous recycle approaches, where plutonium or mixed transuranic (TRU) replace enriched uranium, TRISO fabrication costs typically increase. Based on various factors, as discussed in section 4.2.7, as a first-order approximate, the baseline fabrication cost of \$10,000/kgHM for once-through fuel rises to \$12,000/kgHM under continuous recycle conditions. Repeating the same calculation as carried out for Once-Through concepts, retaining the same 48% allocation for TRISO fabrication, and including the 5% nitriding overhead brings the estimated TRISO production cost to about \$6,048/kgHM.

5.1.2 Prismatic fuel assembly fabrication (including compacts)

Approach to estimate compact fabrication cost

The baseline compact & fuel assembly fabrication costs for TRISO-fueled, graphite-moderated fuels was \$3200/kgHM, encompassing both raw material expenses and manufacturing overhead. The manufacturing share could be identified by separating the material component (based on market data) from this total fabrication cost. Moderator-specific material costs for the different microreactor concepts are then incorporated into the manufacturing baseline to yield a comprehensive fabrication estimate. In summary, this methodology involves (1) disaggregating the graphite baseline costs, (2) identifying the manufacturing component, and (3) combining that manufacturing baseline with the material costs unique to advanced moderators to determine total fabrication costs for novel reactor designs.

Application to baseline graphite case

The total heavy metal inventory for the baseline graphite configuration is 228.7 kgHM. With a per-unit fabrication cost of \$3,200/kgHM, this translates into a overall manufacturing cost of \$732,000, covering both raw materials and process operations.

Per personal communication with Dr. Lance Snead, each machined graphite block is estimated at \$46/kg, which includes an allotment of 60% to raw material cost and the remaining 40% to machining/ waste [35]. This cost breakdown is assumed to be applicable across all reactors based on prismatic concepts for fuel block fabrication. As the total fuel block weighs 6,308.4 kg, the aggregate cost of the fuel blocks (materials plus machining) amounts to \$290,000, of which \$174,000 is material expense and \$116,000 is manufacturing overhead (60:40 split).

For compacts, the baseline graphite process relies on three principal materials: natural graphite (64% by weight), synthetic graphite (16%), and phenolic resin (20%) [27]. A weighted average of \$62.30/kg is derived for the matrix material based on respective costs of \$75, \$65, and \$19.50 per kilogram for natural graphite, synthetic graphite, and phenolic resin. Since the compacts incorporate 1,026.1 kg of graphite, the total compact matrix material costs \$64,000.

Since the overall \$732,000 fabrication cost includes 55 fuel assemblies equipped with 110,880 compacts. By subtracting both the compact matrix cost (\$64,000) and the fuel block material plus the machining cost (\$290,000) from \$732,000, the resulting \$377,680 is attributable to

compact manufacturing. Dividing by the 110,880 compacts yields a per unit compact manufacturing cost of \$3.40 per compact.

a) Consideration for the Once-Through concepts

Extending Cost Estimates to Other Reactor Concepts

Reactor designs employing alternative matrix materials utilize a fabrication process comparable to that of baseline graphite for manufacturing a compact matrix milling/drying, kernel overcoating, warm pressing, and heat treatment. As a result, the \$3.40 per-compact manufacturing is extended to advanced moderator concepts.

b) Consideration for the continuous recycle concepts

Scaling the baseline \$3.40 per-compact manufacturing cost by the proportionate 20% increase associated with plutonium restrictions yields \$4.08 per compact.

5.1.3 QA costs during each of the above processes:

a) Consideration for the Once-Through concepts

Using a per-unit QA cost of \$2,000 per kilogram of heavy metal (kgHM) and a total mass of 229 kgHM, The total QA cost was found to be \$458,000. Assuming that QA costs are equally split between TRISO particle QA and fuel assembly QA, each process was assigned a cost of \$229,000.

For TRISO QA, the cost depends on the number of QA inspections, which is proportional to the number of TRISO particles and, therefore, proportional to the fuel mass. Consequently, as a first-order approximation, TRISO QA costs for different reactor concepts is estimated by multiplying the heavy metal mass by \$1,000/kgHM.

The remaining \$229,000 is dedicated to fuel assembly/ compact QA. Given that the manufacturing process for these compacts is assumed to be the same as that for graphite, QA steps are expected to remain consistent across reactor concepts. Furthermore, because the number of fuel assemblies and compacts does not change among prismatic reactor designs, the total QA cost for fuel assembly fabrication (\$229,000) is expected to remain uniform.

b) Consideration for the continuous recycle concepts

For reactor concepts employing continuous recycle of plutonium-based TRISO fuel, the initial fabrication cost is assumed to rise from \$10,000 per kgHM (once-through case) to \$12,000 per kgHM. Because quality assurance (QA) represents approximately 20% of total fabrication costs, the QA component in this scenario increases proportionally to $12,000 \text{ \$/kgHM} \times 20\% = 2,400 \text{ \$/kgHM}$.

This total QA cost of \$2,400/kgHM is assumed to be split equally between TRISO QA and Compact (and assembly) QA. Again, as before, the TRISO QA costs are a function of the number of the TRISO particles, which also translates to the total heavy metal present. Thus, the TRISO QA costs for different reactor concepts under continuous recycle concepts will be estimated by multiplying the heavy metal mass by \$1,200/kgHM.

For the QA of compacts and fuel blocks, owing to similar considerations for plutonium handling, a premium of 20% is considered, giving the QA cost for the compacts \$274,800. Again, as the number of compacts and fuel blocks is identical, the total QA costs for the block and compacts will be constant for different reactor concepts

5.2 Fuel fabrication costs estimation methodology for pebble-bed concepts

5.2.1 TRISO fabrication costs

a) Consideration for the Once-Through concepts

Because the same UN TRISO is used for prismatic and pebble-bed fuels, baseline costs for TRISO fabrication in a once-through scenario remain the same as for prismatic designs (\$5,040 per kgHM).

b) Consideration for the continuous recycle concepts

As discussed in Once-Through prismatic concepts, TRU-based TRISO production would cost roughly \$6,048 per kgHM.

5.2.2 Pebble fabrication costs

a) Consideration for the Once-Through concepts

Figure 5-2 highlights the principal steps in compact and pebble fabrication. It is evident from the figure that there are similarities between compact and pebble fabrication processes. It is observed that both processes utilize key materials like natural and synthetic graphite and binder resin to prepare the matrix precursor. This precursor is subsequently compacted, overcoated, and heat-treated, which involves similar processing steps for achieving the desired structure and material integrity. Using a binder resin, the compacting stage, and carbonization highlight the comparable stages both fuel forms undergo to meet their specific fabrication requirements. This commonality lends to the applicability of power-law scaling to derive the costs of pebble manufacture based on the compact manufacture cost.

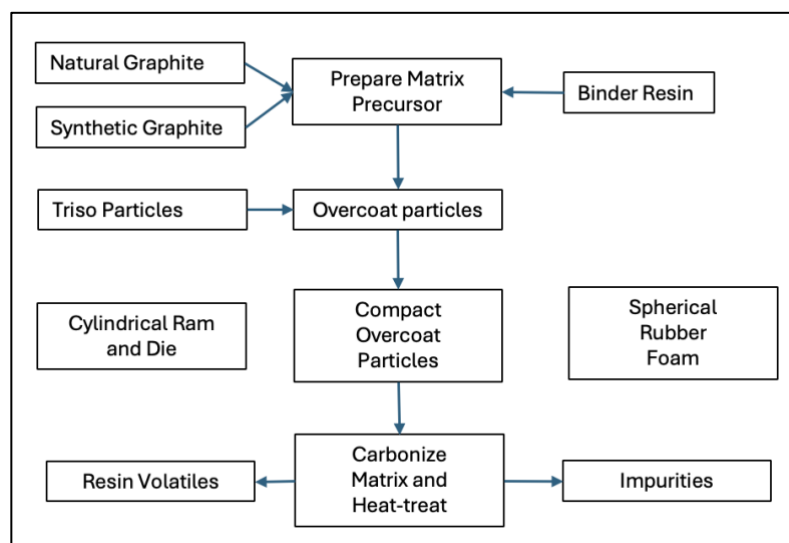


Figure 5-2 Similarity between compact/ pebble fabrication.

Cost Estimation of Manufacturing Pebbles Using Power Law Scaling:

Power law scaling is applied to determine the cost of pebble manufacturing (C_p). The following equation defines the relationship:

$$C_p = C_c \left(\frac{V_p}{V_c} \right)^n \quad \text{Equation 1}$$

The details of the compacts and pebble are as below.

Compact parameters		Pebble parameters	
Volume of compact (V_c)	6.04 cc	Volume of pebble (V_p)	113 cc
Cost of compact (C_c)	\$3.4/compact	Cost of pebble (C_p)	TBD

Plugging the values as defined above in Equation 1 results in the cost of pebble manufacturing $C_p = \$35.4/\text{pebble}$. The estimated cost per pebble of \$35.4 is encouraging as the Module D1-3-19 of advanced fuel cycle cost basis report [13], estimates the fabrication cost of one pebble to be around \$35 per unit.

b) Consideration for the continuous recycle concepts

Based on complexities associated with plutonium handling, adopting continuous recycled fuel in a pebble-bed reactor introduces a proportional cost increase similar to prismatic designs. In other words, if the baseline Once-Through fuel cost is \$10,000 per kgHM and the continuous recycle figure is \$12,000 per kgHM—a 20% uplift—then pebble manufacturing also undergoes a 20% increase. Applying this premium to the \$35.4 baseline yields:

$$C_{\text{pebble, continuous recycle}} = \$35.4 \times 1.20 \approx \$42.48$$

This additional cost reflects stricter handling and processing protocols for plutonium-bearing feedstocks.

5.2.3 Pebble QA cost

a) Consideration for the Once-Through concepts

To establish a cost estimate, it is assumed that the QA processes for pebbles involve similar inspection and quality control steps as those employed for compacts. This assumption allows for an analogous estimation approach, where the cost per unit compact is a proxy for the cost per pebble. The QA cost per compact is derived by dividing the total QA cost of compacts by the number of compacts produced.

$$\text{QA cost per compact} = \text{QA cost per pebble} = (\$0.23 \text{ M}/110880) = \$2.06/\text{compact}$$

b) Consideration for the continuous recycle concepts

Accounting for the increased safeguards and material handling complexities—the QA cost is scaled by the same (20%) proportion, raising the per-pebble QA cost to approximately \$2.50.

6 Methodology and cost estimation for Spent Nuclear Fuel Disposal activity from Microreactors

In this chapter, An equivalency assessment was carried out to adapt traditional spent nuclear fuel (SNF) management methods—originally formulated for large-scale reactors, such as Pressurized Water Reactors (PWRs) and Boiling Water Reactors (BWRs)—to the unique requirements of microreactor SNF. The microreactors considered under the scope of this analysis, employing relatively smaller cores and distinctive fuel burnup, were evaluated against key parameters that typically dictate disposal system design limits. In particular, parameters such as SNF volume, mass, decay heat, neutron and gamma emissions were compared with the design envelopes as applicable to conventional reactor fuel.

Traditional SNF management relies on several well-established techniques, including:

- Interim dry storage in multipurpose canisters (MPCs) and
- Permanent disposal in either deep boreholes or geological repositories.

Each of the above disposal options’ design limits and cost estimates were discussed in sections 4.1.4.6 and 4.1.5.

6.1 Interim storage – microreactor equivalency assessment:

As discussed in Section 4.1.4.6 for interim storage of spent nuclear fuel, multi-purpose canisters (MPCs) have been characterized with design specifications that include a volumetric capacity, mass limit, thermal limit, neutron, and gamma field limits with an accompanying cost of \$1.2 million per canister. These values are shown in the first column of Table 6-1. These reference values were used to perform an equivalency assessment for a baseline graphite microreactor core. The corresponding values for the baseline graphite microreactor are taken from Table 2-1 and shown in the second column of Table 6-1.

After this, the fraction of each parameter (e.g., fraction of volume consumed, fraction of mass capacity used, etc.) was calculated to determine the limiting parameter (maximum). The associated cost was then estimated by multiplying the cost per MPC (\$1.2 million by the fraction) by the fraction/ limiting number of MPCs.

Table 6-1 Equivalency estimation methodology for baseline graphite case.

Design Basis values	Graphite Microreactor	Fraction / Limiting
Volume: 6.95 m ³	4.38 m ³	63%
Mass: 24,595 kg	8,832 kg	36%
Decay Heat: 34 kW (@5 yr)	0.52 kW (@5 yr)	1.5%
Neutron: 2.68E+8 n/s	2.8E+6 n/s	1%
Gamma: 3.85E+15 ph/s	1.7E+15 ph/s	44%
Cost per Cask: \$1.2 M	Limiting parameter: Volume: 63%	\$0.75 M

Discussion: It was seen that the baseline graphite microreactor fuel occupies a volume of 4.38 m³, corresponding to 63% of the canister’s volumetric capacity. The microreactor SNF mass

of 8,832 kg corresponds to only 36% of the canister's mass capacity, and the decay heat, measured at 0.52 kW (five years post-discharge), amounts to approximately 1.5% of the 34 kW limit. Gamma source strength was determined to be about 44% of the canister's allowable gamma emission envelope, whereas neutron emissions were well below 1% of the permissible range. Because the volumetric fraction (63%) was the highest fraction among these parameters, the limiting parameter was established as the MPC volume. This implies that the fuel from a single baseline graphite microreactor core would utilize 63% of the canister's capacity, leading to an estimated cost of \$0.75 million for interim storage.

It is important to clarify that this cost estimation is based on a centralized disposal strategy in which a canister is not disposed of until it is completely filled. In practice, spent nuclear fuel from one or more reactors will be consolidated into a single MPC until 100% of the strictest design limit (with volume being the controlling parameter in this case) are reached. Thus, while the baseline graphite microreactor fuel occupies only 63% of a canister's capacity on its own, additional spent fuel would be added to bring the canister to full capacity before disposal. This centralized approach will ensure optimal utilization of each canister, maximizes storage efficiency, and aligns with regulatory and safety requirements for spent fuel disposal.

The methodology described above was applied to different prismatic concepts and pebble bed concepts as derived from Table 2-1 and Table 2-3 and the resulting values are summarized in Table 6-2 for the interim storage of the prismatic and pebble bed concepts.

Table 6-2 Limiting parameter identification and storage costs for interim storage (full core basis). The values in rows 1-5 indicate the fraction of interim storage casks required for disposal of full core as dictated by criteria in column 1.

Limiting criteria	Prismatic concepts				Pebble bed concepts			
	BeO	Be	YH	ZrH	BeO	Be	YH	ZrH
Volume	63%	51.9%	63%	51.9%	25.8%	34.8%	45.1%	34.8%
Mass	61.3%	44.8%	69.2%	58.8%	22.9%	29.8%	49.3%	40%
Decay heat	2.5%	3.1%	10.7%	9.2%	4.2%	6.8%	10.7%	11.1%
Neutron field	4.7%	10.3%	81.3%	75.8%	23.3%	86.5%	117.9%	222.6%
Gamma field	65.8%	83.2%	259.3%	230.8%	116.9%	180.9%	266.5%	278.2%
Limiting MPC	65.8%	83.2%	259.3%	230.8%	116.9%	180.9%	266.5%	278.2%
Cost (\$M)	0.78	0.99	3.11	2.76	1.4	2.17	3.19	3.34

Since the gamma field is the limiting factor for all the reactor concepts, deconsolidation will not yield any benefit due to volume reduction in interim storage costs.

6.2 Deep borehole - microreactor concepts equivalency assessment

As summarized in Section 4.1.5, the deep borehole disposal concept employs canisters with a fill volume of 38,639 cm³, a typical waste mass capacity of approximately 729.07 kg, and a thermal capacity of 340 W, each costing about \$0.1 million. For different microreactors, the multiple of each limiting parameter was calculated using corresponding values from Table 2-1

(prismatic) and Table 2-3 (pebble bed), respectively. The number of canisters was determined by the highest of the three fractions—volume, mass, or decay heat—and then multiplied by \$0.1 million per canister to yield the total disposal cost. Table 6-3 summarizes the total cost of deep borehole disposal for prismatic and pebble bed microreactors.

Table 6-3 Limiting parameter identification and storage costs (full core basis) for deep borehole disposal. The values in rows 1-3 indicate the number of borehole casks required for disposal of full core as dictated by criteria in column 1.

Limiting criteria	Prismatic concepts				Pebble bed concepts			
	BeO	Be	YH	ZrH	BeO	Be	YH	ZrH
Volume	114	114	94	114	47	63	82	63
Mass	13	21	16	24	8	11	17	14
Decay heat	1	2	2	8	3	5	8	8
Limiting # of canisters	114	114	94	114	47	63	82	63
Cost (\$M)	11.4	11.4	9.43	11.4	4.7	6.3	8.2	6.3

6.3 Geological repository microreactor equivalency assessment

As detailed in Section 4.1.5.2, the structural specifications for each geological repository canister include a total available volume of 6.95 m³, total mass capacity of 24,595 kg, and is capable of withstanding up to 10 kW of decay heat. A typical Cost per canister is also estimated to be \$3.24 million. The same equivalency approach was applied to the different prismatic and pebble bed options, and the resulting cost values for the geological repository disposal option are summarized in Table 6-4.

Table 6-4 Limiting parameter identification and storage costs(full core basis) for salt repository disposal. The values in rows 1-3 indicate the number of MPC's required for disposal of full core as dictated by criteria in column 1.

Limiting Factor	Prismatic concepts				Pebble bed concepts			
	BeO	Be	YH	ZrH	BeO	Be	YH	ZrH
Volume	63%	63%	51.9%	63%	25.8%	34.8%	45.1%	34.8%
Mass	35.9%	61.3%	44.8%	69.2	22.9%	29.8%	49.3%	40%
Decay heat	3%	5%	6.3%	25.1%	8.6%	14.6%	24.5%	24.7%
Limiting MPC	63%	63%	51.9%	69.2%	25.8%	34.8%	49.3%	40%
Cost (\$M)	2.04	2.04	1.68	2.24	0.83	1.13	1.6	1.3

Cost summary for once-through-cycle back-end disposal option

The ultimate disposal costs for the SNF of the full microreactor core were evaluated under prismatic and pebble-bed core configurations. Table 6-5 consolidates the results for both deep borehole and salt repository options.

In general, deep borehole disposal costs are 5–8 times higher than corresponding salt repository options for the disposal of SNF from advanced microreactors, making salt-based geological disposal comparatively more economical. Therefore, subsequent LCOF calculations in

this study assume salt repository disposal as the preferred option for long-term waste management.

Table 6-5 Permanent disposal cost comparison. (full core basis)

Core configuration	Disposal option	MgO-BeO	MgO-Be	MgO-YH	MgO-ZrH
Prismatic core	Deep bore hole storage cost	\$ 11.4 M	\$ 9.43 M	\$ 11.4 M	\$ 9.43 M
	Salt repository storage cost	\$ 2.04 M	\$ 1.68 M	\$ 2.24 M	\$ 1.91 M
Pebble bed core	Deep bore hole storage cost	\$ 4.7 M	\$ 6.3 M	\$ 8.2 M	\$ 6.3 M
	Salt repository storage cost	\$ 0.83 M	\$ 1.13 M	\$ 1.6 M	\$ 1.3 M

In conclusion, the equivalency assessment carried out has provided a pathway by which microreactor SNF can be aligned with proven SNF disposal methods. The key constraints are identified, and a cost model is prepared, allowing informed decisions to be made in selecting back-end management strategies.

Limitation of analysis

Although parameters from standard SNF canisters were used for the above analyses, no disposal option is currently licensed to handle HALEU-based SNF directly. The bounding analysis provides a first-order approximation to determine the associated costs by assuring that the microreactor SNF remains within typical design envelopes. Further licensing and design adaptations would be required to accommodate HALEU-specific requirements.

6.4 Back-End disposal constraints and costs

One of the primary objectives for developing advanced microreactor fuel cycles is to minimize the back-end disposal footprint. The structural or moderator material (e.g., graphite or MgO-based composites) represents a large fraction of the spent nuclear fuel (SNF) volume, even though it contains negligible fissile material. Across both prismatic and pebble-bed microreactors, (Table 6-3 and Table 6-4) repeatedly show that volume is the limiting factor for canister loading, surpassing mass and decay-heat constraints in most scenarios. As soon as the canister's internal volume is filled, no additional SNF may be added—even if mass or heat limits are not fully utilized. As a result, volume becomes the key driver of total disposal capacity and strongly influences the repository footprint.

Deconsolidation seeks to mitigate this issue by selectively removing the non-fissile matrix material—through mechanical, chemical, or electrochemical processing—so that only the “fuel-bearing” portion remains for disposal. Deconsolidation thus allows for fewer canisters to hold the same thermal inventory by reducing both the mass and volume of the SNF. This section outlines how deconsolidation is modeled and the threshold-cost methodology used to gauge whether the process is cost-effective.

Cost of SNF Disposal After Deconsolidation

During deconsolidation, the matrix material (e.g., MgO plus entrained moderator) is partially or fully separated from the irradiated fuel. The reduced mass and volume of the left TRISO particles are then re-evaluated to determine the new limiting criteria. Table 6-3 and Table 6-4 are regenerated under new core mass and volume conditions. Decay heat, however, remains unchanged by matrix removal. Recalculating the required canister count and disposal cost

under these conditions quantifies the deconsolidation benefit. The results for this case are presented in Section 8.3.

Threshold-Cost Analysis

Since the exact cost of deconsolidation is currently unknown. A threshold deconsolidation cost ($C_{\text{decon threshold}}$) that serves as a benchmark for assessing its feasibility is calculated to capture the economic trade-offs.

$$C_{\text{decon threshold}} = \frac{(\text{Disposal cost without deconsolidation}) - (\text{Disposal cost with deconsolidation})}{\text{Heavy metal mass}}$$

If the actual deconsolidation cost remains below this threshold, the net savings in disposal outweigh the cost of matrix removal. Conversely, once deconsolidation expense rises above $C_{\text{decon threshold}}$, the economic gains from fewer canisters are reduced. That being said, even when deconsolidation costs exceed this threshold, the reduced land footprint may still offer qualitative or strategic benefits (e.g., smaller repository size, enhanced public acceptance, or simpler logistics), which might justify its adoption despite reduced direct cost savings.

7 LCOF Estimation

In this chapter, the generalized methodology from chapter 3 is applied to once-through and continuous recycling concepts by adapting them to the technical details of each cycle. By detailing each step of the calculation this chapter clearly demonstrates how the LCOF can be systematically estimated across different reactor designs. Sensitivity and Monte Carlo calculations are also discussed, along with the parameter ranges.

7.1 Levelized Cost of Fuel (LCOF) estimation for once-through cycle

Equations to calculate the yellow cake, conversion, and enrichment requirements.

The total mass of core fuel is easily determined once the discharge burnup, refueling interval, and capacity factor are known. Based on an assumed tail enrichment of 0.22%, the amount of natural uranium feed and SWU needed per kilogram of enriched fuel is also calculated. Table 7-1 lists the heavy metal mass, ore mass, and SWU required for the Once-Through concepts. The equations used to derive these values are given in Appendix 2.

Table 7-1 Mass of ore, SWU, and fuel mass for different concepts

	Prismatic concepts					Pebble bed concepts			
	Graphite	MgOBeO	MgOBe	MgOYH	MgOZrH	MgOBeO	MgOBe	MgOYH	MgOZrH
Mass of HM (kg)	228.7	326.8	326.7	1471.1	980.8	382.1	515.3	987.4	737.4
Mass of Ore (t)	9.3	13.2	13.2	59.8	39.8	15.5	20.9	40.1	29.9
SWU required (tSWU)	10.8	14.6	14.6	65.7	43.8	16.1	21.7	41.7	31.1

Application of methodology

Step-1 (Identifying major activities and timeline)

The nuclear fuel cycle has a structured timeline, with various processes occurring at specific timelines relative to the reactor core load and unloading. For this analysis, a simplifying assumption is made regarding the different timelines for the once-through cycle as follows. The front end of the cycle starts with mining and milling, which occurs two years before the core load. Conversion follows 1.5 years before core load, and enrichment occurs one year prior. Fabrication completes the front-end processes 6 months before the core load.

On the back end, the spent fuel is typically stored in storage wells located on the fuel deck of the plant reactor building [36]. Interim storage occurs five years after core unloading. Final disposal, involving either deep borehole disposal or salt repository, is scheduled 25 years after core unloading. The major steps and the typical timelines for the Once-Through fuel cycle are shown graphically in Figure 7-1.

Step 2 (Finding the cost associated with each activity)

The cost calculation for different activities of once-through prismatic and pebble-bed IMF (Inert Matrix Fuel) concepts are summarized in Table 7-2 and Table 7-3. These tables show how each activity's cost is calculated, referencing formulas and data from previous sections.

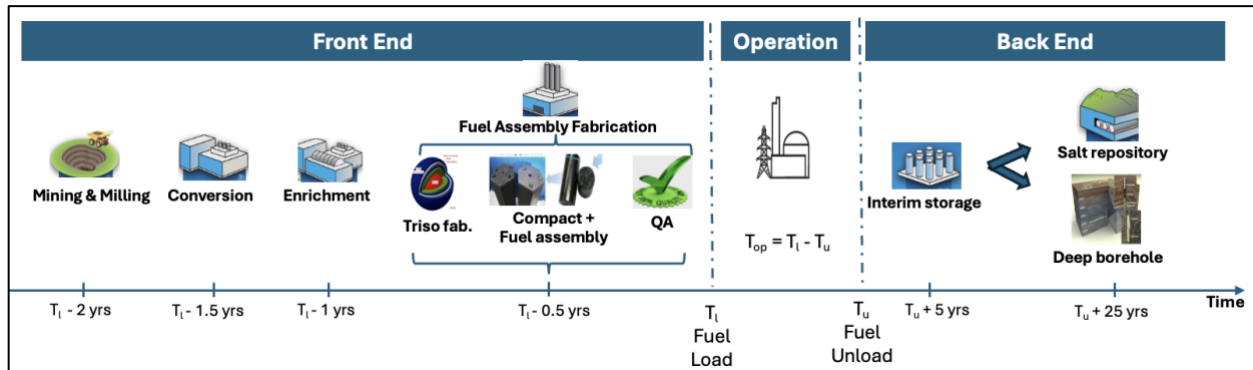


Figure 7-1 Major activities in a Once-Through prismatic fuel cycle with timeline

Table 7-2 Cost basis table for Once-Through prismatic IMF concepts

Fuel cycle activity		Time, t (years)	Activity Cost Calculation
Mining and Milling		-2	Per unit mass yellow cake cost (Section 4.1.1) X Mass of Ore (Table 7-1)
Conversion		-1.5	Per unit conversion cost (Section 4.1.2) X Mass of Ore (Table 7-1)
Enrichment		-1	Per SWU cost (Section 4.1.3) X SWU required (Table 7-1)
Fabrication (FAB)	TRISO	-.5	Per unit TRISO cost (Section 5.1.1a) X Heavy metal mass in fuel (Table 7-1)
	Compact material	-.5	Per Unit material cost in compact (Section 4.3) X Mass of compact (Table 2-1)
	Compact manufacture	-.5	Per Unit compact manufacture cost (Section 5.1.2a) X Number of compacts (Table 2-1)
	Fuel block material	-.5	Per Unit material cost (Section 4.3) X Mass of material in Fuel block (Table 2-1)
	Fuel block manufacture	-.5	66% of fuel block material cost
	QA	-.5	\$1,000/kgHM X Heavy metal mass in fuel (Table 2-1) + \$ 229,000 (Section 5.1.3a)
Interim storage (INT)		T _{op} +5	Calculated in Table 6-2
Salt repository (SR)		T _{op} +25	Calculated in Table 6-4

Table 7-3 Cost basis table for Once-Through pebble-bed IMF concept

Fuel cycle activity		Time, t (years)	Activity Cost Calculation
Mining and Milling		-2	Per unit mass yellow cake cost (Section 4.1.1) X Mass of Ore (Table 7-1)
Conversion		-1.5	Per unit conversion cost (Section 4.1.2) X Mass of Ore (Table 7-1)
Enrichment		-1	Per SWU cost (Section 4.1.3) X SWU required (Table 7-1)
Fabrication (FAB)	TRISO	-.5	Per unit TRISO fabrication cost (Section 5.2.1a) X Heavy metal mass in fuel (Table 2-3)
	Pebble material	-.5	Per unit cost of material in pebble (Section 4.3) X Mass of pebble material (Table 2-3)
	Pebble manufacture	-.5	Per pebble manufacture cost (Section 5.2.2a) X Number of pebbles (Table 2-3)
	QA	-.5	QA cost per pebble (Section 5.2.3a) X Number of pebbles (Table 2-3)
Interim storage (int)		T _{op} +5	Calculated in Table 6-2
Salt repository (sr)		T _{op} +25	Calculated in Table 6-4

Step-3 (Calculating the present value)

For each activity in Table 7-2 and Table 7-3, present value is calculated using Equation 2.

$$PV = \frac{\text{Activity Cost}}{(1 + r)^t} \quad \text{Equation 2}$$

Where:

r: discount rate (6%), t: time of activity wrt fuel load (in years). US EIA report [37] uses WACCs to calculate LCOE for plants entering service in 2024 and 2040 as 5.6% and 6.5%, respectively. For the purpose of this analysis, a average WACC of 6% is assumed.

Step-4 (Calculating LCOF (Component wise and aggregate))

First, the present value of these costs is annualized using the capital recovery factor (CRF) calculated using Equation 3.

$$CRF = \frac{r \cdot (1 + r)^{t_{op}}}{(1 + r)^{t_{op}} - 1} \quad \text{Equation 3}$$

Where:

r: discount rate (6%, as used for PV calculation in step-3),
 t_{op} : reactor operating time (varies by concept, derived from Table 2-1 for prismatic concepts, Table 2-3 for pebble bed concepts)

Second, the electricity units generated in one year (P) is calculated using Equation 4.

$$P = \text{Plant capacity} \times CF \times 8760 \quad \text{Equation 4}$$

Where:

Plant capacity = 5 MWe (Assuming plant efficiency of 50% for all concepts, Efficiency as high as 53% is proposed for GA EM² advanced reactor [38])
 CF = Capacity factor (Assumed 93% based on current US fleet albeit optimistic considering frequent outages in initial years of operation.)
 8760 = hours in one year

Finally, the LCOF is calculated by dividing the annualized cost by the annual electricity generation.

7.2 Levelized Cost of Fuel (LCOF) estimation for continuous recycle fuel cycle

As introduced in Section 3.1, continuous recycle scenarios add complexity by reusing materials from a stage-1 reactor in stage-2 microreactors.

Step-1 (Identifying major activities and timeline)

Typical timelines assumed for this analysis are as follows. On the front end of the Sodium-Cooled Fast Reactor (SFR) fuel cycle, mining and milling of fresh ore begin about one year prior to core load. Six months before loading, the fabrication of the contact-handled blanket and remote-handled driver fuel is finalized. On the back end, spent fuel remains in a spent fuel pool for five years, after which it is reprocessed. A one-year interval follows for the interim storage of recovered transuranic and uranium, culminating in the final disposal of remaining high-level waste approximately six years after core unloading. Comparable timelines are employed for the microreactor cycle, where the front end involving fabricating plutonium-based TRISO fuel is

carried out six months before reactor loading, and the back-end timeline mirrors those of the SFR processes. Figure 7-2 graphically illustrates the major activities and timelines for continuous recycle fuel cycle.

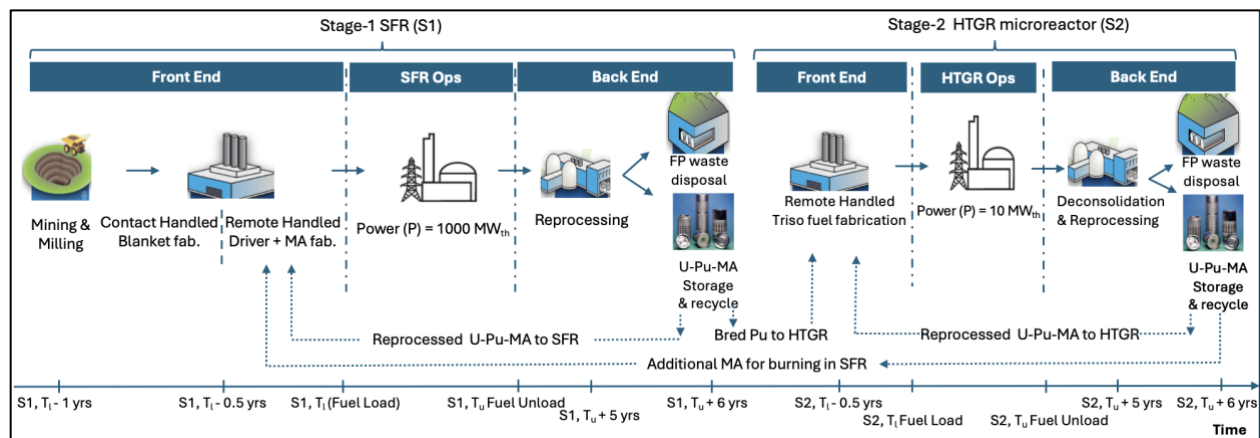


Figure 7-2 Major activities in a continuous recycle fuel cycle with timeline

Step 2 (Finding the cost associated with each activity)

Table 7-4, Table 7-5 and Table 7-6 are the cost basis tables used to calculate the cost of the fuel cycle activities for the SFR, Prismatic microreactor, and pebble bed microreactor.

Table 7-4 Cost basis for stage-1 SFR

Fuel cycle activity	Time, t (years)	Activity Cost Calculation
Mining and Milling	-1	Per unit mass ore cost (Section 4.2.1) X Mass of Ore (Appendix 1)
Contact handled blanket fabrication	-0.5	Per unit mass blanket fabrication cost (Section 4.2.2) X Mass of fuel in blanket (Appendix 1)
Remote handled driver fabrication	-0.5	Per unit mass driver fabrication cost (Section 4.2.3) X Mass of fuel in driver (Appendix 1)
Reprocessing costs	$T_{op-sfr} + 5$	Per unit mass reprocessing cost (Section 4.2.4) X Total Mass of fuel (Appendix 1)
FP disposal costs	$T_{op-sfr} + 6$	Per unit mass fission product disposal cost (Section 4.2.6) X Mass of Fission product (Appendix 1)
U-Pu-MA handling & storage costs	$T_{op-sfr} + 6$	Per unit mass U-Pu-Ma storage cost (Section 4.2.5) X Mass of Separated U-Pu-Ma (Appendix 1)

Table 7-5 Cost basis for continuous recycle prismatic concepts

Fuel cycle activity		Time, t (years)	Activity Cost Calculation
Fabrication	TRISO	-0.5	TRU based TRISO fabrication cost/kgHM (Section 5.1.1b) x fuel mass (Table 2-2)
	Compact material	-0.5	Cost of material per unit mass (Section 4.3) x material mass in compact (Table 2-2)
	Compact manufacture	-0.5	Manufacture cost per compact (Section 5.1.2b) x Number of compacts (Table 2-2)
	Fuel block material	-0.5	Cost of material per unit mass (Section 4.3) x material mass in fuel block (Table 2-2)

	Fuel block manufacture	-0.5	66% of total material cost
	QA	-0.5	Unit TRISO QA cost (Section 5.1.3b) X Mass of HM in fuel (Table 2-2) + Compact QA cost (Section 5.1.3b)
Deconsolidation & Reprocessing costs		$T_{op-mr} + 5$	Per unit mass deconsolidation & reprocessing cost (Section 4.2.8) X Mass of fuel (Table 2-2)
FP disposal costs		$T_{op-mr} + 6$	Per unit fission product disposal cost (Section 4.2.10) X Mass of fission product (Table 2-2)
U-Pu-MA handling & storage costs		$T_{op-mr} + 6$	Per unit U-Pu-Ma storage cost (Section 4.2.9) X Mass of separated U-Pu-Ma (Table 2-2)

Table 7-6 Cost basis for continuous recycle pebble bed concepts

Fuel cycle activity		Time, t (years)	Activity Cost Calculation
Fabrication	TRISO	-0.5	Pu TRISO fabrication cost/kgHM (Section 5.2.1b) x Fuel mass (Table 2-4)
	Pebble material	-0.5	Unit material cost (Section 4.3) x Mass of material (Table 2-4)
	Pebble manufacture	-0.5	Unit pebble cost (Section 5.2.2b) x Number of pebbles (Table 2-4)
	QA	-0.5	Unit pebble QA Cost (Section 5.2.3b) x Number of pebbles (Table 2-4)
Deconsolidation & Reprocessing costs		$T_{op-mr} + 5$	Per unit mass Deconsolidation & reprocessing cost (Section 4.2.8) x Fuel mass (Table 2-4)
FP disposal costs		$T_{op-mr} + 6$	Per unit fission product disposal cost (Section 4.2.10) X Mass of fission product (Table 2-4)
U-Pu-MA handling & storage costs		$T_{op-mr} + 6$	Per unit U-Pu-Ma storage cost (Section 4.2.9) X Mass of separated U-Pu-Ma (Table 2-4)

Step-3 (Calculating the present value)

For each activity in Table 7-4, Table 7-5, and Table 7-6, calculate the present value using Equation 2.

Step-4 (Calculating LCOF (Component wise and aggregate))

(a) Standalone microreactor (Calculating LCOF (Component wise and aggregate))

The present value of the costs as calculated in Table 7-5 for standalone continuous recycle prismatic concepts and Table 7-6 for standalone continuous recycle pebble bed concepts is annualized using the capital recovery factor (CRF) calculated using Equation 3. The annual electricity units produced (P) is calculated using Equation 4. Finally, the LCOF is calculated by dividing the annualized cost by the annual electricity generated.

(b) Fleet mode (Calculating LCOF (Component wise and aggregate))

The present value of costs associated with stage-1 (SFR) as calculated in Table 7-4 and stage-2 (Micro reactor) as calculated in Table 7-5 for prismatic design and Table 7-6 for standalone pebble bed concepts is annualized using Equation 5.

$$C_{\text{combined}} = r \cdot \frac{PV_1 + N \cdot PV_2 \cdot e^{-rT_2}}{E_1 \cdot (1 - e^{-rT_1}) + N \cdot E_2 \cdot (e^{-rT_2} - e^{-rT_3})} \quad \text{Equation 5}$$

Where:

E1 = Annual electricity generated from SFR = SFR plant capacity X CF X 8760

SFR plant capacity = 330 MWe

E2 = Annual electricity generated from MR = MR plant capacity X CF X 8760

Micro reactor plant capacity = 5 MWe (All concepts)

N = Number of MR per SFR

(Table 2-2 for prismatic concepts, Table 2-4 for pebble bed concepts)

CF = Capacity factor (Assumed 93% based on current US fleet)

8760 = hours in one year

r: discount rate (6%)

T₁ = SFR operating duration = 4.9 years

T₂ = MR beginning of fuel load from SFR fuel load = 10.4 years

T₃ = MR end of operation from SFR fuel load = 10.4 + MR operating time

(Table 2-2 for prismatic concepts, Table 2-4 for pebble bed concepts)

7.3 Sensitivity analysis

To estimate the primary cost drivers, a sensitivity analysis is carried out by varying one parameter at a time by $\pm 20\%$ and looking at the resulting effect on LCOF. The process and material cost variables changed in the sensitivity analysis are shown in Table 7-7.

Table 7-7 Variables considered for sensitivity analysis:

Once-Through cycle		Continuous recycle fuel cycle	
Process costs	Material Costs	Process costs	Material Costs
Mining & Milling cost	MgO	Contact handled blanket fabrication cost	MgO
Conversion cost	BeO	Remote handled driver fabrication cost	BeO
Enrichment cost	Be	Reprocessing cost	Be
Fuel fabrication cost	YH	Fission product disposal cost	YH
	ZrH	Recycled Pu TRISO Fabrication cost	ZrH

7.4 Montecarlo analysis

Monte Carlo (MC) simulations is carried out to account for the uncertainty in the model parameters. The parameters considered for the Montecarlo analysis, along with the ranges, is discussed next

Fabrication cost variation

The Advanced Fuel Cycle Cost Basis report [13] indicates that lower-bound TRISO fuel fabrication costs of \$1,000/kgHM are achievable in optimized production scenarios. This cost specifically represents NOAK facilities operating at high production volumes (hundreds of MTU/year) while focusing exclusively on TRISO particle production, excluding the additional manufacturing steps for final fuel forms such as compacts or pebbles. This bottom range

explicitly assumes highly automated production lines servicing multiple reactor fuel vendors and excludes the higher costs associated with HEU TRISO production that would require Category-I facilities (Facilities enriching uranium to $\geq 20\%$ U-235 (HEU production)). As an enrichment up to 19.9% in Category-II facility (Facilities enriching uranium to 10-20% U-235) is required for the fuel considered in this analysis, as well as with the inclusion of pebble/compact materials, an increased lower bound of \$2,000/ kgHM (100% margin) is assumed for analysis.

Conversely, the Advanced Fuel Cycle Cost Basis report [13] also discusses projected costs up to \$10,000/kgHM for very small facilities (<5 MTU/yr) that are more FOAK than NOAK. These higher costs are particularly relevant for the next decade as early facilities come online, notably including the complete manufacturing process through to final fuel forms such as blocks, planks, or pebbles. This value serves as the higher bound for Monte Carlo analysis.

Enrichment cost variation

The cost structure of uranium enrichment services demonstrates significant variation based on enrichment levels, primarily due to facility requirements. For standard enrichment up to 6% U-235, the current spot price is established at 138 USD per Separative Work Unit (SWU), reflecting operations in conventional Category III facilities.

For enrichment levels exceeding 10%, which requires Category II fuel fabrication facilities, industry experts indicate costs might be approximately 3 to 5 times higher than current prices [39]. It is worth noting that the actual costs may vary depending on factors such as enrichment technology advancements, economies of scale, and changes in regulatory requirements. However, the general principle of higher costs for increased enrichment levels remains valid and is essential for consideration for future higher enrichment scenarios. An upper limit of \$500/ SWU is assumed for the Montecarlo analysis.

Entrained moderator cost variation

The Monte Carlo analysis for cost uncertainty of key metals (Beryllium, Yttrium, Zirconium) utilized historical price trends and manufacturing process assumptions. Historical price data for Beryllium, Yttrium, and Zirconium were extracted from the USGS database [40] from 2001 to 2022 to establish baseline costs and variability ranges, are plotted in Figure 7-3.

Historical price deviations were then analyzed to quantify uncertainty ranges. Zirconium showed substantial volatility with maximum and minimum deviations of +346% (14.4 to 64.2 USD/kg) and -52% (14.4 to 6.9 USD/kg), respectively. Yttrium demonstrated even greater variation, ranging from +446% (19.7 to 107.3 USD/kg) to -15% (19.7 to 16.7 USD/kg). Beryllium exhibited more moderate fluctuations of +16% (316.4 to 366.4 USD/kg) and -61% (316.4 to 124.5 USD/kg). These ranges form the basis for subsequent Monte Carlo simulations in the cost uncertainty analysis.

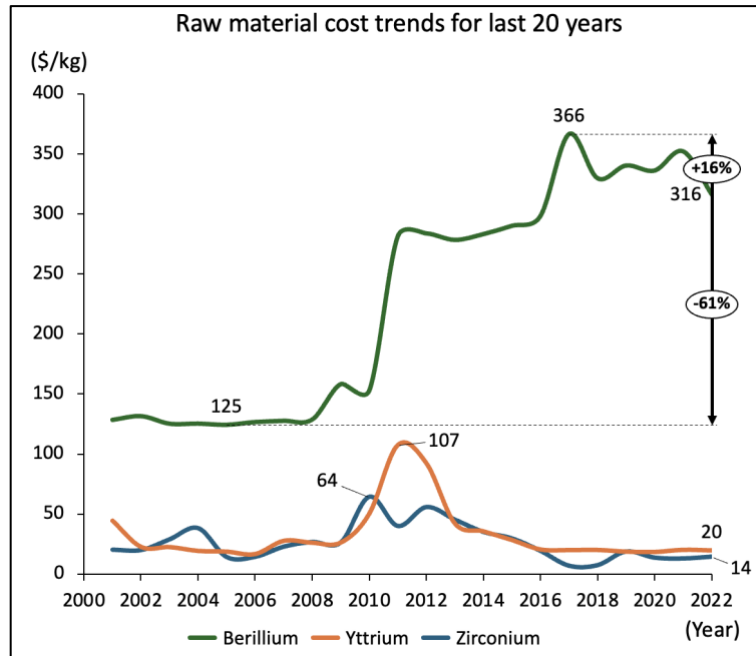


Figure 7-3 Historical data of Beryllium, Yttrium and Zirconium

Monte Carlo cost variation

Applying these deviations to the baseline cost from Section 4.3 (BeO-\$816/kg, Be-\$2313/kg, YH-\$175/kg, ZrH-\$160/kg) yields the following Monte Carlo cost ranges: Beryllium Oxide: USD 321–945/kg, Beryllium Metal: USD 910–2,678/kg, Yttrium hydride: USD 149–955/kg, Zirconium hydride: USD 76–714/kg

Table 7-8 Summary of the Monte Carlo range for process and material costs

Parameters		Low value	High value
Fabrication cost (Clean TRISO fabrication)		\$2000/ kgHM	\$10000/ kgHM
Fabrication cost (Recycled TRISO fabrication)		\$4000/ kgHM	\$12000
Enrichment cost		\$138/ SWU	\$500/ SWU
Cost of entrained moderator	BeO	\$321/kg	\$945/kg
	Be	\$910/kg	\$2678/kg
	YH	\$149/kg	\$955/kg
	ZrH	\$76/kg	\$714/kg

A uniform probability distribution is assumed for each parameter in a Monte Carlo simulation rather than assigning a fixed value. The code then runs 200,000 versions of the LCOF model, randomly picking parameter values according to uniform distribution each time based on Table 7-8. The result is a distribution of levelized costs, which represents the uncertainty of the real world.

8 Results & Discussion LCOF using deterministic approach, Sensitivity Analysis & Montecarlo Analysis

This chapter presents the findings from an economic assessment of advanced microreactor concepts. Prismatic and pebble bed microreactor configurations featuring four different moderator materials under Once-Through and continuous recycle fuel-cycle strategies are compared to offer a comprehensive perspective on deterministic and probabilistic economic performance.

Chapter Organization

Section 8.1: Once-Through Prismatic Microreactors

An analysis of the LCOF results for prismatic cores under a once-through fuel strategy is presented. Sensitivity and Monte Carlo techniques are applied to highlight major cost drivers and variability, focusing on how different moderators influence economic performance.

Section 8.2: Once-Through Pebble-Bed Microreactors

A parallel investigation is performed for pebble-bed designs utilizing a once-through cycle, and comparisons with prismatic outcomes are provided.

Section 8.3: Deconsolidation Merits

The practice of removing inert moderator material from spent fuel is examined. Reductions in repository footprint, disposal canisters, and associated back-end costs are quantified, along with an analysis of threshold deconsolidation costs under both deep borehole and geological repository scenarios.

Section 8.4: Continuous Recycle (Prismatic, Stand-alone Only)

The economics of a multi-recycle model are investigated on a standalone basis for prismatic microreactors. Deconsolidation, reprocessing, and waste disposal are incorporated to determine the effects on LCOF, emphasizing moderator-based trade-offs in fabricating and reprocessing TRISO fuel.

Section 8.5: Continuous Recycle with SFR + Prismatic Microreactor

The interaction of a Sodium Fast Reactor (Stage 1) and prismatic microreactor (Stage 2) is assessed, noting how costs related to driver fabrication, reprocessing, and waste management are allocated. The extent to which the SFR dominates the overall LCOF is highlighted.

Section 8.6: Continuous Recycle (Pebble-Bed, Stand-alone Only)

A standalone continuous recycle strategy is addressed for pebble-bed microreactors, including assumptions on extended burnup and ultra-long residence times.

Section 8.7: Continuous Recycle with SFR + Pebble-Bed Microreactor

A two-stage nuclear system is considered, wherein an SFR supplies recycled TRU for a pebble-bed microreactor. The contribution of microreactor-specific fabrication and moderator material costs relative to the SFR's share is analyzed.

8.1 Once-Through cycle | Prismatic microreactor

This section analyzes the Levelized Cost of Fuel (LCOF) for various Once-Through prismatic microreactor concepts based on the methodology outlined in Chapter 7. The following discussion presents a comparative evaluation of the results and compares them to the baseline graphite case.

8.1.1 LCOF cost drivers

Figure 8-1 illustrates each concept's LCOF results utilizing a stacked bar chart. These visualizations show the overall cost distribution and the contribution of individual cost components.

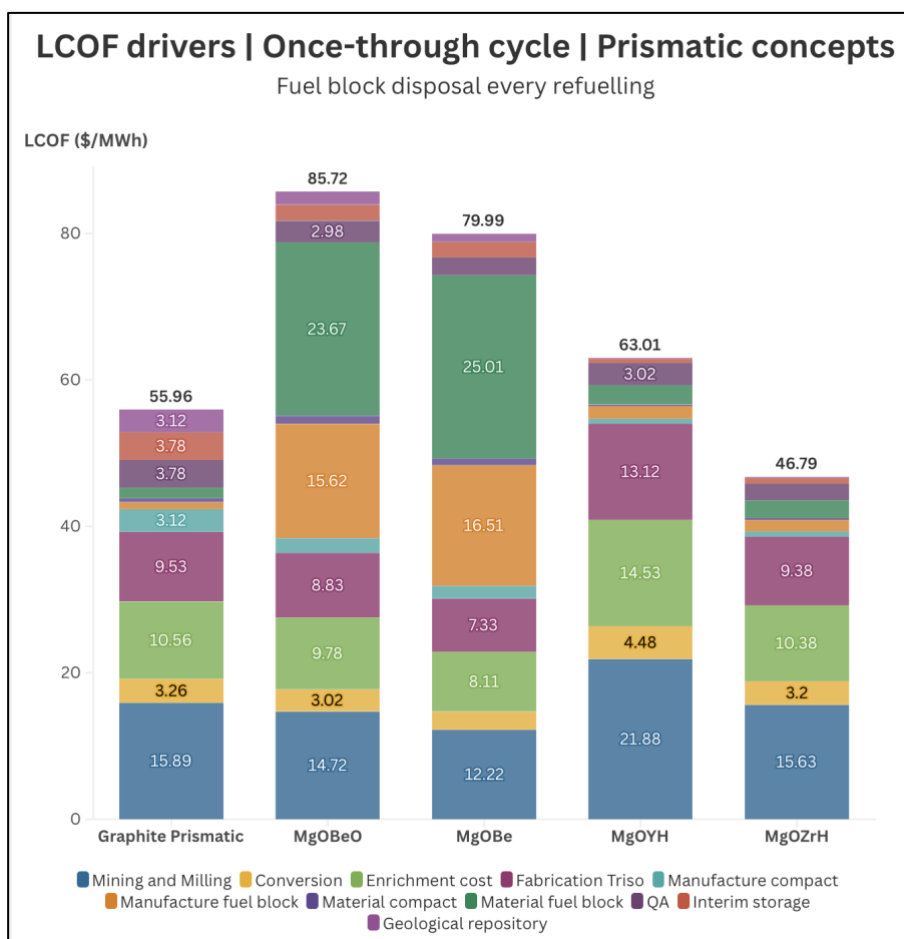


Figure 8-1 LCOF distribution across different Once-Through prismatic reactor concepts [fuel block single use]

The baseline graphite design, at \$55.96/MWh, is a reference for all other configurations. MgO–BeO has the highest LCOF at \$85.72/MWh, roughly 53% higher than the baseline, owing to the elevated price of beryllium oxide. MgO–Be reaches \$79.99/MWh, about 43% above the graphite benchmark, and faces similarly high material costs due to specialized handling requirements for beryllium. MgO–YH exhibits \$63.01/MWh, representing a 13% increase over graphite, driven primarily by additional mining, milling, and enrichment costs accompanying its higher initial uranium requirements. Finally, MgO–ZrH achieves the most favorable

deterministic value at \$46.79/MWh, approximately 16% lower than the baseline, reflecting relatively modest zirconium hydride expenses and manageable manufacturing overhead.

It is clearly seen that the material and manufacturing costs associated with fuel block during each fuel load are the major cost drivers. Thus, recycling fuel blocks could provide a strong value proposition to improve the overall economics of these concepts.

Discussion of fuel block recycling in once-through prismatic core concepts

The economic analysis of fuel block recycling in once-through prismatic concepts reveals compelling advantages, as shown in Figure 8-2. The most immediate benefit is the substantial cost reduction across all designs, with beryllium-based cores demonstrating significant improvements - MgO-Be achieving a 52% LCOF reduction (from \$79.99/MWh to \$38.54/MWh) and MgO-BeO showing a 46% decrease (from \$85.72/MWh to \$46.49/MWh). Even designs with more modest improvements (5-8% for graphite prismatic, MgO-YH, and MgO-ZrH cores) show meaningful cost benefits through eliminated manufacturing costs and reduced material requirements.

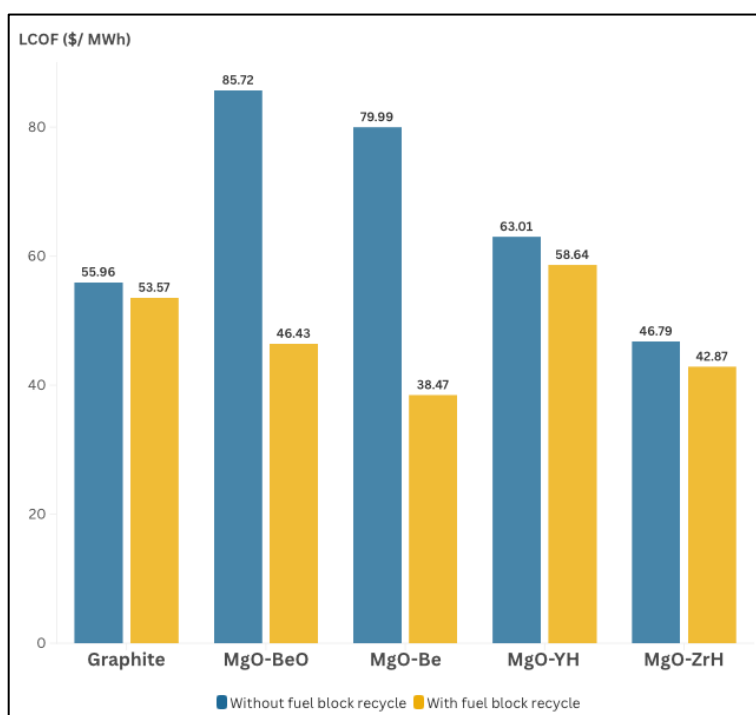


Figure 8-2 LCOF distribution across different Once-Through prismatic reactor concepts w/wo fuel block recycling

Beyond economic considerations, recycling offers significant advantages in safety and resource utilization. For beryllium-containing designs, reduced handling frequency minimizes occupational exposure risks. The strategy promotes efficient resource utilization of specialized materials and significantly reduces waste volume, as only spent fuel compacts require disposal. This approach could potentially streamline waste management procedures while providing operators with greater flexibility in fuel management strategies.

However, several critical challenges must be addressed before the implementation of fuel block recycling. The primary concern lies in validating material performance under extended

operating conditions. Long-term material behavior and mechanical integrity over multiple cycles require thorough assessment. Fuel block recycling will require comprehensive development of technical requirements, safety protocols, and quality assurance measures. These process development and handling costs, which are not included in the current LCOF analysis, could impact the ultimate economic benefits.

Nevertheless, the substantial cost reductions observed, combined with safety and resource utilization benefits, justify the continued development of this approach. Future work should focus on material performance studies and detailed economic assessments incorporating facility costs and risk mitigation measures.

Moderator cost threshold analysis for prismatic microreactors: Achieving LCOF parity with baseline.

Under current manufacturing processes, the Levelized Cost of Fuel (LCOF) for MgO-BeO, MgO-Be, and MgO-YH prismatic microreactor concepts exceeds the baseline graphite design. The higher expense of entrained moderator materials largely drives this cost differential. To establish the moderator cost thresholds required for these reactors to reach parity with the baseline graphite LCOF, Excel's Goal Seek function was used to set each concept's LCOF to \$55.96/MWh.

It was observed that the concepts incorporating yttrium hydride retain higher LCOF values than the baseline graphite design, regardless of moderator cost, indicating persistent economic challenges. Prismatic cores that rely on beryllium moderators become more cost-competitive when raw beryllium costs drop below \$798/kg. Similarly, BeO costs must fall below \$54/kg to achieve an LCOF on par with baseline graphite. These findings underscore the need for strategies to reduce the cost of entrained moderator materials like improved sourcing or long-term contracts to improve the economic appeal of advanced microreactor configurations.

The following subsections incorporate sensitivity and Monte Carlo analyses to assess the degree of cost risk when key parameters, including moderator pricing and upstream fuel processes like enrichment and fabrication, vary under realistic market conditions.

8.1.2 Sensitivity Analysis

Figure 8-3 summarizes the impact of $\pm 20\%$ variations in process and material cost parameters on the LCOF of each design. Key observations are summarised below.

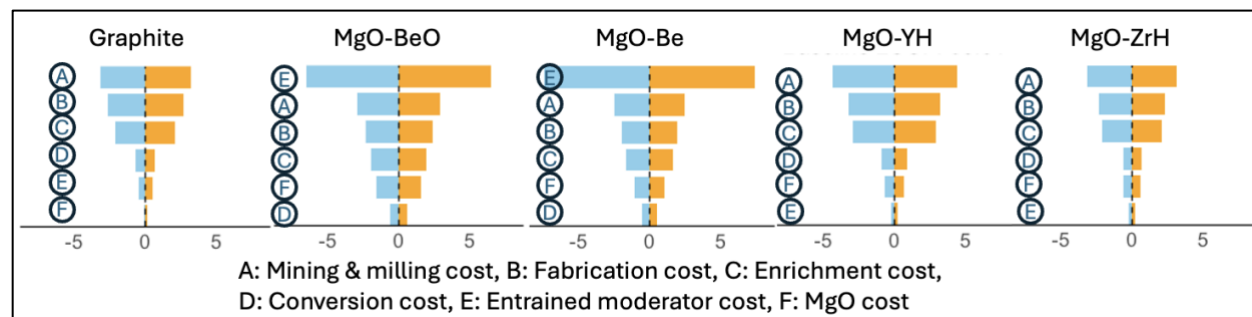


Figure 8-3 Sensitivity analysis of LCOF components for different OT prismatic reactor concepts

The baseline graphite configuration exhibits its strongest sensitivity to upstream fuel processes, especially mining and milling at about $\pm\$3.2/\text{MWh}$, while fuel fabrication demonstrates a moderate influence of $\pm\$2.7/\text{MWh}$, and conversion exerts minimal impact of approximately $\pm\$0.6/\text{MWh}$. These findings underscore how graphite's overall cost structure remains balanced, with no single component overwhelmingly driving LCOF fluctuations.

For advanced moderators, MgO–BeO shows heightened vulnerability to the price of beryllium oxide, with variations near $\pm\$6.5/\text{MWh}$, reflecting both the elevated cost of BeO as a raw material and the associated machining/fabrication losses pose challenges to amplify overall cost swings. MgO–Be exhibits similar instability, with the sensitivity to beryllium moderator costs approaching $\pm\$7.4/\text{MWh}$. This design faces added handling constraints associated with beryllium, which can further magnify the effect of any price shifts.

MgO–YH, on the other hand, reveals a higher dependence on mining and milling costs at about $\pm\$4.4/\text{MWh}$, owing to its higher uranium requirements, while enrichment changes of around $\pm\$2.9/\text{MWh}$ also influence the final LCOF. Finally, MgO–ZrH demonstrates a relatively balanced sensitivity profile, with mining and milling again taking the lead at $\pm\$3.1/\text{MWh}$, whereas the cost of zirconium hydride remains comparatively modest. This outcome suggests that stable and reasonably priced ZrH supplies could ensure a strong cost-benefit advantage for MgO–ZrH, provided other supply chain elements remain predictable.

Overall, the sensitivity analysis shows that while the baseline graphite concept maintains moderate and predictable cost drivers, advanced moderator designs can exhibit substantial swings in LCOF depending on raw material availability, specialized handling requirements, and broader uranium market variations. These observations highlight the necessity of secure and cost-effective supply chains for key materials and fuel block production improvements that could mitigate the most extreme cost fluctuations.

8.1.3 Monte Carlo analysis

Figure 8-4 presents the Monte Carlo simulation results that account for concurrent uncertainties in enrichment, fabrication, and moderator material pricing. This probabilistic approach offers a broader perspective on how real-world volatility may amplify total fuel-cycle expenditures, moving beyond the single-point estimates of deterministic calculations.

The baseline graphite design in these simulations has a mean LCOF of $\$65.73/\text{MWh}$, roughly 18% higher than its deterministic value of $\$55.88$. The relatively narrow spread (from about $\$49.37$ to $\$81.26$) and a standard deviation of 7.77 reflect graphite's well-established supply infrastructure and simpler fabrication processes. In contrast, MgO–ZrH exhibits the most pronounced gap between deterministic and mean LCOF figures, rising from $\$46.78$ to $\$76.80$. This 64% difference suggests that uncertainties in zirconium hydride sourcing and potential enrichment cost spikes can substantially affect its overall cost benefits.

MgO–Be has a mean LCOF of $\$94.63/\text{MWh}$, which exceeds its deterministic figure of $\$79.99$ by around 18%. Although this gap is smaller than that observed in MgO–ZrH, it underscores the cost implications associated with potential market volatility and higher enrichment costs. MgO–BeO experiences an approximate 23% jump from $\$85.72$ to $\$105.01/\text{MWh}$, reflecting both the

high base price of beryllium oxide and the possibility of disruptions in BeO supply or manufacturing.

Finally, MgO–YH stands out as the most volatile option, registering a mean LCOF of \$102.61/MWh compared to its deterministic outcome of \$63.01, implying a 63% increase. This volatility arises from uncertainties in yttrium hydride pricing, combined with the hydride design’s heavier reliance on initial heavy metal, thus increasing the dependence on potentially expensive Cat-II enrichment facilities. Across all advanced moderators, results show that realistic market and process instabilities can drive mean LCOFs between 15% and 60% above deterministic calculations, underscoring the importance of thorough risk assessment in microreactor economics.

8.1.4 Key implications and recommendations

The analysis carried out demonstrates how moderator selection can influence Once-through prismatic microreactor economics. Although MgO–ZrH appears highly competitive under deterministic assumptions, its cost advantage depends on secure, reasonably priced zirconium hydride sources.

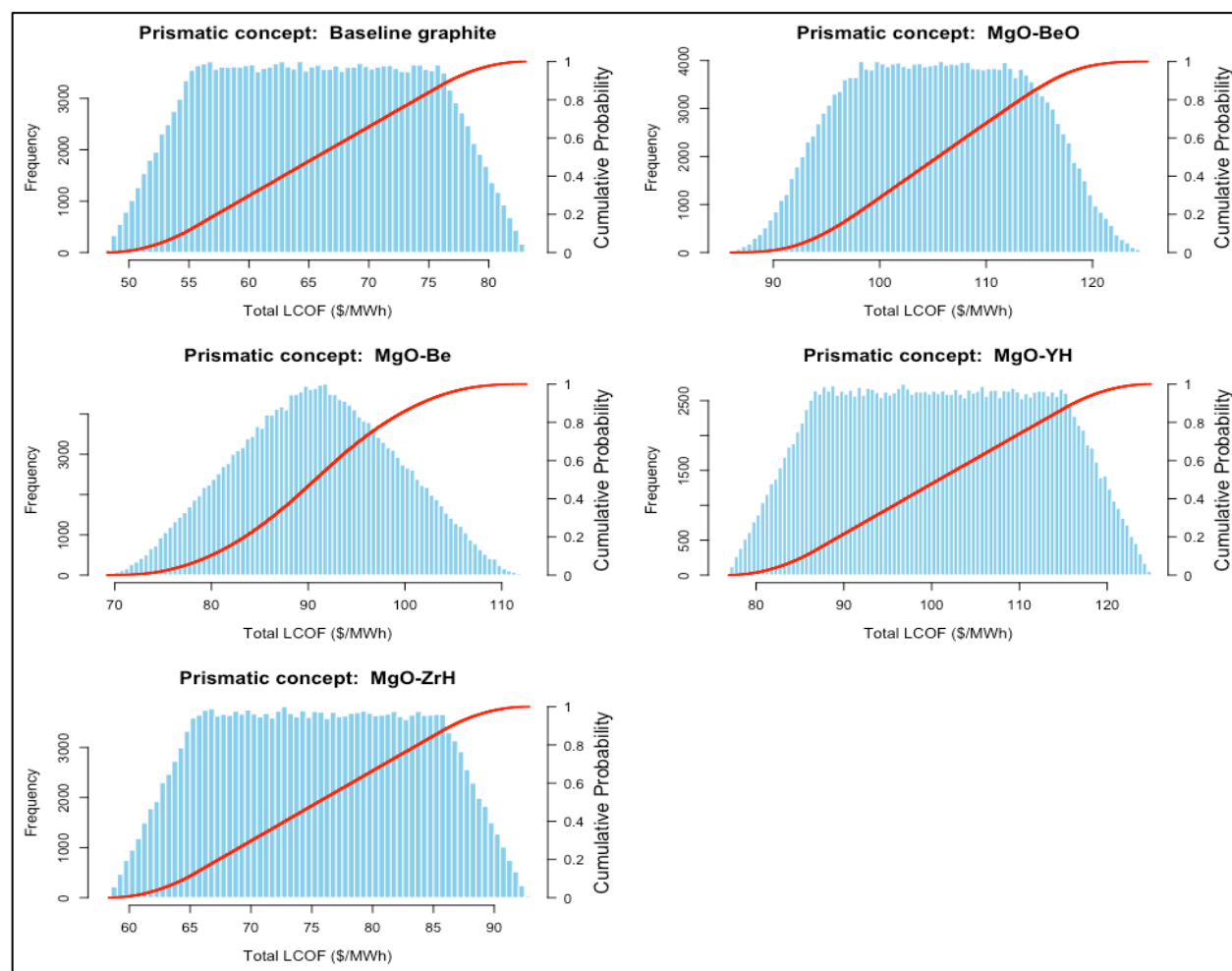


Figure 8-4 Histogram and cumulative distribution function (CDF) of LCOF for different OT prismatic reactor concepts. The blue histograms show the frequency distribution of LCOF outcomes, while the red curves represent cumulative probabilities, providing insights into the likelihood of achieving specific cost targets.

Proactive industry engagement, along with further research and development to streamline ZrH production, could help realize the full economic potential of this concept. Conversely, beryllium-based designs carry large cost premiums but might remain appealing if technological breakthroughs in beryllium extraction, fabrication, and recycling significantly lower costs.

Across all prismatic configurations, upstream fuel processes such as uranium mining and milling remain major cost contributors, signaling advanced contracting strategies can help reduce LCOF volatility. The gap between deterministic and probabilistic outcomes, which in many cases ranges from 15% to over 60%, highlights that any single-point estimate may underestimate the real-world challenges of market pricing, technological challenges, and complex supply chains. Consequently, risk assessments should remain integral to design and commercialization decisions, factoring not just baseline cost expectations but also the variance around them.

8.2 Once-Through cycle | Pebble-bed microreactor

This section analyzes the Levelized Cost of Fuel (LCOF) for various pebble bed microreactor concepts in the Once-Through scenario.

8.2.1 LCOF cost drivers

Figure 8-5 presents a stacked bar chart of deterministic LCOF outcomes, highlighting how front-end and back-end costs contribute to each design's economic performance. MgO–ZrH demonstrates the most competitive LCOF at \$33.12/MWh, driven primarily by mining and milling (\$11.28/MWh) and enrichment (\$7.49/MWh) activities. This design achieves a 73% reduction in material costs compared to its prismatic counterpart, underscoring the inherent material efficiency of the pebble bed architecture. MgO–BeO, at \$39.67/MWh, is about 19.8% higher than MgO–ZrH and still avoids the severe moderator cost penalties observed in prismatic systems. Its mining costs of \$11.37/MWh and enrichment costs of \$7.55/MWh reflect a more balanced front-end expenditure, while material expenses decline to \$7.23/MWh, marking a substantial reduction from the \$23.67/MWh recorded in prismatic designs.

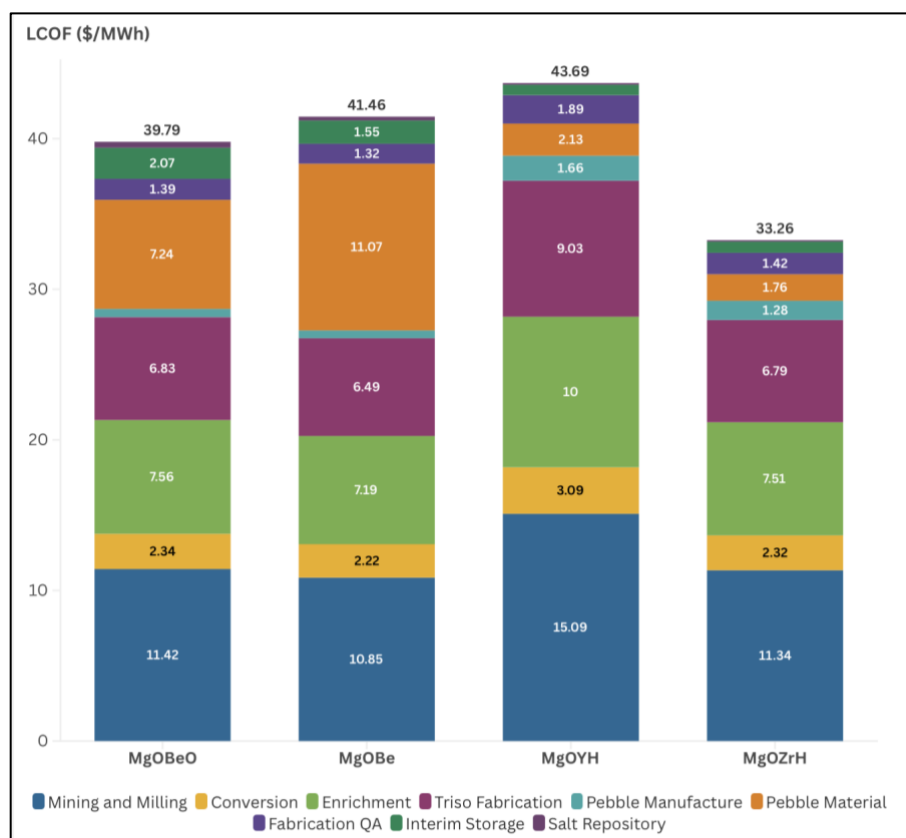


Figure 8-5 LCOF distribution across different Once-through pebble-bed reactor concepts

MgO–Be exhibits an LCOF of \$41.49/MWh, 25.3% higher than MgO–ZrH. Although beryllium-related expenses remain a concern, the pebble bed form effectively reduces them relative to prismatic configurations; pebble material costs here register \$11.09/MWh, significantly below earlier block-manufacturing figures. Meanwhile, MgO–YH reaches \$43.77/MWh, the highest among the four variants. Elevated mining (\$15.11/MWh) and enrichment (\$10.03/MWh) requirements dominate front-end expenditures, yet pebble-based design choices help maintain

more reasonable manufacturing and material costs than the prismatic equivalent. Across all cases, back-end costs—such as interim storage and geological repository—show little variation, implying that optimizing front-end processes and manufacturing strategies holds the greatest potential for cost reductions.

These comparisons highlight several advantages of pebble bed architecture. More consistent fabrication costs, significantly lower moderator expenses, and a narrower LCOF range collectively demonstrate a more stable and scalable platform for commercial deployment. Unlike prismatic systems, whose LCOFs can vary by nearly 40 units, pebble bed concepts exhibit a tighter span of around 10.65 units between the lowest and highest values. This narrower band underscores how pebble bed designs moderate the economic impact of specialized materials, offering greater flexibility in selecting moderators without risking prohibitive cost escalation.

8.2.2 Sensitivity analysis

The results of the sensitivity analysis are shown in Figure 8-6. The sensitivity analysis shows several critical patterns across the designs:

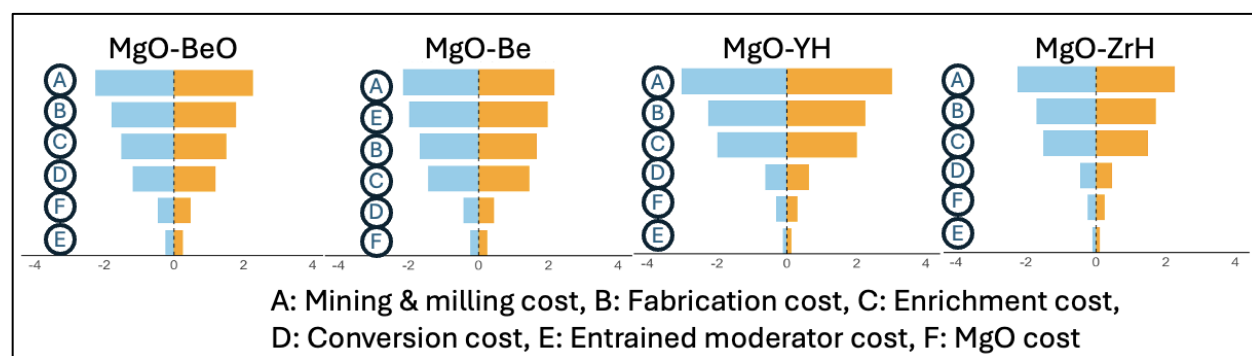


Figure 8-6 Sensitivity analysis of LCOF components for different Once-Through Pebble bed reactor concepts

MgO-BeO emerges with a primary sensitivity to mining costs ($\pm\$2.2/\text{MWh}$), which constitute about 5.4% of its baseline LCOF. Secondary drivers include enrichment ($\pm\$1.5/\text{MWh}$) and fabrication expenses ($\pm\$1.7/\text{MWh}$). The cost of the entrained moderator affects MgO-BeO by about $\pm\$1.1/\text{MWh}$, a notable decline from the pronounced moderator sensitivity observed in prismatic designs. MgO-Be reveals a similar emphasis on mining ($\pm\$2.2/\text{MWh}$) and fabrication ($\pm\$1.7/\text{MWh}$) but shows a somewhat higher entrained moderator sensitivity of $\pm\$2.0/\text{MWh}$. Although this remains substantial within the pebble bed framework, it remains far below prismatic beryllium sensitivities, often exceeding $\pm\$7.0/\text{MWh}$. Enrichment sensitivity aligns with other concepts at around $\pm\$1.5/\text{MWh}$.

MgO-YH registers the highest mining cost sensitivity ($\pm\$3.0/\text{MWh}$) among these configurations, reflecting its elevated uranium consumption. It also exhibits a comparatively strong response to fabrication changes ($\pm\$2.2/\text{MWh}$) yet shows minimal entrained moderator sensitivity ($\pm\$0.1/\text{MWh}$), owing to lower YH costs. Meanwhile, MgO-ZrH maintains a balanced profile with mining and fabrication, each near $\pm\$2.2/\text{MWh}$, and minimal fluctuation in entrained moderator expenses ($\pm\$0.1/\text{MWh}$). Consistent low sensitivity to ZrH pricing reinforces MgO-ZrH as the most economically stable configuration in this series.

Overall, the analysis highlights how mining and fabrication concerns, rather than moderator expenses, dominate economic risk in pebble bed architectures, contrasting sharply with prismatic designs. By effectively mitigating the steep material cost sensitivity typically seen in advanced moderators, pebble bed concepts offer a more predictable cost structure, potentially making them more attractive for commercial-scale adoption.

8.2.3 Monte Carlo analysis

A Monte Carlo analysis used overlapping uncertainties in fabrication, enrichment, and moderator material costs. Figure 8-7 presents histograms illustrating the distribution of possible LCOF values for each configuration, along with cumulative distribution functions (CDFs) that summarize the overall probability range.

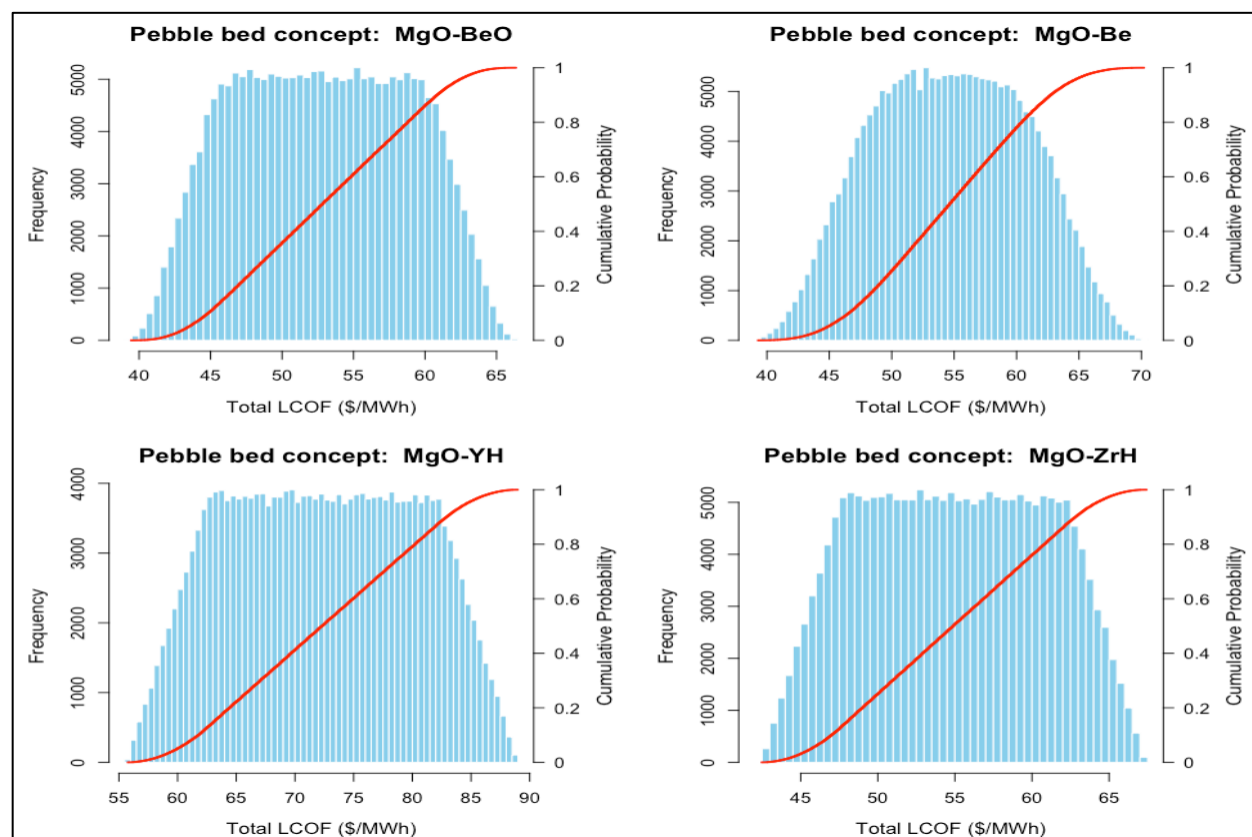


Figure 8-7 Histogram and cumulative distribution function (CDF) of LCOF for different OT Pebble-bed reactor concepts

MgO-BeO achieves a mean LCOF of \$52.66/MWh within a spread of \$38.16–\$67.26 ($\sigma = 6.05$). This indicates considerably reduced uncertainty compared to the prismatic MgO-BeO concept. MgO-Be's mean cost of \$56.32/MWh spans \$40.90–\$71.82 ($\sigma = 6.04$). Its absolute uncertainty is notably lower than in prismatic equivalents, which often exceeded \$70–\$80/MWh in mean cost, showing how the pebble bed arrangement moderates high beryllium-related financial risks.

MgO-YH, at a mean of \$73.60/MWh, shows a range of \$55.98–\$91.36 ($\sigma = 7.88$) and thus the largest uncertainty band among the pebble bed variants. However, it still maintains more consistent cost variability than its prismatic counterpart, whose higher initial fuel loading

translates to steeper LCOF fluctuations. Finally, MgO–ZrH demonstrates the most stable economic outlook, at \$55.75/MWh on average, with a range of \$42.50–\$69.10 ($\sigma = 5.89$). This consistency matches its prismatic version’s relative performance but at substantially lower absolute costs and narrower variability.

Two chief patterns emerge across all pebble bed configurations. First, their relative uncertainty levels fall within a tighter band of 10.6–11.5% of the mean cost, a marked improvement over prismatic designs. Second, their absolute uncertainty is also reduced, as seen in lower standard deviations. Together, these patterns underscore pebble bed reactors’ ability to provide more predictable economic performance, a key consideration for commercial projects where risk mitigation and financial stability frequently hold much importance.

8.2.4 Key implications and recommendations

Although MgO–ZrH offers the most favorable deterministic outcome, Monte Carlo simulations reveal that fluctuations in zirconium hydride supply and production costs can diminish its advantage if not carefully managed. Continued research on high-temperature hydrogenation processes and ensuring reliable sourcing could strengthen MgO–ZrH’s competitiveness by reducing cost overruns under uncertain market conditions.

Beryllium-based concepts, MgO–Be and MgO–BeO, demonstrate improved cost structures in pebble bed form but still rely on manageable beryllium sourcing. Technological innovations that reduce material costs remain central to stabilizing their economics. Across all four designs, the sensitivity analysis highlights uranium market volatility as a principal risk factor, signaling that long-term contracting or diversified fuel supply sources may be critical in minimizing price spikes for large-scale reactor fleets.

In sum, the pebble bed architecture emerges as a substantially more flexible platform for advanced moderator materials, offering narrower cost ranges and improved risk mitigation relative to prismatic designs. These findings suggest that future microreactor deployment could benefit from focusing on pebble bed configurations, particularly where cost predictability and resilience to material fluctuations are vital.

8.3 Deconsolidation merits and limiting cost for the deconsolidation process

As detailed in Chapter 6, many advanced microreactor designs generate a large volume of spent nuclear fuel (SNF). Even though the inert moderator holds negligible fissile content, it occupies significant canister volume—often exceeding the mass and decay heat as the primary limiting factor for disposal loading.

Benefits of deconsolidation

Dissolving the matrix reduces the mass and volume of disposed SNF, altering the limiting criteria for fuel disposal. Using the methodology as discussed in Section 6.4 the new limiting factor is recalculated for the deconsolidated SNF. The limiting number of canisters required per microreactor for the deconsolidated core under deep borehole concepts is shown in Table 8-1.

Table 8-1 Equivalent deep borehole canisters required per microreactor (after deconsolidation). The values in rows 1-3 indicate the number of borehole canisters dictated by criteria in column 1

Limiting Criteria	Prismatic Core					Pebble-bed Core			
	Graphite	MgOBeO	MgOBe	MgOYH	MgOZrH	MgOBeO	MgOBe	MgOYH	MgOZrH
Volume	2	2	2	8	6	3	3	6	4
Mass	1	1	1	3	2	1	1	2	2
Decay heat	1	2	2	8	7	3	5	8	8

Table 8-2 below shows the new equivalent number of MPC for the geological repository per microreactor for the different concepts.

Table 8-2 Equivalent MPCs required per microreactor for the geological repository (after deconsolidation). The values in rows 1-3 indicate the percentage of MPC filled dictated by criteria in column 1

Limiting Criteria	Prismatic Core					Pebble-bed Core			
	Graphite	MgOBeO	MgOBe	MgOYH	MgOZrH	MgOBeO	MgOBe	MgOYH	MgOZrH
Volume	0.96%	0.96%	0.96%	4.34%	2.89%	1.13%	1.53%	2.83%	2.18%
Mass	1.46%	1.84%	1.84%	8.29%	5.53%	2.16%	2.92%	5.4%	4.16%
Decay heat	3.0%	5.0%	6.3%	25.1%	21.2%	8.2%	14.6%	24.5%	24.5%

Overall, by comparing the initial estimates with no-deconsolidation (Table 6-3 and Table 6-4) vs. deconsolidation (Table 8-1, Table 8-2) it is clear that the repository burden—measured in total canisters—is reduced by tens of percent to well over 90% in many scenarios.

The reduced number of deep borehole canisters or multi-purpose canisters reduces the back end's expenditure. The reduced LCOF for the no-deconsolidation vs deconsolidated cases was calculated only for the back end part and is as below in Figure 8-8 and Figure 8-9.

While the disposal cost is a small percentage of the overall Levelized Cost of Fuel (LCOF), the analyses show a noteworthy percentage reduction in back-end costs once deconsolidation is applied. More importantly, the repository footprint (a strategic and environmental consideration) is substantially reduced since fewer canisters mean fewer drifts in a geologic repository or fewer boreholes in a deep borehole site.

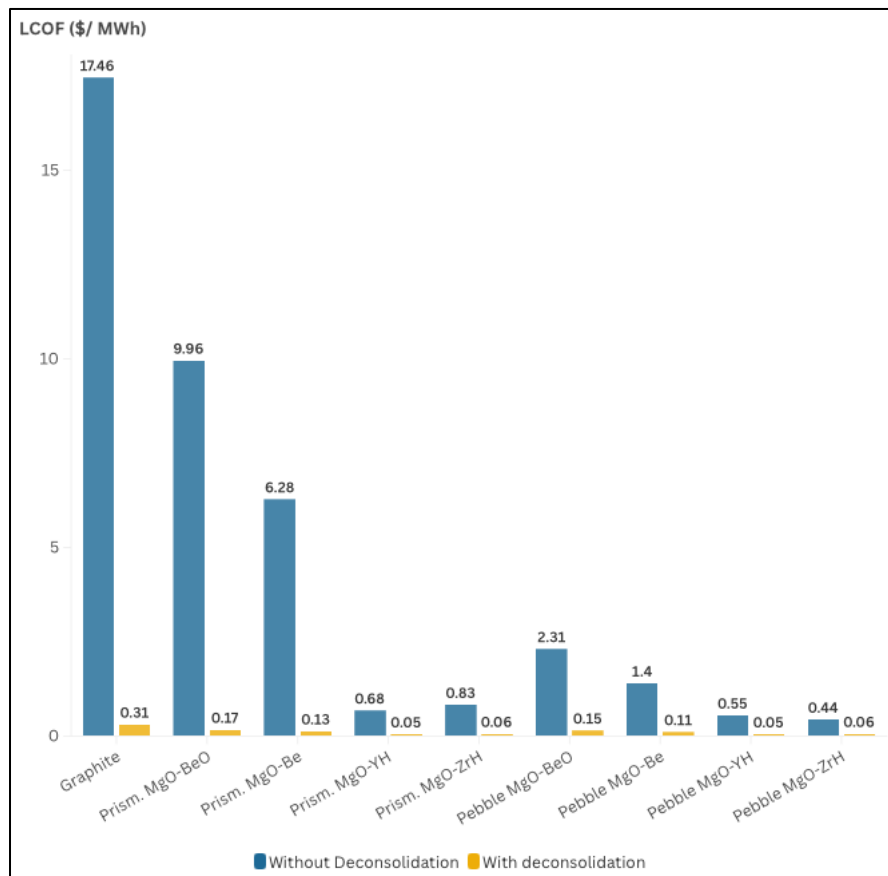


Figure 8-8 Disposal contribution to LCOF with and without deconsolidation for deep borehole

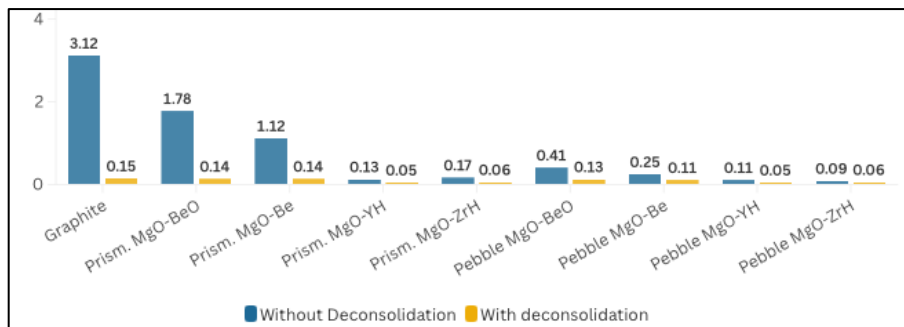


Figure 8-9 Disposal contribution to LCOF with and without deconsolidation for disposal in geological repository

As described in Section 6.4 (Threshold-Cost Analysis), the net economic benefit of deconsolidation is determined by threshold deconsolidation cost. Based on the canister-reduction data and disposal cost assumptions, Table 8-3 provides the maximum allowable deconsolidation cost (\$/kgHM) for each fuel-moderator combination based on the canister-reduction data and disposal cost assumptions.

The threshold cost can be very high for graphite fuels (where volume-limited canisters may be reduced by 95–99%), making deconsolidation economically viable even at substantial processing expenses. Deconsolidation must be relatively more cost-efficient to secure net savings for hydride-based moderators or certain pebble-bed configurations—where the baseline canister penalty is less. In qualitative terms, even if the direct cost threshold is

exceeded, a large footprint reduction can still be strategically beneficial for siting, public acceptance, and regulatory flexibility.

Table 8-3 Threshold deconsolidation costs for economic benefit

Moderator concept	Prismatic Concepts \$/kgHM	Pebble-bed Concepts \$/kgHM
Graphite	49,418	NA*
MgO-BeO	22,347	5,183
MgO-Be	15,254	3,409
MgO-YH	1,558	1,650
MgO-ZrH	2,057	1,653

*Graphite moderated pebble-bed design were not considered due to low burnup, driven primarily by the size constraints of fitting in a CONEX box.

In summary, deconsolidation substantially lowers the required canisters for both deep borehole and geologic repository concepts, resulting in large reductions in disposal footprint. While the resultant back-end cost savings are a relatively small portion of the total LCOF, the substantial footprint minimization is a critical benefit that can improve the overall feasibility, public acceptance, and environmental profile of once-through fuel cycles for advanced microreactors.

8.4 Continuous recycle (Only stage-2) | Prismatic microreactor

This section examines continuous recycling (CR) strategies for prismatic microreactors under a standalone Stage-2 framework. Unlike once-through cycles, CR approaches eliminate the enrichment requirement but introduce additional steps—such as deconsolidation, reprocessing, and by-product (fission product and minor actinide) handling.

8.4.1 LCOF cost drivers

Figure 8-10 provides a stacked bar chart comparing the LCOF for each prismatic reactor concept under continuous recycle conditions. These LCOFs integrate costs for TRISO fabrication, moderator materials, and recycling operations (deconsolidation, reprocessing, FP disposal, and MA storage), allowing a direct comparison of each advanced moderator against the baseline prismatic graphite configuration presented in Section 8.1, which had an LCOF of approximately \$55.96/MWh in a once-through scenario.

In the standalone framework, MgO–ZrH exhibits the lowest deterministic LCOF at \$33.38/MWh, representing a 40% reduction relative to the once-through graphite baseline. MgO–BeO follows closely at \$33.83/MWh but is still 39% lower than the graphite reference. MgO–Be at \$37.03/MWh, which is roughly 34% below the graphite baseline. Meanwhile, MgO–YH stands at \$50.68/MWh, or about 9% lower than the once-through graphite level.

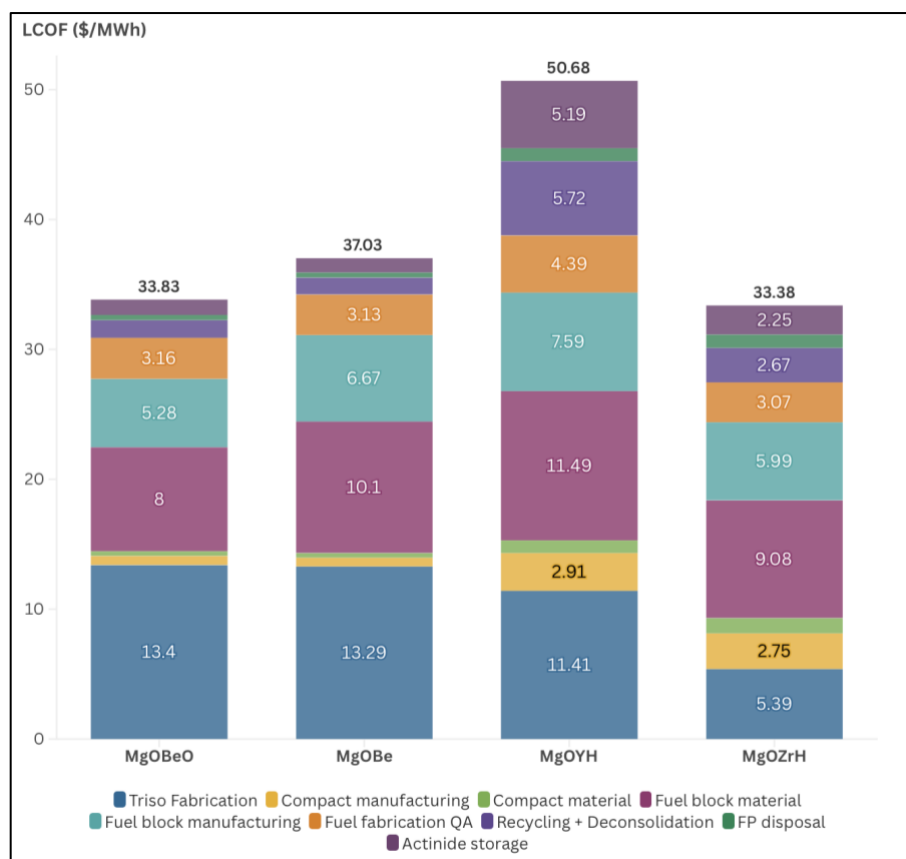


Figure 8-10 LCOF distribution for standalone stage-2 reactor concepts

A closer examination of the cost breakdown explains why MgO–ZrH and MgO–BeO are at the lower end of the LCOF range. In MgO–ZrH, TRISO fabrication (\$5.39/MWh) remains notably lower than in other designs, while moderate overhead for deconsolidation (\$2.67/MWh), and MA storage (\$2.25/MWh) keeps recycling expenses from escalating. MgO–BeO features a balanced distribution, as TRISO fabrication (\$13.40/MWh) and block manufacturing (\$5.28/MWh) stay moderate, and total recycling costs add about \$3–\$4/MWh. One of the reasons for the lower material costs is also that the costs are spread over a longer duration thus increasing cost competitiveness.

MgO–Be shows a modest premium compared to MgO–BeO, stemming from higher block manufacturing (\$6.67/MWh). Nonetheless, these expenditures still place MgO–Be well below the once-through graphite LCOF. By contrast, though about 9% cheaper than the once-through graphite baseline, MgO–YH exhibits a higher overall cost than the other CR designs. With \$11.41/MWh in TRISO fabrication, roughly \$19.08/MWh for block materials & manufacturing costs, and over \$5.70/MWh in reprocessing, YH’s higher fuel requirements drive a significant portion of its \$50.68/MWh total, leaving it the least competitive option under continuous recycle. Also, owing to shorter incore residence time, the back-end costs are not discounted to a greater extent and become a bigger contributing factor to LCOF.

8.4.2 Sensitivity analysis

Figure 8-11 illustrates how $\pm 20\%$ shifts in fabrication cost, MgO cost, entrained moderator cost, deconsolidation & reprocessing cost, MA storage cost, and FP disposal cost impact each configuration’s baseline LCOF. The following summary highlights the most influential parameters for each design.

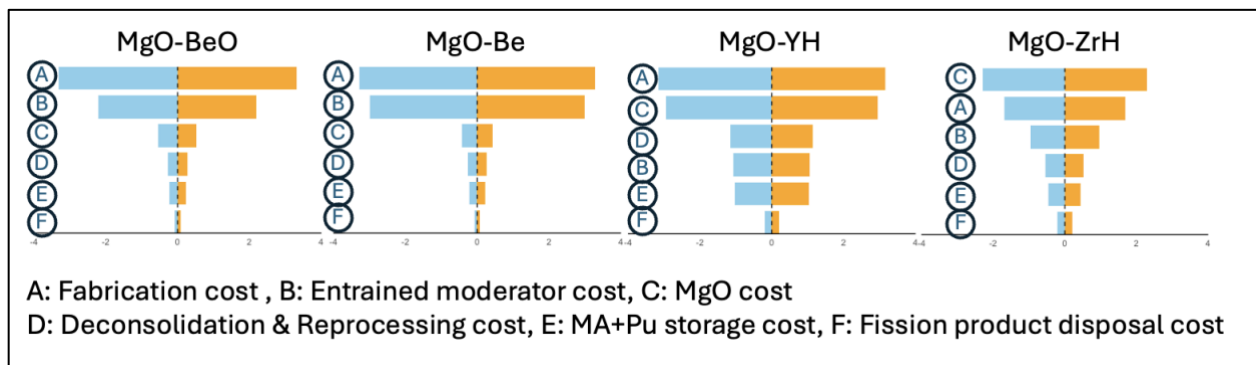


Figure 8-11 Sensitivity analysis for continuous recycle prismatic concepts

MgO–ZrH exhibits the most resilient profile, with a modest fabrication cost sensitivity of $\pm \$1.69/\text{MWh}$. Changes in MgO pricing ($\pm \$2.29/\text{MWh}$) and ZrH costs ($\pm \$0.96/\text{MWh}$) prove equally manageable, indicating that neither manufacturing adjustments nor entrained moderator supply issues would substantially reduce its LCOF advantage. By contrast, MgO–BeO experiences greater fabrication sensitivity ($\pm \$3.32/\text{MWh}$), suggesting that TRU-based TRISO fabrication plays a significant role in controlling its cost, whereas MgO pricing ($\pm \$0.53/\text{MWh}$) remains comparatively inconsequential. The entrained moderator component (BeO), however, can shift costs by $\pm \$2.20/\text{MWh}$, highlighting the importance of ensuring stable beryllium oxide supply chains.

MgO–Be mirrors MgO–BeO’s elevated fabrication risk ($\pm\$3.29/\text{MWh}$) but exhibits a stronger moderator price impact ($\pm\$3.00/\text{MWh}$), reflecting the volatility associated with beryllium sourcing. In contrast, MgO–YH’s sensitivity profile centers on fabrication ($\pm\$3.16/\text{MWh}$) and MgO costs ($\pm\$2.94/\text{MWh}$), while YH-related fluctuations ($\pm\$1.06/\text{MWh}$) are relatively contained. Nonetheless, the higher uranium loads make MgO–YH particularly susceptible to cost spikes when multiple parameters shift unfavorably. These patterns reinforce the importance of efficient TRU-based TRISO manufacturing, stable raw-material supply chains, and streamlined recycling processes to minimize cost variability under continuous recycling schemes.

8.4.3 Monte Carlo analysis

A Monte Carlo simulation provides further insight into how these designs might perform under concurrent uncertainties in fabrication, and moderator pricing. Figure 8-12 depicts each configuration’s LCOF distribution and cumulative probability curve.

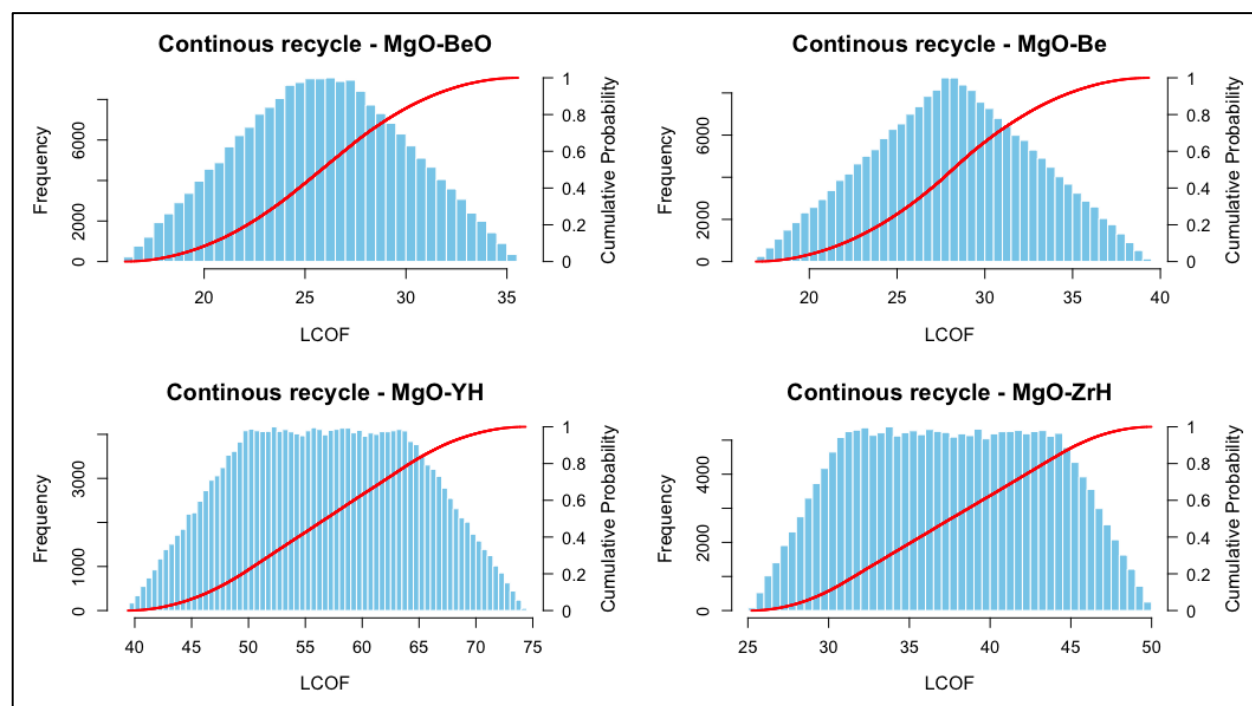


Figure 8-12 LCOF Probability distributions for continuous recycle prismatic reactor Concepts (Stage-2 microreactor only).

MgO–Be achieves a mean LCOF of $\$28.17/\text{MWh}$ (range: $\$18.32$ – $\$37.06$, $\sigma = 4.26$), notably below its deterministic figure of $\$37.03/\text{MWh}$, implying that favorable assumptions concerning beryllium costs and lower TRU based TRISO fabrication costs frequently coincide in the probabilistic space. MgO–BeO similarly attains a mean of $\$26.22/\text{MWh}$ (range: $\$16.64$ – $\$35.36$, $\sigma = 3.94$), falling below its deterministic estimate of $\$33.83$. This gap reveals potential synergies where stable BeO supplies and efficient recycled TRU TRISO fuel fabrication produce outcomes well below the once-through graphite reference.

MgO–ZrH, by contrast, yields a mean LCOF of $\$37.08/\text{MWh}$ (range: $\$26.56$ – $\$49.18$, $\sigma = 5.72$), slightly higher than its deterministic value of $\$33.38$ but still substantially below the once-through graphite baseline. While periodic unfavorable draws—such as elevated zirconium

hydride prices reduce some of MgO–ZrH’s deterministic edge, its average cost remains competitive. MgO–YH reports a mean LCOF of \$56.27/MWh (range: \$40.53–\$73.09, $\sigma = 7.68$), exceeding its deterministic \$50.68 and hovering near the once-through graphite reference, underscoring how uncertainties in material costs can drive this design’s cost far beyond the other CR variants.

Compared to once-through scenarios, these Monte Carlo outcomes demonstrate how advanced moderators can exploit continuous recycle efficiencies to place their mean LCOFs below or well below the original graphite benchmark. MgO–Be and MgO–BeO, in particular, exhibit upside potential when reduced fuel fabrication parameters and stable moderator supplies align, although they remain vulnerable to beryllium market volatility. MgO–ZrH stands out for consistent performance across most simulations, while MgO–YH’s higher initial fuel requirements leave it prone to higher aggregate costs than other concepts, even though it occasionally dips below the once-through graphite baseline.

8.4.4 Key Implications and Recommendations

The sensitivity and Monte Carlo analyses confirm that fabrication and recycled TRU fabrication costs dominate LCOF determination for continuous recycle microreactors, much like once-through designs. However, by expanding the fuel-cycle scope to include recycling, these Stage-2 concepts can achieve substantial cost reductions—ranging from about 9% to 40% below the once-through graphite baseline—depending on moderator choice and supply-chain consistency. MgO–ZrH stands out for its stable deterministic performance, although occasional adverse parameter draws can lift its average cost closer to other options. MgO–BeO and MgO–Be reveal upside potential in scenarios where beryllium sourcing, handling, and fuel fabrication prove unfavorable. Meanwhile, MgO–YH persists as the most expensive design.

Overall, transitioning to continuous recycling alters the cost equation by adding reprocessing and disposal steps while simultaneously removing enrichment costs. Nonetheless, each configuration requires sound management of fuel fabrication and supply chain challenges to maintain a distinct advantage over the once-through graphite baseline.

8.5 Continuous recycle (Stage-1 & Stage-2 combined) | Prismatic micro Reactor

This section extends the previous prismatic microreactor studies by coupling a sodium-cooled fast reactor (SFR) as Stage-1 under a continuous recycle model. Unlike the single-reactor scenarios, the SFR handles much of the system's electricity unit generation and reprocessing infrastructure, with microreactors drawing on its recycled actinides.

In the prismatic microreactor continuous recycle designs, hydride-based systems demonstrate significantly lower plutonium loading requirements, allowing a single SFR to supply enough plutonium for 13.3 and 14.3 micro-reactors with MgO-YH and MgO-ZrH respectively. In contrast, beryllium-based variants can handle higher plutonium per fuel load, supporting approximately 1.25 microreactors per SFR (specifically 1.26 for MgO-BeO and 1.24 for MgO-Be).

8.5.1 LCOF cost drivers

Figure 8-13 shows a stacked bar chart of the LCOF for the prismatic microreactor concepts when coupled with an SFR under continuous recycle scenario. These data reflect cost contributions from both the SFR (driver fabrication, blanket, reprocessing, and disposal) and the microreactors (TRISO manufacturing, moderator materials, reprocessing, and disposal). Across all concepts, SFR-related activities account for 87–92% of the total LCOF, indicating that microreactor differences, though consequential, are overshadowed by the SFR's cost structure.

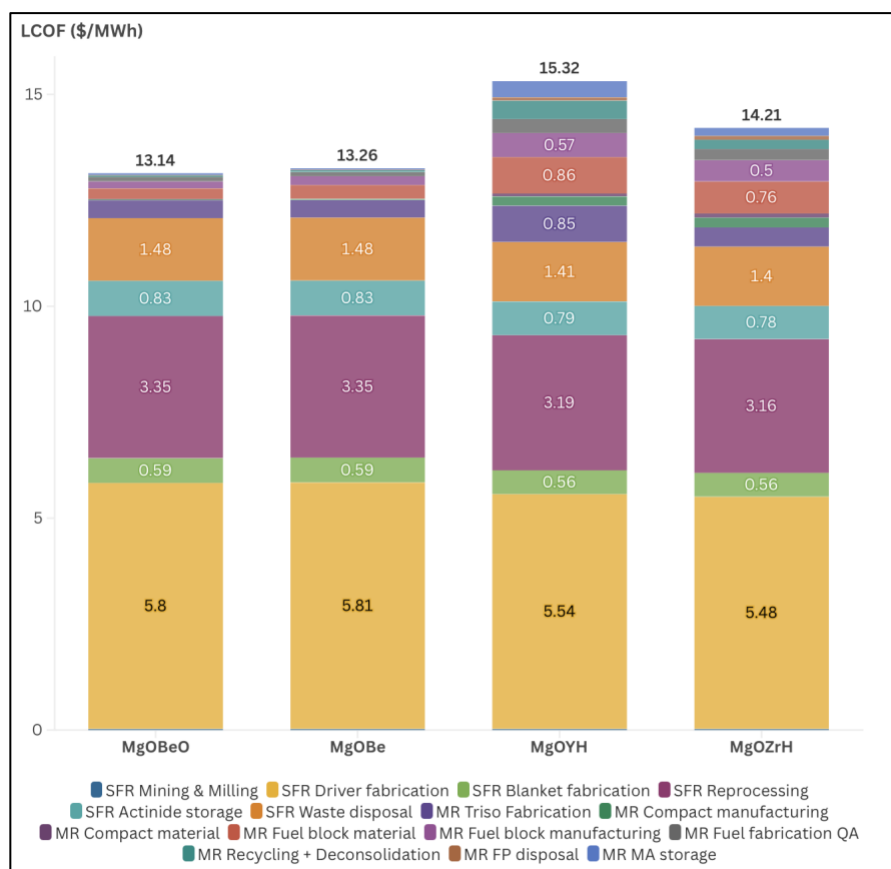


Figure 8-13 LCOF Distribution Across Combined Stage-1 and Stage-2 Reactor Concepts

MgO–BeO achieves an LCOF of \$13.14/MWh, placing it among the least costly beryllium-based moderators. Approximately 90% of this figure is linked to SFR operations, particularly driver fabrication (\$5.80/MWh) and reprocessing (\$3.30/MWh). Stage-2 costs, including TRISO fabrication (roughly \$0.40/MWh) and BeO supply, contribute to the remaining 8%. MgO–Be sits marginally higher at \$13.25/MWh, driven by slightly elevated beryllium manufacturing expenses relative to BeO. Nonetheless, cost differences at the microreactor level remain modest at about \$0.10/MWh, leaving the overall figure dominated by the same SFR cost drivers that shape the MgO–BeO design.

MgO–YH, at \$15.31/MWh, stands out as the most expensive concept within this combined configuration. The primary driver is yttrium hydride’s higher TRISO fabrication requirements (\$3.20/MWh) with more microreactors being supported, increasing microreactor costs beyond beryllium-based alternatives. MgO–ZrH occupies an intermediate position at \$14.21/MWh, with an additional \$0.50–\$0.80/MWh attributed to Stage-2 fuel block overhead for zirconium hydride. Reprocessing expenses remain below \$3.20/MWh, indicating that ZrH’s cost premium arises partly due to the higher number of microreactors being serviced.

In summary, although the microreactor moderator choice influences the final LCOF by a few dollars per MWh, the SFR’s cost structure—particularly driver fabrication and reprocessing—ultimately accounts for most of the variance.

8.5.2 Sensitivity analysis

Figure 8-14 depicts the impact of $\pm 20\%$ variations in key parameters on the combined LCOF for the SFR + microreactor configuration. The results highlight how fluctuations in these inputs modulate the final cost for each concept.

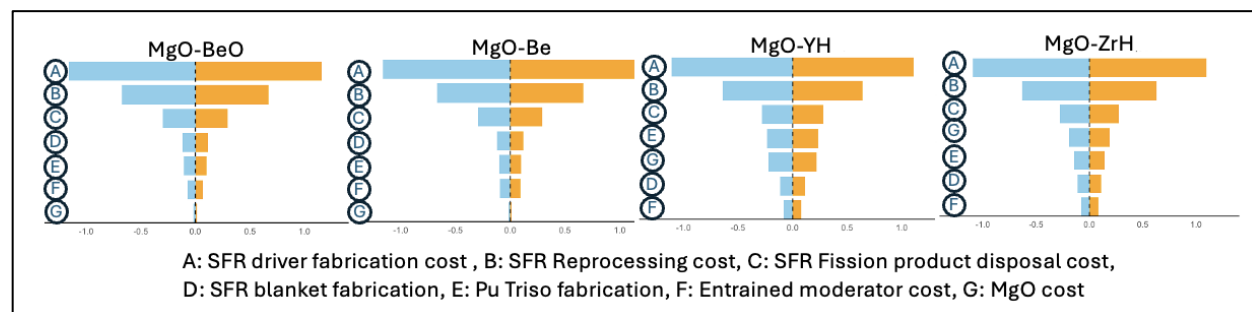


Figure 8-14 Sensitivity Analysis of LCOF for Combined SFR + Microreactor Prismatic Reactor Concepts

Because the SFR constitutes the largest fraction of the total LCOF, shifts in driver fabrication and reprocessing dominate overall risk. For instance, a 20% hike in driver fabrication can increase MgO–Be’s LCOF from \$13.25/MWh to around \$14.40/MWh, while a similar decrease drops it below \$12.10/MWh. Reprocessing cost swings across all designs typically add or subtract \$0.60–\$1.10.

Moderator costs exert more modest effects. In MgO–BeO and MgO–Be, a $\pm 20\%$ swing in beryllium pricing shifts the LCOF by about $\pm \$0.10$ – $\$0.15$, while hydride concepts (MgO–ZrH, MgO–YH) see $\pm \$0.20$ – $\$0.30$ changes due to higher manufacturing costs arising from servicing more number of microreactors. These narrower ranges highlight that the microreactor

parameters, although nonnegligible, exert less leverage than the SFR's driver fabrication and reprocessing efficiency.

8.5.3 Monte Carlo analysis

This section presents the Monte Carlo analysis for the Levelized Cost of Fuel (LCOF) in continuous recycle prismatic reactor concepts for the combined SFR + Microreactor system. Figure 8-15 presents histograms and cumulative probability curves.

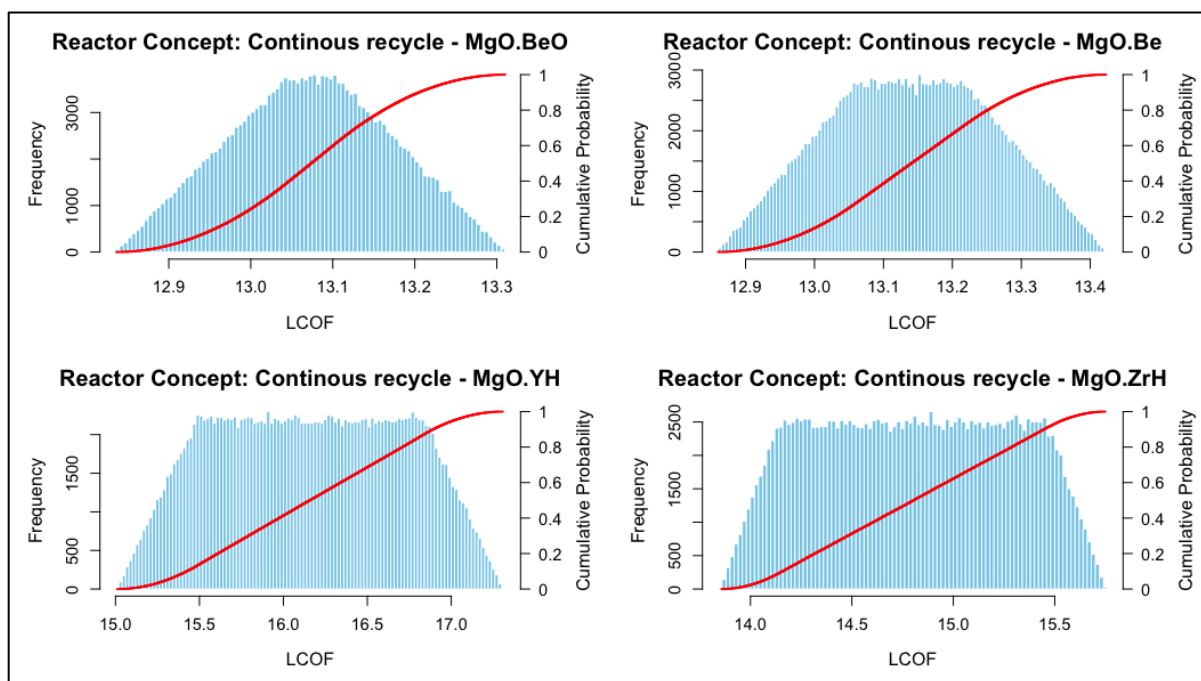


Figure 8-15 LCOF probability distributions for continuous recycle prismatic reactor concepts.

MgO–Be yields a mean LCOF of \$13.14/MWh (range: \$12.88–\$13.39, $\sigma = 0.12$), closely matching its deterministic value of \$13.25. Favorable assumptions regarding beryllium supply and TRU-based TRISO fabrication occasionally bring costs down to \$12.90 or below, but outcomes rarely exceed \$13.40. MgO–BeO shows similar behavior, with a mean LCOF of \$13.08/MWh (range: \$12.85–\$13.28, $\sigma = 0.09$). Its comparatively tight distribution suggests stable BeO expenses.

MgO–ZrH registers a mean LCOF of \$14.80/MWh (range: \$13.94–\$15.69, $\sigma = 0.46$), slightly above its deterministic estimate (\$14.21). Adverse draws in ZrH supply can approach \$15.50, indicating some susceptibility to escalations in hydride processing. MgO–YH, by contrast, has a mean of \$16.16/MWh (range: \$15.20–\$17.28, $\sigma = 0.55$), surpassing its deterministic \$15.31. This outcome underscores how increased initial fuel loads also required higher reprocessing requirements and expanded cost risk, placing YH consistently above beryllium or zirconium hydride designs in a probabilistic setting.

Overall, the steep cumulative curves for MgO–Be and MgO–BeO indicate tight clustering of outcomes near \$13/MWh, highlighting a relatively high degree of cost predictability in both beryllium concepts. MgO–ZrH's broader range suggests greater sensitivity to supply chain and manufacturing parameters, while MgO–YH sustains the greatest economic uncertainty. These

results confirm that the SFR's dominant role partially stabilizes total costs, and differences in TRU-based TRISO production, fuel block production, and reprocessing overhead still yield minor costs spread across the four microreactor variants.

8.5.4 Key implications and recommendations

By integrating an SFR as Stage-1 under a continuous recycle scenario, the reactor's driver fabrication and reprocessing expenses overshadow distinctions in microreactor concepts, comprising 87–92% of the total LCOF. Overall, while the SFR dictates the majority of cost outcomes in this continuous recycle arrangement, entrained moderator selection in microreactors still impacts final economics. Across all options, improvements in SFR driver fabrication and reprocessing remain the most influential lever for reducing LCOF and improving the viability of continuous recycle nuclear deployment strategy.

8.6 Continuous recycle (Only Stage-2) | Pebble-bed micro reactor

This section examines continuous recycling (CR) strategies for pebble bed based microreactors under a standalone Stage-2 framework.

8.6.1 LCOF cost drivers

The stacked bar chart in Figure 8-16 illustrates dominant cost drivers within pebble systems, where moderator mass is reduced by 87–93% compared to equivalent prismatic designs. These dramatic material savings, coupled with unprecedented burnup levels and century-scale residence times, underlie the distinctive cost structures described below.

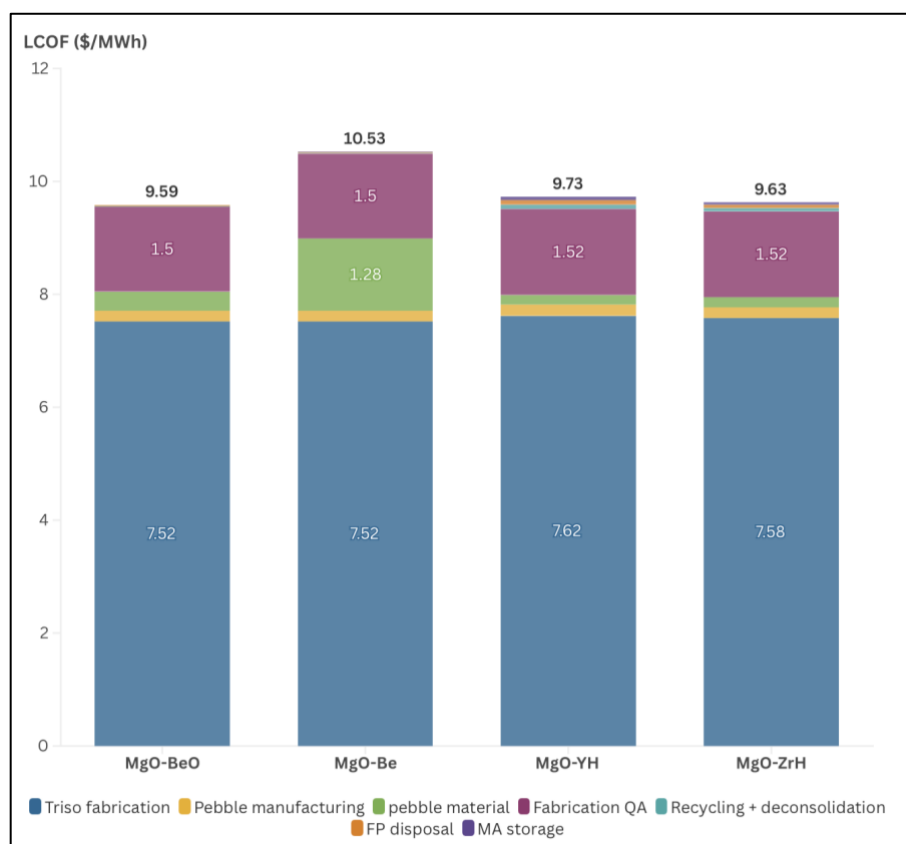


Figure 8-16 LCOF distribution across continuous recycle pebble reactor concepts (microreactor Only)

A systematic breakdown of each configuration's LCOF reveals notable differences in cost distribution. MgO-BeO at \$9.59/MWh stands marginally below MgO-ZrH (\$9.64/MWh), MgO-YH (\$9.74/MWh), and MgO-Be (\$10.53/MWh). Despite small percentage disparities, the TRISO fabrication step remains dominant across all concepts (\$7.52–\$7.62/MWh), while variations in pebble material, manufacturing, and back-end charges account for the remaining differences.

Combined Impact of High Burnup and Long Residence Time

Crucial to understanding these low LCOF values are the exceptional burnup levels (ranging from 287.5 to 415.3 GWd/MT) and extended core residence times (up to nearly a century in some beryllium designs). For example, MgO-BeO's \$9.59/MWh partially stems from a 415.3 GWd/MT burnup and a 99.9-year residence, while MgO-Be, at \$10.53/MWh, benefits from 411.6

GWd/MT and a 99.0-year residence. MgO–YH and MgO–ZrH, with burnups of 287.5–314.1 GWd/MT and core lifetimes of 69–75 years, cluster between \$9.64 and \$9.74/MWh. These extended residence times reduce annualized back-end costs, as reprocessing may be required only once per century, driving recycling charges below \$0.22/MWh in even the most conservative cost scenarios.

It is important to note, however, that such high burnup figures significantly exceed current TRISO fuel performance, while multi-decade or century-scale residence times remain unproven for these material configurations. Consequently, the favorable cost structures observed here depend on successfully demonstrating advanced TRISO capabilities in extended operation. These results thus underscore theoretically achievable targets rather than guaranteed commercial results.

8.6.2 Sensitivity analysis

Figure 8-17 explores how $\pm 20\%$ changes in key cost inputs—fabrication costs, MgO cost, entrained moderator costs, and back-end processes costs—affect the LCOF. Compared to prismatic architectures, the pebble bed concepts exhibit distinct and generally lower sensitivities to material cost variations.

Across all composite moderator designs examined TRU-based TRISO fuel assembly fabrication emerges as the dominant cost driver, dwarfing the comparatively small contributions from the rest of the parameters. In particular, MgO–ZrH stands out for its overall stability, with a fabrication overhead of $\pm \$1.82/\text{MWh}$ —accounting for about 18.9% of the \$9.64/MWh baseline—and negligible sensitivity to MgO or the moderator supply. A similar pattern arises with MgO–BeO, where fabrication changes ($\pm \$1.80/\text{MWh}$) represent 18.8% of total costs, while entrained BeO fluctuations remain minimal ($\pm \$0.05/\text{MWh}$) due to efficient resource usage and century-scale residence times. By contrast, MgO–Be faces a moderately higher beryllium moderator variability ($\pm \$0.24/\text{MWh}$), though still considerably below prismatic benchmarks. MgO–YH registers the fabrication sensitivity ($\pm \$1.83/\text{MWh}$) but displays minimal hydride cost volatility ($\pm \$0.01/\text{MWh}$). These findings emphasize that refining plutonium-based TRISO manufacturing processes offers the most substantial economic leverage, particularly when extended burnups and prolonged core lifespans help spread overhead across multiple reactor years.

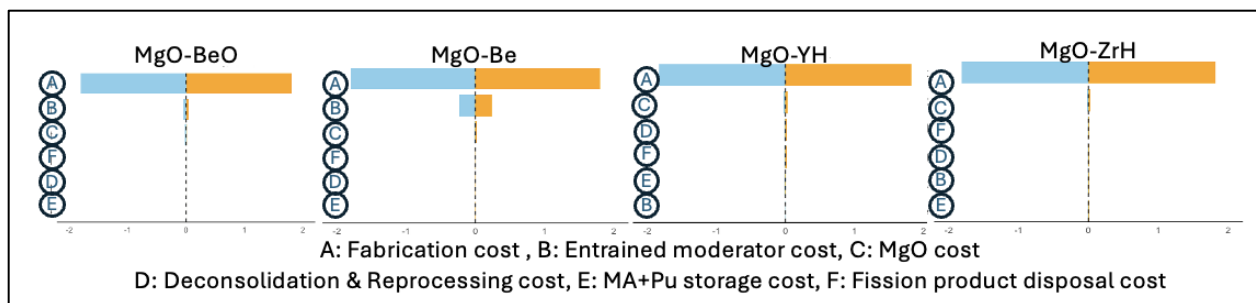


Figure 8-17 Sensitivity analysis of LCOF for continuous recycle pebble concepts (microreactor Only)

8.6.3 Monte Carlo analysis

Figure 8-18 presents Monte Carlo simulation results, capturing how uncertainties in fabrication, material costs, and recycling parameters converge in a probabilistic LCOF distribution. Each design's mean LCOF falls below its deterministic value, reflecting the “probabilistic advantage” that arises when extended core life and reduced material usage enable a wider range of favorable outcomes.

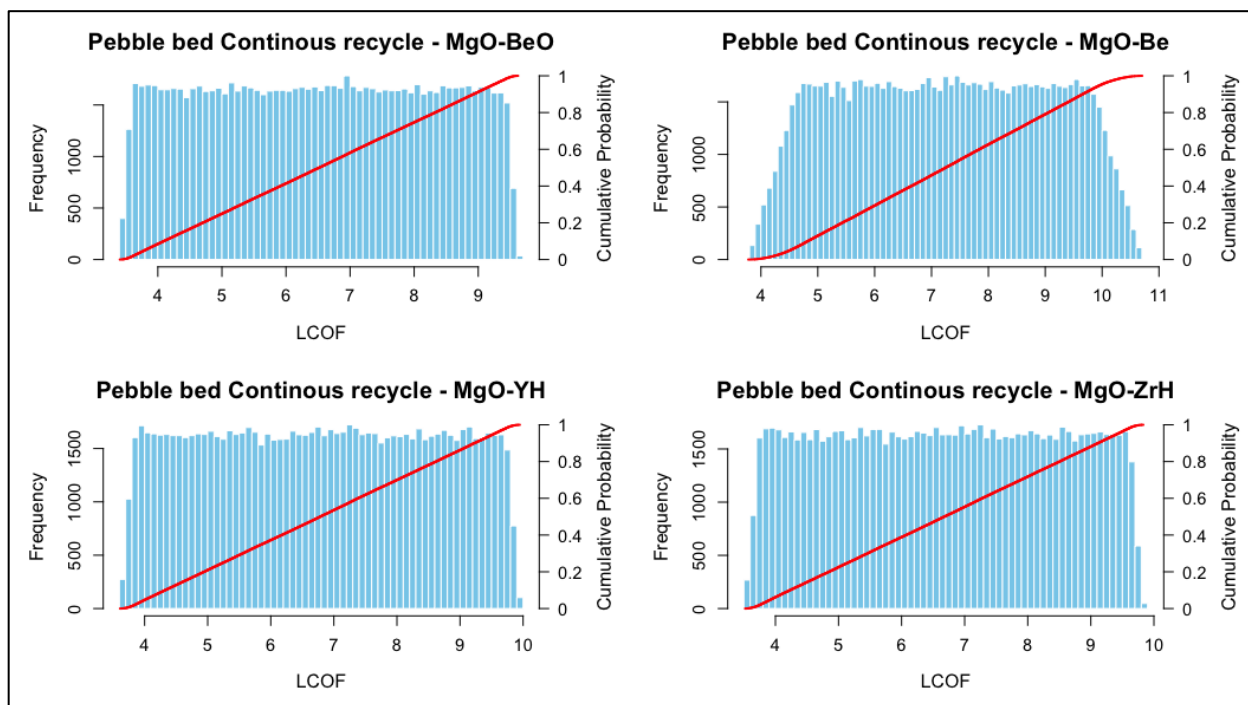


Figure 8-18 LCOF probability distributions for pebble bed continuous recycle concepts. The blue histograms depict the frequency of LCOF outcomes, while the red curves represent the cumulative probability, highlighting the likelihood of achieving specific cost targets.

MgO–ZrH yields a mean LCOF of \$6.69/MWh (range: \$3.54–\$9.84, $\sigma = 1.77$), representing a 31% decrease from \$9.64/MWh. This narrower range indicates less dependence on material costs. MgO–BeO follows at \$7.26/MWh (range: \$3.82–\$10.70, $\sigma = 1.77$), about 24% below its deterministic \$9.59, suggesting strong upside potential in scenarios where TRU-based fabrication and recycling achieve optimal performance. MgO–Be offers the most pronounced difference, with a mean of \$6.52/MWh (range: \$3.41–\$9.62, $\sigma = 1.75$), down 38% from \$10.53/MWh, hinting that beryllium concerns can be mitigated under the right cost and operational conditions. MgO–YH shows a mean of \$6.79/MWh (range: \$3.63–\$9.94, $\sigma = 1.78$), or 30% below its \$9.74/MWh baseline.

8.6.4 Key implications and recommendations

Across all designs, nearly uniform standard deviations (1.75–1.78) signal a shared stabilizing mechanism—stemming from reduced moderator mass, high burnup, and extended residence times that disperse costs over extensive operating intervals. However, successfully realizing these benefits depends on confirming TRU-based TRISO fuel reliability at 200+ GWd/MT or higher and validating multi-decade system longevity. While the data suggest that well-managed pebble bed systems can mitigate material cost volatility and leverage advantageous recycling

strategies, scaling these outcomes for commercial deployment requires extensive R&D to demonstrate the feasibility and safety of the underlying reactor and fuel technologies.

8.7 Continuous recycle (stage-1 & stage-2 combined)| Pebble bed microreactor

This section assesses a two-stage nuclear system wherein Stage-1 is a sodium-cooled fast reactor (SFR), and Stage-2 is a pebble bed microreactor. As with the prismatic analysis, all spent fuel is continuously recycled, with plutonium recovered by the SFR for reuse in the microreactor. Like the prismatic concepts, the SFR dominates total electricity generation and strongly influences overall economics.

Higher loading of TRU per microreactor is possible across all microreactor fuel designs. For example, one SFR can support 0.78 and 0.72 microreactors for MgO-YH and MgO-ZrH, respectively. Beryllium-based designs (MgO-BeO and MgO-Be) support still higher TRU loading at 0.57 microreactors per SFR.

8.7.1 LCOF cost drivers

Figure 8-19 illustrates the LCOF for the four combined SFR + pebble bed microreactor concepts. The results reveal uniform LCOF values that converge within a \$0.04 band, indicating that the SFR's cost structure largely overshadows differences in the microreactor design.

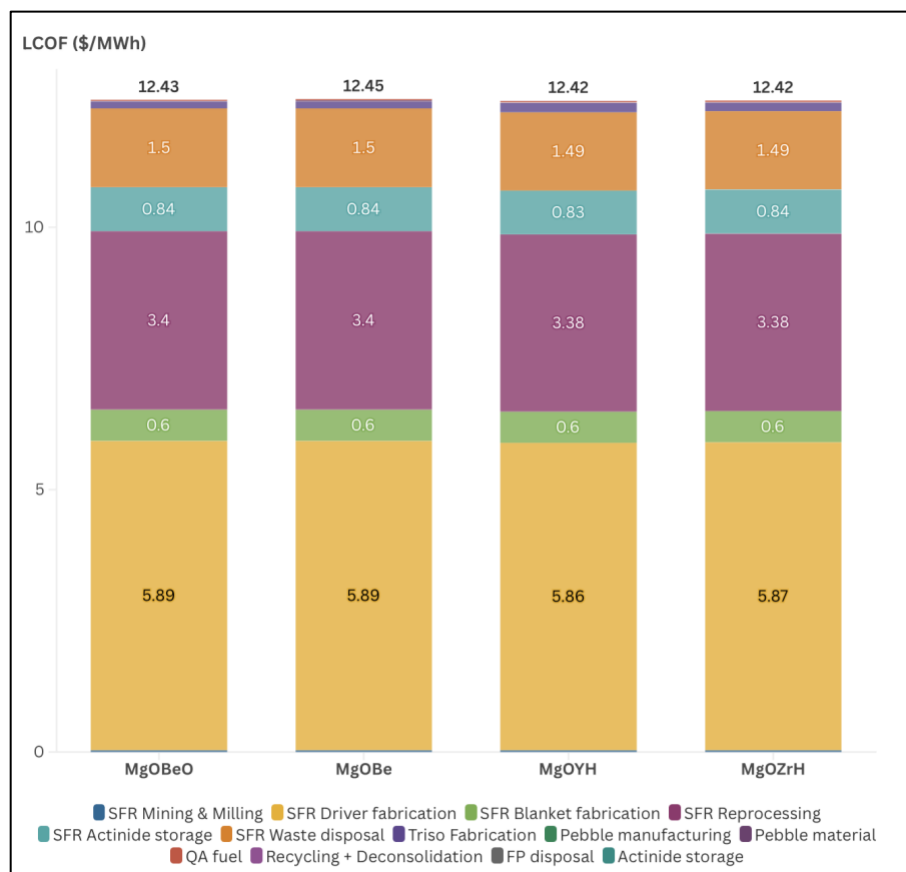


Figure 8-19 LCOF distribution across combined SFR + Microreactor pebble-bed reactor concepts

MgO–BeO, at \$12.4311/MWh, devotes approximately \$12.27 (or ~98.7% of the total) to SFR-related driver and reprocessing expenses, leaving just \$0.16 for microreactor-specific charges such as TRISO fabrication. MgO–Be follows at \$12.4474/MWh, differing from MgO–BeO by only \$0.016; beryllium moderator costs produce a negligible increment and the SFR baseline of

around \$12.30 remains dominant. MgO–YH, at \$12.4171/MWh, exhibits the lowest deterministic value among the four but still falls within a $\pm\$0.03$ range of its counterparts. Overall, the SFR constitutes 98–99% of total LCOF across all moderators, confining microreactor costs to about 1–2% of the final figure and resulting in an extremely tight cluster of \$12.41–\$12.45/MWh.

8.7.2 Sensitivity analysis

Figure 8-20 explores how $\pm 20\%$ variations in key parameters affect the LCOF for each moderator design. These parameters include SFR driver fabrication costs, SFR reprocessing costs, SFR blanket fabrication costs, fission product disposal, and Plutonium-based TRISO manufacturing. The results show that SFR cost levers, particularly driver fabrication and reprocessing, produce the most substantial swings, eclipsing fluctuations related to pebble bed TRISO or moderator materials.

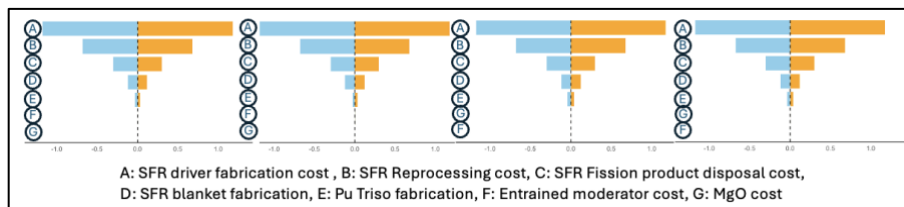


Figure 8-20 Sensitivity analysis of LCOF for combined SFR + microreactor pebble reactor concepts

Raising driver costs by 20% can push LCOF above \$13.60 for MgO–BeO or MgO–Be, and similarly for YH or ZrH. Lowering driver cost by 20% can drive LCOF below \$11.25, creating a total range of roughly $\pm\$1.18$ from the baseline of about \$12.40–\$12.45. Blanket fabrication and fission product disposal exert smaller impacts of $\pm\$0.12$ – $\$0.30$. Adjusting Plutonium TRISO fabrication costs or entrained moderator pricing typically shifts LCOF by less than \$0.06, highlighting that even higher beryllium uncertainties cannot significantly alter a cost baseline dominated by the SFR. This pattern mirrors the prismatic analysis, where Stage 1 processes remain the main determinant of final fuel costs.

8.7.3 Monte Carlo analysis

Figure 8-21 presents the Monte Carlo outcomes for these combined SFR + pebble microreactor systems, capturing probabilistic uncertainties in fuel fabrication and entrained moderator-cost parameters. Each distribution shows a narrow clustering of LCOF results, centering on values just above \$13/MWh in most scenarios.

MgO–Be has a mean LCOF of \$13.14/MWh (range: \$12.88–\$13.39, $\sigma = 0.12$), remaining close to its deterministic baseline and indicating that beryllium cost and microreactor fabrication uncertainties pale in comparison to SFR-driven parameters. MgO–BeO at \$13.12/MWh, with a similarly tight spread of \$12.87–\$13.37 ($\sigma = 0.12$). MgO–YH has a slightly broader range (\$12.83–\$13.33, $\sigma = 0.13$) while still clustering near \$13.08. MgO–ZrH registers \$13.10/MWh with a comparable range, verifying that even worst-case draws rarely exceed \$13.40. These results confirm the strong dominance of SFR cost factors, with microreactor choices playing only a minor role in shifting LCOF distributions.

8.7.4 Key implications and recommendations

The analysis underscores that the SFR remains the primary economic driver for continuous recycle pebble microreactor concepts, accounting for 98–99% of total fuel costs and confining the microreactor's share to only \$0.12–\$0.18 out of \$12.40–\$12.45. This dominance is even more pronounced than in prismatic cases, where microreactors could reach 2–5% of final LCOF. Stage 1 driver fabrication produces $\pm\$1$ – $\$1.30$ swings from the baseline, while microreactor variables shift outcomes by as little as \$0.06–\$0.08. Consequently, microreactor moderator selection appears nearly inconsequential in fleet-scale economics for this combined system.

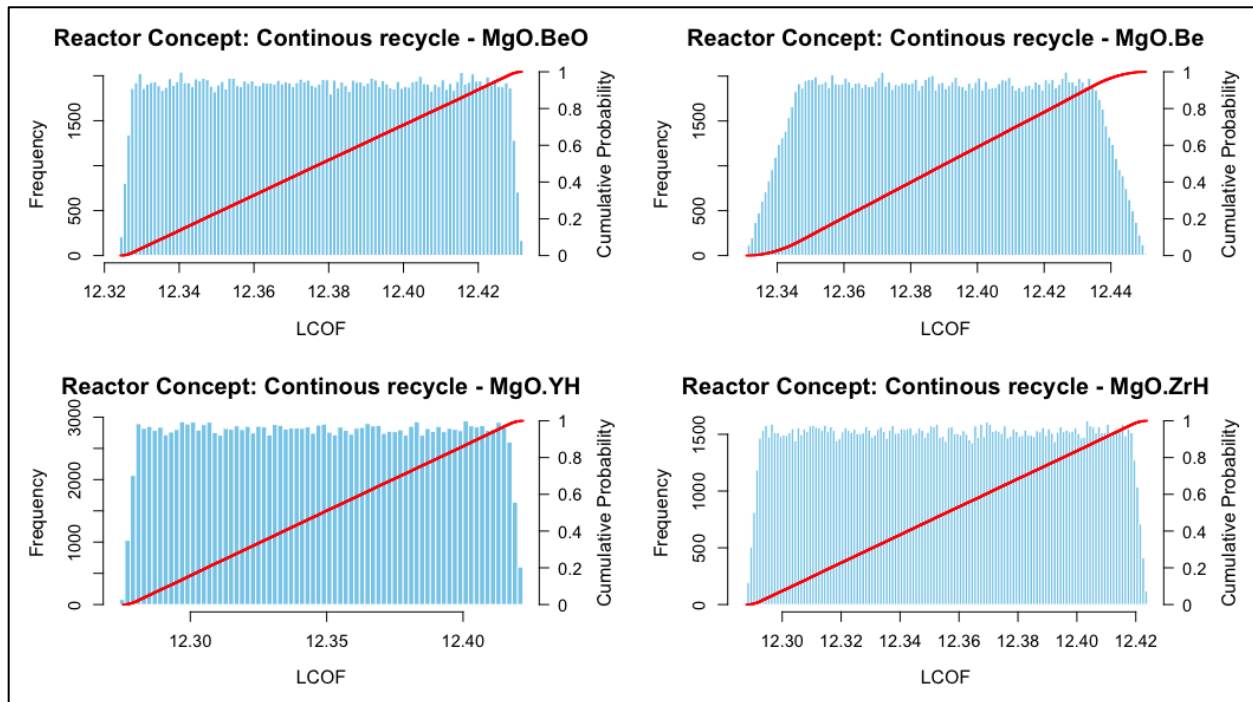


Figure 8-21: LCOF probability distributions for continuous recycle prismatic reactor concepts.

In any scenario, enhancing SFR driver performance, improving reprocessing throughput, and optimizing blanket fabrication will produce more pronounced LCOF reductions than refinements to pebble bed TRISO fabrication or moderator materials.

9 Conclusion and future work

This thesis analyzed the Levelized Cost of Fuel (LCOF) for advanced microreactor designs under two major fuel cycles—once-through and continuous recycle—and two core architectures—prismatic blocks and pebble beds. The study assessed the economic impact of four moderator materials, MgO–Be, MgO–BeO, MgO–YH, and MgO–ZrH, and compared it to the baseline graphite case. A comprehensive overview of the cost drivers, uncertainties, and potential for cost reduction was developed by employing deterministic modeling, sensitivity analyses, and Monte Carlo simulations.

Considering the Once-Through cycle for prismatic microreactors, the baseline graphite design LCOF was established at \$55.88/MWh. This served as a benchmark against which alternative moderators were measured. Among these, MgO–ZrH emerged as a particularly compelling option, offering an approximately 16% lower LCOF (down to \$46.78/MWh) due to moderate zirconium hydride prices and manageable block fabrication costs. In contrast, beryllium-based designs (MgO–Be and MgO–BeO) were burdened by high raw material costs, producing LCOFs of around \$79.99/MWh and \$85.72/MWh, respectively. Yttrium hydride (MgO–YH), at \$63.01/MWh, was between graphite and the beryllium moderators but faced the challenge of increased fuel requirements driving up mining & milling and enrichment expenses. Sensitivity analyses revealed that, in general, front-end fuel costs (especially enrichment) were consistently dominant, but for beryllium-based options, even modest cost fluctuations in raw beryllium or beryllium oxide significantly impacted the total LCOF by up to \pm \$7/MWh. Thus, it underscores the fact that advanced moderator adoption must be paired with stable material costs. Otherwise, it risks eroding the economic advantages.

The analysis demonstrated a pronounced drop in LCOF relative to their prismatic counterparts for once-through pebble-bed microreactors primarily driven by the higher realized burnup and lower material costs associated with the entrained moderator. MgO–ZrH LCOF dropped from \$46.78 in prismatic form to \$33.12/MWh in pebble form, highlighting the efficiency gains in moderator material usage and less wastage during pebble manufacturing methods. Even beryllium-based pebble designs, which were expensive in prismatic format, achieved more moderate LCOFs: MgO–BeO at \$39.67/MWh and MgO–Be at \$41.49/MWh. MgO–YH, also improved from \$63.01/MWh (prismatic) to \$43.77/MWh (pebble). Here, sensitivity analyses indicated that front-end uranium supply (i.e., mining & milling, enrichment) was the main cost driver, while moderator price volatility contributed far less than in the prismatic block scenario. Thus, the once-through pebble bed approach mitigated advanced moderator cost risk by reducing the required mass of moderator material.

In moving to continuous recycle concepts, the thesis examined LCOF using two key frameworks: standalone microreactors (Stage-2 only) and microreactors coupled to a sodium-cooled fast reactor (Stage-1 + Stage-2). For prismatic Stage-2 only, the LCOF ranged from around \$33–\$37/MWh for MgO–ZrH, MgO–BeO, and MgO–Be, up to \$50.68/MWh for MgO–YH. These values are lower than their once-through equivalents because reprocessing and deconsolidation costs, while significant, can be more than offset by reduced enrichment needs. Nonetheless, Monte Carlo simulations revealed that beryllium-based options can yield lower mean costs than deterministic baselines under favorable beryllium market conditions, while YH-based systems often trended higher than their deterministic figure due to higher heavy metal

demands. In prismatic reactors coupled with an SFR, the cost of the microreactor's moderator and fabrication contributed only 8–13% of the total, leaving the SFR's driver fabrication and reprocessing (nearly \$12–\$14/MWh out of \$13–\$15/MWh total) as the core economic driver. Consequently, even large cost swings in Stage 2 parameters had a marginal effect on final LCOFs, demonstrating that synergy with a fast reactor can overshadow microreactor-level design differences.

Beyond prismatic blocks, continuous recycle for pebble-bed microreactors offered perhaps the most promising economic potential, especially if extremely high burnups (287–415 GWd/MT) and extended residence times (50 to 100+ years) could be experimentally validated. The thesis estimates that in such scenarios, MgO–BeO or ZrH pebble designs might achieve deterministic LCOFs near \$9–\$10/MWh. Even the higher-cost beryllium designs (MgO–Be) and fuel-intensive YH designs (MgO–YH) could reach around \$10.53–\$9.74/MWh, respectively. These optimistic values, however, rely on maintaining TRISO fuel integrity over exceptionally long irradiation periods—an assumption requiring substantial research and development. Sensitivity analysis showed that Plutonium-based TRISO fabrication is the largest cost lever, whereas moderator material becomes a minor factor when used in smaller quantities in pebble form. If a pebble-bed microreactor is paired with an SFR (Stage-1 + Stage-2), the SFR portion dominates at 98–99% of total LCOF (\$12–\$13/MWh overall), rendering differences among MgO–Be, MgO–BeO, MgO–ZrH, and MgO–YH nearly inconsequential from an economic standpoint.

Finally, inert-matrix removal, or “deconsolidation,” emerged as a powerful method to reduce the volume of spent nuclear fuel requiring significant disposal. By removing the inert matrix—such as graphite in baseline concepts or MgO-based composites in advanced moderator designs—only the highly radioactive TRISO particles remain, thereby lowering the total disposal volume by as much as 90–98% in some reactor configurations. Although waste disposal constitutes only a modest proportion of the LCOF (particularly when compared to enrichment or fabrication), this steep decline in required repository capacity carries important siting and public acceptance benefits.

Three major recommendations follow from these findings. First, focusing on the pebble-bed version of advanced moderators for once-through cycles will likely yield more stable and lower LCOFs than prismatic designs because of smaller moderator mass requirements and less wastage during block fabrication. Second, prismatic cores can realize moderate cost reductions for continuous-recycle systems if efficient TRISO production and a low-cost supply of specialized moderators are assured; however, pebble-bed architectures could capture still larger savings if extremely high burnups become demonstrable. Third, in scenarios where microreactors operate in tandem with a large fast reactor, the SFR cost structure effectively overshadows microreactor-level differences, so advanced microreactors would benefit most if the fast reactor driver fabrication and reprocessing cost could be driven down.

Limitations of current work: Data limitations

Many simplifying assumptions are made regarding process and material costs. Actual fabrication costs may differ considerably based on regulatory environments, vendor capabilities, and market price fluctuations. The estimates, including those derived from personal communications and analogous assumptions, offer approximations rather than

absolute values. Consequently, these results should not be considered definitive engineering data but rather a preliminary framework to guide decision-making and identify areas requiring further, more detailed analysis.

Future work

One key direction for future research is improving fuel block fabrication and reducing raw material expense, especially for moderators whose costs can drive LCOFs above \$80/MWh in prismatic once-through designs (e.g., MgO–BeO at \$85.72/MWh or MgO–Be at \$79.99/MWh). Achieving cost parity with graphite (\$55.88/MWh) would require, for instance, lowering BeO prices to \$54/kg or beryllium costs below \$798/kg. Research into novel synthesis routes (e.g., advanced sintering for BeO) or additive manufacturing strategies to enhance block manufacture could significantly shift the feasible cost boundary, especially if they reduce manufacturing complexity. Similarly, zirconium hydride (MgO–ZrH), while more economically favorable in deterministic models (\$46.78/MWh prismatic), still faces the risk of supply chain bottlenecks or processing uncertainties that can inflate mean LCOFs to the \$60–\$80/MWh range in Monte Carlo scenarios. Addressing these risks through scaled-up hydride production lines, improved hydrogenation controls, or international supply agreements would stabilize costs and maintain MgO–ZrH’s competitive edge.

Another major avenue involves validating and refining the high burnup assumptions supporting the more optimistic LCOF outcomes—particularly for pebble-bed microreactors. This thesis identified scenarios in which beryllium- or zirconium hydride-based pebble cores could drop below \$10–\$11/MWh if they achieve burnups of 287–415 GWd/MT and multi-decade residence times. While these numbers showcase the theoretical limits of TRISO-based fuels, large-scale demonstration projects would be needed to confirm long-term mechanical stability, fission product retention, and moderator integrity over decades of operation. Even partial success—reaching, say, 250 GWd/MT instead of 400—could still yield LCOFs in the \$15–\$20/MWh range, a significant improvement over the baseline graphite case. Parallel to in-core testing, developing advanced in-situ inspection and remote handling devices can help mitigate the added costs of extended operation, ensuring that maintenance overheads do not erode the targeted LCOF reductions from high burnups.

References

- [1] J. Buongiorno, B. Carmichael, B. Dunkin, J. Parsons, and D. Smit, “Can Nuclear Batteries Be Economically Competitive in Large Markets?,” *Energies*, vol. 14, no. 14, p. 4385, Jul. 2021, doi: 10.3390/en14144385.
- [2] “Project PELE Mobile Nuclear Reactor – DoD Research & Engineering, OUSD(R&E).” Accessed: Jan. 29, 2025. [Online]. Available: https://www.cto.mil/pele_eis/
- [3] “The Value of Nuclear Microreactors in Providing Heat and Electricity to Alaskan Communities -,” CEEPR. Accessed: Jan. 29, 2025. [Online]. Available: <https://ceepr.mit.edu/workingpaper/the-value-of-nuclear-microreactors-in-providing-heat-and-electricity-to-alaskan-communities/>
- [4] E. M. Duchnowski, R. F. Kile, L. L. Snead, J. R. Trelewicz, and N. R. Brown, “Reactor performance and safety characteristics of two-phase composite moderator concepts for modular high temperature gas cooled reactors,” *Nucl. Eng. Des.*, vol. 368, p. 110824, Nov. 2020, doi: 10.1016/j.nucengdes.2020.110824.
- [5] “MATRICY: Matrix Engineered TRISO Compacts Enabling Advanced Reactor Fuel Cycles | ARPA-E.” Accessed: Jan. 29, 2025. [Online]. Available: <https://arpa-e.energy.gov/programs-and-initiatives/search-all-projects/matricy-matrix-engineered-triso-compacts-enabling-advanced-reactor-fuel-cycles>
- [6] E. M. Duchnowski *et al.*, “Pre-conceptual high temperature gas cooled microreactor design utilizing two-phase composite moderators. Part II: Design space and safety characteristics,” *Prog. Nucl. Energy*, vol. 149, p. 104258, Jul. 2022, doi: 10.1016/j.pnucene.2022.104258.
- [7] E. M. Duchnowski, D. Doyle, N. R. Brown, and J. R. Trelewicz, “Matrix Engineered TRISO Compacts Enabling Advanced Reactor Fuel Cycles,” Milestone M2.2, Sep. 2023.
- [8] L. L. Snead *et al.*, “Development and potential of composite moderators for elevated temperature nuclear applications,” *J. Asian Ceram. Soc.*, vol. 10, no. 1, pp. 9–32, Jan. 2022, doi: 10.1080/21870764.2021.1993592.
- [9] C. Ang *et al.*, “Fabrication of Two-Phase Composite Moderators as Potential Lifetime Reactor Components,” in *Transactions of the American Nuclear Society - Volume 121*, AMNS, 2019, pp. 1445–1447. doi: 10.13182/T31286.
- [10] E. M. Duchnowski, R. F. Kile, K. Bott, L. L. Snead, J. R. Trelewicz, and N. R. Brown, “Pre-conceptual high temperature gas-cooled microreactor design utilizing two-phase composite moderators. Part I: Microreactor design and reactor performance,” *Prog. Nucl. Energy*, vol. 149, p. 104257, Jul. 2022, doi: 10.1016/j.pnucene.2022.104257.
- [11] F. Ganda, B. Dixon, E. Hoffman, T. K. Kim, T. Taiwo, and R. Wigeland, “Economic Analysis of Complex Nuclear Fuel Cycles with NE-COST,” *Nucl. Technol.*, vol. 193, no. 2, pp. 219–233, Feb. 2016, doi: 10.13182/NT14-113.
- [12] UXC.COM, “UXc Weekly Publication.” Oct. 23, 2023. [Online]. Available: <https://www.uxc.com/docs/p/product/UxW37-43.pdf>
- [13] B. W. Dixon, F. Ganda, K. A. Williams, E. Hoffman, and J. K. Hanson, “Advanced Fuel Cycle Cost Basis – 2017 Edition,” NTRD-FCO-2017-000265, Sep. 2017.
- [14] J. Mc Murray *et al.*, “Production of Low-Enriched Uranium Nitride Kernels for TRISO Particle Irradiation Testing,” Fuel Cycle Research & Development Advanced Fuels Campaign ORNL/SR-2016/268, Jun. 2016.
- [15] P. A. Demkowicz, “TRISO Fuel: Design, Manufacturing, and Performance,” INL/MIS-19-52869-Revision-0, Jul. 2019.

- [16] D. Petti and M. Barrachin, "High Temperature Gas Cooled Reactor Fuels and Materials," Vienna, Austria, IAEA-TECDOC-1645, Mar. 2010. [Online]. Available: https://www-pub.iaea.org/mtcd/publications/pdf/te_1645_cd/pdf/tecdoc_1645.pdf
- [17] D. Petti, J. Maki, J. Buongiorno, R. Hobbins, and G. Miller, "Key Differences in the Fabrication, Irradiation and Safety Testing of U.S. and German TRISO-coated Particle Fuel and Their Implications on Fuel Performance," Idaho National Laboratory, Idaho Falls, Idaho, INEEL/EXT-02-00300, Jun. 2002.
- [18] J. Phillips and E. Shaber, "Compact Process Development at Babcock & Wilcox," Idaho National Laboratory, Idaho Falls, INL/EXT-11-23166, Mar. 2012.
- [19] B. Liu, "'HTGR Fuel Fabrication and Quality Control,' IAEA Course on High Temperature Gas Cooled Reactor Technologies.," Biejing, China, IAEA meeting, Oct. 2012.
- [20] "Advances in High Temperature Gas Cooled Reactor Fuel Technology," Tec Doc IAEA-TECDOC-CD-1674, Dec. 2012.
- [21] Holtec international FSAR, "Holtec International Final Safety Analysis Report for the HI-STORM 100 Cask System." 2016. [Online]. Available: <https://www.nrc.gov/docs/ML1613/ML16138A100.pdf>
- [22] J. S. Gibbs, "FEASIBILITY OF LATERAL EMPLACEMENT IN VERY DEEP BOREHOLE DISPOSAL OF HIGH LEVEL NUCLEAR WASTE," 2010.
- [23] Sandia National Laboratories, "DPC Disposal Concepts of Operations," M3SF-20SN010305052 Rev. 1, Mar. 2021.
- [24] E. Hardin *et al.*, "Repository Reference Disposal Concepts and Thermal Load Management Analysis," Sandia National Laboratory, FCRD-UFD-2012-00219 Rev. 2, Nov. 2012.
- [25] J. T. Carter and T. F. Severynse, "Electrochemical Reprocessing and Capital Cost Estimate, Report Number DCRD-SYSA-2010-000107," Savannah River Site, Aug. 2010.
- [26] M. A. Rose, W. C. Phillips, R. O. Hoover, and M. E. Woods, "An Assessment of Applying Pyroprocessing Technology to Advanced Pebble-Type Fuels," ANL/CFCT-23/6, Mar. 2023.
- [27] S. K. Kim, W. I. Ko, and Y. H. Lee, "Economic Viability of Metallic Sodium-Cooled Fast Reactor Fuel in Korea," *Sci. Technol. Nucl. Install.*, vol. 2013, pp. 1–10, 2013, doi: 10.1155/2013/412349.
- [28] M. J. Lineberry, R. D. Phipps, and J. P. Burelbach, "Commercial-size IFR Fuel Cycle Facility: Conceptual Design and Cost Estimate, DOE Document No. ANL-IFR-25," Oct. 1985.
- [29] J.-H. Lee, J.-B. Shim, E.-H. Kim, J.-H. Yoo, S.-W. Park, and C. T. Snyder, "A Feasibility Study for the Development of Alternative Methods to Treat a Spent Triso Fuel," *Nucl. Technol.*, vol. 162, no. 2, pp. 250–258, May 2008, doi: 10.13182/NT08-A3953.
- [30] J. Trelewicz *et al.*, "Technology Enabling Zero-EPZ Micro Modular Reactors," Milestone M1.1.2.
- [31] J. Buongiorno, J. W. Sterbentz, and P. E. MacDonald, "Study of Solid Moderators for the Thermal-Spectrum Supercritical Water-Cooled Reactor," *Nucl. Technol.*, vol. 153, no. 3, pp. 282–303, Mar. 2006, doi: 10.13182/NT06-A3708.
- [32] "Zirconium and Hafnium Statistics and Information | U.S. Geological Survey." Accessed: Jan. 22, 2025. [Online]. Available: <https://www.usgs.gov/centers/national-minerals-information-center/zirconium-and-hafnium-statistics-and-information>
- [33] "BLS Data Viewer." Accessed: Jan. 23, 2025. [Online]. Available: <https://data.bls.gov/dataViewer/view/timeseries/CUUR0000SA0;jsessionid=F01730E239E328BC74156EE40E4F90B2>
- [34] Dr. D. Petti, Nov. 19, 2023.
- [35] Dr. L. Snead, Sep. 19, 2024.

- [36] "FSV History." Accessed: Feb. 04, 2025. [Online]. Available: <https://www.fsvfolks.org/FSVHistory.html>
- [37] "Levelized Costs of New Generation Resources in the Annual Energy Outlook 2022," 2022.
- [38] "Advanced Reactors," General Atomics. Accessed: Feb. 04, 2025. [Online]. Available: <https://www.ga.com/nuclear-fission/advanced-reactors>
- [39] J. Hinze, Oct. 24, 2024.
- [40] "USGS Scientific Investigations Report 2012–5188: Metal Prices in the United States Through 2010." Accessed: Jan. 23, 2025. [Online]. Available: <https://pubs.usgs.gov/sir/2012/5188/>

Appendix 1 Sodium-cooled fast reactor design specification

Parameter	Value
Reactor power (MWth)	1000
Cycle length (years)	4.9
Fresh fuel composition	
Fresh Uranium + Recycled Uranium (kg)	24175.2
Plutonium (kg)	2919.6
Minor Actinides (kg)	270.4
Spent fuel composition	
Recycled Uranium (kg)	21947.8
Plutonium (kg)	3115.7
Minor Actinides (kg)	221.0
Fission Products (kg)	1806.5

Derivation of driver and blanket mass distribution

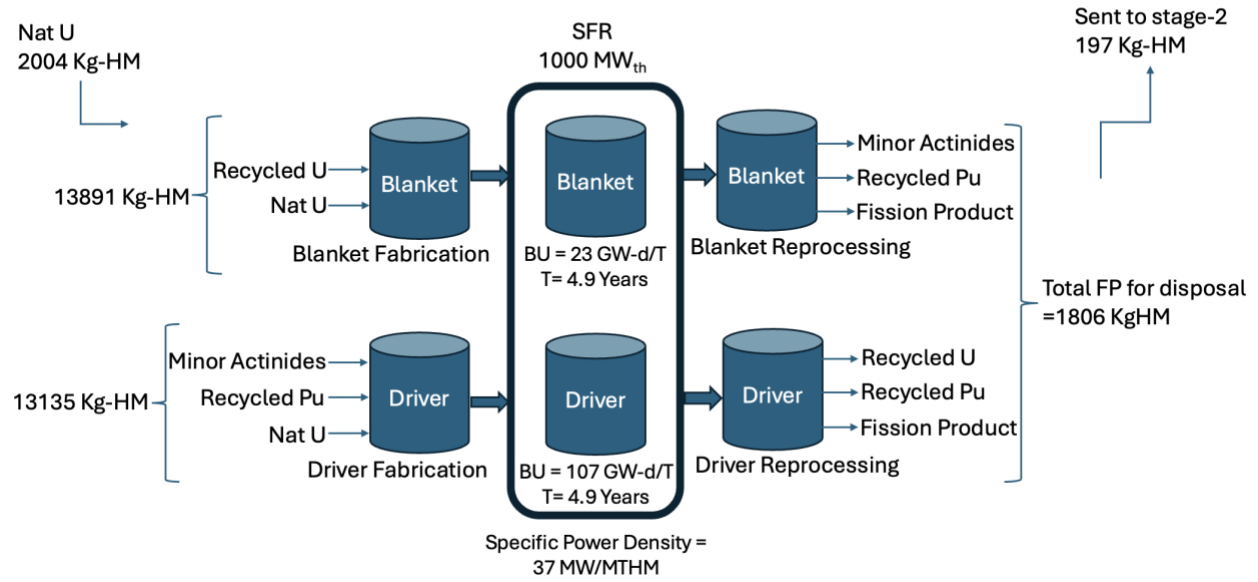
Parameter	Value
Reactor power (MWth)	1000
Cycle length (years)	4.9
Specific power density (MW/ MT-HM)	37
Blanket discharge burnup (GW-d/MT)	23
Driver discharge burnup (GW-d/MT)	107

Formula	Calculation	
	Driver	Blanket
Burnup (GWday/MTiHM) -> A	107	23
In core residence time (EFPY) -> B	4.9	4.9
Average Power Density (MWth/MTiHM) -> $C=1000A/B365$	59.83	12.86
Weight Ratio	x	1-x
Solving for x $\{59.83x+12.86(1-x)=37\}$	0.51	0.49

Comment

51 % of the total mass is driver (13891.4 Kg-HM), and 49% of the total mass is Blanket (13135.6 Kg-HM).

Mass balance for SFR



Appendix 2 Calculations for the front end of the cycle

The mass of uranium loaded in the core

$$\text{Mass of Fuel in kgHM: } M_p = \frac{1000 \times Q \times 365 \times T \times CF}{1000 \times BU}$$

Mass of ore

$$\text{Value Function for Enriched Fuel: } V_p = (1 - 2p) \times \ln\left(\frac{1 - p}{p}\right)$$

$$\text{Value Function for Uranium Feed: } V_f = (1 - 2f) \times \ln\left(\frac{1 - f}{f}\right)$$

$$\text{Value Function for Uranium Tail: } V_t = (1 - 2t) \times \ln\left(\frac{1 - t}{t}\right)$$

$$\text{Amount of Uranium Feed in kg: } M_f = \frac{p - t}{f - t} \times M_p$$

SWU requirement

$$\text{Amount of Uranium Tail in kg: } M_t = M_f \times \frac{p - f}{p - t}$$

SWU per Unit Mass of Uranium Product (in SWU/ kgHM):

$$\text{SWU} = \frac{M_p \times V_p + M_t \times V_t - M_f \times V_f}{M_p}$$

Where,

Symbol	Meaning / Definition
M_p	Mass of enriched fuel (Heavy Metal) loaded in the core
Q	Reactor power rating
T	Time of operation or fuel cycle length
CF	Capacity factor
BU	Discharge burnup of fuel
p	Product enrichment
f	Feed enrichment
t	Tails enrichment
V_p	Value function for the enriched product
V_f	Value function for the uranium feed
V_t	Value function for the uranium tails
M_f	Mass of uranium feed required
M_t	Mass of uranium tails produced
SWU	Separative Work Units required